ANNUAL REPORT

NASA GRANT NSG-1288

GAS CORE REACTORS FOR ACTINIDE TRANSMUTATION AND BREEDER APPLICATIONS

J. D. Clement and J. H. Rust

NASA Program Manager, F. Hohl

Prepared for the

National Aeronautics and Space Administration

by the

School of Nuclear Engineering
Georgia Institute of Technology
Atlanta, Georgia 30332

April 1, 1978

ANNUAL REPORT

NASA GRANT NSG-1288

GAS CORE REACTORS FOR ACTINIDE TRANSMUTATION AND BREEDER APPLICATIONS

J. D. Clement and J. H. Rust

NASA Program Manager, F. Hohl

Prepared for the

National Aeronautics and Space Administration

by the

School of Nuclear Engineering
Georgia Institute of Technology
Atlanta, Georgia 30332

April 1, 1978

ACKNOWLEDGMENTS

This work was supported by NASA Grant NSG-1288, Supplement No. 1. The authors wish to express their appreciation to the program manager, Dr. Frank Hohl, for helpful suggestions during the performance of the research.

The following graduate students, supported by the grant, made significant contributions to the research project: Stanley Chow and Pak Tai Wan.

In addition, the NASA research program was also used as a design project for the Nuclear Engineering design course in the academic curriculum. The following graduate students taking the course were of great assistance in the research work: Constantine Bratianu, Stanley Chow, Trent Primm, and Scott Revolinski.

TABLE OF CONTENTS

LIST OF FIGURES

LIST OF FIGURES (Continued)

LIST OF TABLES

LIST OF TABLES

Abstract

The work summarized in this report, which was carried out as a part of a NASA sponsored fissioning plasma research program, consisted of design power plant studies for four types of reactor systems: uranium plasma core breeder, uranium plasma core actinide transmuter, UF_6 breeder and UF_6 actinide transmuter.

The plasma core systems can be coupled to MHD generators to obtain high efficiency electrical power generation. A power plant employing a ternary cycle of MHD generator, gas turbine, and steam cycle may have efficiencies of 60 to 70 percent for reactor exit temperatures of $3000^{\circ}K$ to $4000^{\circ}K$, respectively. The material problems are severe so that this system will require long research and development times and can, therefore, be regarded as an advanced system.

On the other hand, the UF_6 reactor would require only a modest extension of present day technology for its development. A 1074 MWt UF_6 breeder reactor was designed with a breeding ratio of 1.002 to guard against diversion of fuel. Using molten salt technology and a superheated steam cycle, an efficiency of 39.2% was obtained for the plant and the U^{233} inventory in the core and heat exchangers was limited to 105 kg.

It was found that the UF_6 reactor can produce high fluxes (10^{14} n/cm^2-sec) necessary for efficient burnup of actinides. However, the buildup of fissile isotopes posed severe heat transfer problems. Therefore, the flux in the actinide region must be decreased with time. Consequently, only beginning-of-life conditions were considered for the power plant design. A 577 MWt UF_6 actinide transmutation reactor power plant was

designed to operate with 39.3% efficiency and 102 kg of U^{233} in the core and heat exchangers for beginning-of-life conditions. Additional work is needed to solve the heat transfer problems.

1. INTRODUCTION

The need to produce more electricity within certain social, economic, and political constraints has forced the United States to reevaluate many of its energy policies. In particular, the nuclear industry is beset by problems of dwindling uranium resources, waste management, and nuclear proliferation among others. The political and social pressures have been great enough to delay commercialization of the liquid metal fast breeder reactor for an indefinite period and has prompted a growing effort to look at alternative systems.

One such alternative is the gas core reactor which has been supported by the National Aeronautics and Space Administration for almost twenty years. The original goal in research and development of the gas core reactor was to produce a space propulsion reactor that would be capable of fast, manned expeditions to neighboring planets.[1]

Although budgetary and policy factors terminated the development of nuclear powered propulsion engines, NASA has continued to sponsor fissioning plasma research consisting of cavity reactor criticality tests, fluid mechanics tests, investigation of uranium optical emission spectra, radiant heat transfer studies, and related theoretical work.[2,3] Research has shown that UF_6 fueled reactor can be quite versatile with respect to power, pressure, operating temperature, and modes of power extraction.[4] Possible power conversion systems include Brayton cycles, Rankine cycles, MHD generators, and thermionic diodes. Power extraction may also be possible in the form of coherent light from interactions of fission fragments with a laser gas mixture.

NASA is also conducting a series of UF_6 non-flowing and flowing critical experiments at the Los Alamos Scientific Laboratory.[5] If preceding steps are successful, a reactor experiment may be performed in the early 1980's at the Nuclear Rocket Development Station for a uranium plasma at 6000°K and producing 5 MW of thermal power.

In addition, the International Security Affairs Office of the U.S. Energy Research and Development Administration (now the Department of Energy) has sponsored research on non-proliferating gas core reactor power plants.[6-9] Initial studies show that fuel inventories may be a factor of 10 less than those in current U.S. power reactors.

A study[10] was also conducted by the University of Florida on heterogeneous gas core reactors (HGCR) for power generation. An approximately 50-50 mixture of UF_6 and He was used as the gaseous fuel. Designs for a 3000 MWt light-water moderated, and a 1000 MWt heavy-water moderated HGCRs were presented.

The Georgia Institute of Technology has been engaged in various gas core reactor power plant concepts under NASA sponsorship. One such concept utilized a uranium plasma, breeder reactor employing a MHD generator for the topping cycle.[11,12] Power plant efficiencies of 70 percent are attainable with this high temperature reactor.

More recent work done at Georgia Tech involves the application of UF_6 reactors for breeding and actinide transmutation purposes.[13,14] Several advantages of these systems were identified.

An advantage of UF_6 reactor systems is the continuous on-line reprocessing of fluid fuels. By bleeding off a small percentage of the UF_6 from the primary loop, fission product and actinide buildup can be continuously removed by reprocessing. This results in a better fuel economy for the reactor.

The UF_6 reactor is inherently safe because the conventional loss-of-coolant accident cannot occur, the core contains a minimum amount of radioactive fission products, and the temperature coefficient of reactivity is negative which prevents accidental power excursions.

Reference 13 indicates that UF_6 breeder reactors may have breeding ratios of 1.25 - 1.26 for core diameters varying from 1 to 5 m and that fuel doubling times may be as small as a few years. Reference 14 shows that the gas core actinide transmutation reactor may be capable of burning up 10.3 metric tons of actinides in 40 years as compared to 2.93 and 0.423 for the liquid metal fast breeder reactor and the light water reactor, respectively.

One significant advantage of the gas core reactors over conventional reactors is that it has a smaller critical mass. This is important since reducing system uranium inventory may reduce the risk of fuel diversion. However, this will place an added design constraint. For example, a breeder reactor may be designed with a breeding ratio just sufficient to fuel itself. The rationale behind this design is that any diversion of fuel would cause the reactor to shut down. The resulting loss of the use of a power reactor may be a deterrent to fuel diversion.

This report reexamines both plasma core and UF_6 breeder and actinide transmutation reactors in the light of reducing fuel inventories. However, full optimizations of these systems were beyond the scope of this study.

Chapter 2 summarizes the results for high temperature uranium plasma breeder and actinide transmutation power plants employing MHD topping cycles. A detailed study was made in Ref. 15. Chapter 3 analyzes the UF_6 breeder power plants while Chapter 4 analyzes UF_6 actinide transmutation power plants. Finally, conclusions and recommendations are presented in Chapter 5.

References for Chapter 1

1. Ragsdale, R. G., "To Mars in 30 Days by Gas Core Nuclear Rocket," Astronautics and Aeronautics, 10, No.1 (1971).

2. Thom, K., Schneider, R. T., and Schwenk, F.C., "Physics and Potentials of Fissioning Plasmas for Space Power and Propulsion," International Astronautical Federation 25th Congress, Paper No. 74087, Amsterdam (October 1974).

3. Schwenk, F. C. and Thom, K. T., "Gaseous Fuel Nuclear Reactor Research," paper presented at the Oklahoma State University Conference on Frontiers of Power Technology (October 1974).

4. Rodgers, R. J., Latham, T. S., and Krascella, N. L., "Investigation of Applications for High-Power, Self-Critical Fissioning Uranium Plasma Reactors," NASA CR-145048 (September 1976).

5. Rodgers, R. J., Latham, T. S., and Krascella, N.L., "Analyses of Low-Power and Plasma Core Cavity Reactor Experiments," United Aircraft Research Laboratories Report R75-911908-1 (May 1975).

6. Lowry, L. L., "Gas Core Reactor Power Plants Designed for Low Proliferation Potentials," LA-6900-MS (September 1977).

7. Soran, P. D. and Hansen, G. E., "Neutronics of a Mixed-Flow Gas-Core Reactor," LA-7036-MS (November 1977).

8. Lowry, L. L., Helmick, H. H., and Kendall, J. S., "The Nonproliferation Features of the Gas Core Reactor," Transactions of the American Nuclear Society, 27, 933 (November 27-December 2, 1977).

9. Mc Laughlin, T. P., Soran, P. D., and Hansen, G.E., "Gas Core Reactors: Neutronics, SNM Proliferation, and Resource Utilization," Transactions of the American Nuclear Society, 27, 934-35 (November 27-December 2, 1977).

10. Han, K. I., Dugan, E. T., and Diaz, N. J., "Heterogeneous Gas Core Reactor Power Plants," Transactions of the American Nuclear Society, 27, 722-724 (November 27-December 2, 1977).

11. Williams, J. R. and Clement, J.D., "Exploratory Study of Several Advanced Nuclear-MHD Power Plant Systems," Final Status Report, NASA Grant NGR-11-002-145, Georgia Institute of Technology, Atlanta, Georgia (March 1973).

12. Williams, J. R. and Clement, J.D., "Satellite Nuclear Power Station - An Engineering Analysis," NASA Grant NGR-11-002-145, Georgia Institute of Technology, Atlanta, Georgia (March 1973).

13. Clement, J. D. and Rust, J. H., "Analysis of UF_6 Breeder Reactor Power Plants," Final Report, NASA Grant NSG-1168, Georgia Institute of Technology, Atlanta, Georgia (February 1976).

14. Clement, J. D. and Rust, J. H., "Analysis of the Gas Core Actinide Transmutation Reactor (GCATR)," Annual Report, NASA Grant NSG-1288, Georgia Institute of Technology, Atlanta, Georgia (February 1977).

15. Clement, J. D. and Rust, J.H., "Analysis of the Gas Core Actinide Transmutation Reactor (GCATR)," Semi-Annual Report, NASA Grant NSG-1288, Supplement No.1, Georgia Institute of Technology, Atlanta, Georgia (September 1977).

2. HIGH TEMPERATURE URANIUM PLASMA POWER PLANTS

The work summarized in this chapter, which is described in detail in Ref. 1, consists of design power plant studies for applications of the plasma core reactor as a breeder and as an actinide transmuter. In addition to these applications, the system produced electrical power with a high efficiency.

A reactor subsystem was designed for each of the two applications. Tables 2.1 and 2.2 summarize the reactor design parameters for the breeder and the actinide transmuter, respectively.

For the breeder reactor, neutronics calculations were carried out for a U-233 plasma core with a molten salt breeding blanket. The primary objectives of the overall nuclear design were to design a reactor with a low critical mass (less than a few hundred kilograms U-233) and also a breeding ratio of 1.01. The later objective was a safety precaution to guard against diversion of fissionable material during blanket reprocessing. Since only enough U-233 would be bred in the blanket to replenish the amount depleted in the core, any diversion of U-233 during reprocessing would result in an insufficient amount of fissionable material to replenish the core and the reactor would shut down. Both of the above objectives were met in the final design. It is also possible to design for much higher breeding ratios in the range 1.1-1.2.

The Plasma Core Actinide Transmutation reactor was designed to transmute the nuclear waste from conventional LWR's. Each LWR is loaded with

Table 2.1 Plasma Core Breeder Reactor Reference Design

Dimensions of Reactor Regions	
U^{233} Plasma	- 165 cm O.D.
Helium	- 285 cm O.D.
BeO Moderator	- 325 cm O.D.
Molten Salt*	- 355 cm O.D.
BeO Reflector	- 375 cm O.D.
Fe Pressure Shell	- 415 cm O.D.
Critical Mass	- 26.3 kg
Breeding Ratio	- 1.0099
Power	- 2000 MWt
Average Thermal Flux in Plasma	- 3.42×10^{15} $\bar{n}/cm^2$-sec
Reactor Pressure	- 200 atm
Average Temperatures	
U^{233} Plasma	- 25,000°K
Helium	- 3,000°K
Molten Salt	- 1,015°K
Molten Salt Mass Flow Rate	- 542 kg/sec

*Molten Salt Composition - 71.7% LiF (99.995% Li^7), 16% BeF_2, 12.3% ThF_4

Table 2.2 Plasma Core Actinide Transmutation Reactor Reference Design

Dimensions of Reactor Regions

U^{233} Plasma	-	200 cm thickness
He	-	120 cm thickness
Be Moderator	-	17 cm thickness
*Act. Oxide + Zr + He	-	0.85 cm thickness
Be Reflector	-	80-90 cm thickness

Critical Mass	-	380 kg
Mass of Actinides	-	1.27 metric tonne
Power	-	2000 MWt
Average Thermal Flux in Plasma	-	2.06×10^{14} n/cm^2-sec
Average Thermal Flux in Actinides	-	1.23×10^{14} n/cm^2-sec
Reactor Pressure	-	200 atm.

Temperatures

U^{233} Plasma	-	25000°K
He	-	3000°K
Be Moderator	-	1000°K
Act. Oxide + Zr + He	-	800°K
Be Reflector	-	400-600°K

*Actinide Composition: 74% Np^{237}; 7% Am^{241}; 14% Am^{24}; 4% Cm^{244}.

88 metric tonnes of uranium (3.3% U^{235}) and operated until a burnup of 33,000 MWD/MTU is reached. The fuel is discharged from the reactor and cooled for 160 days. Next, the spent fuel is reprocessed during which 100% of Np, Am, Cm, and higher actinides are separated from the other components. The concentrations of these actinides are calculated by ORIGEN[2] and tabulated. These actinides are then manufactured as oxides into zirconium clad fuel rods and charged as fuel assemblies in the reflector region of the plasma core actinide transmutation reactor. Results of actinide burnup calculations for an equilibrium plasma core transmuter servicing 27 PWR's show that after 12 cycles the actinide inventory has stabilized to about 2.6 times its initial loading. There are two mechanisms for the removal of actinides:

(1) They are fissioned directly in the plasma core actinide transmuter

(2) They are removed as U or Pu.

The U and Pu can be used in other reactors. In the equilibrium cycle, about 7% of the actinides are directly fissioned away, while about 31% is removed by reprocessing.

Fluid mechanics, heat transfer, and mechanical design considerations for both reactors are also described in Ref. 1.

Since it is desirable to have the Plasma Core Breeder Reactor (PCBR) be a self-contained unit, generating its own new fuel, an on-line reprocessing system for the molten salt blanket is a necessity. Reference 1 describes protactinium removal and salt purification processes, calculations of expected flow rates, and equilibrium concentrations of various isotopes present in the system.

In order to achieve maximum effectiveness from the high temperature coolants from either of the two plasma core reactors, it was decided that a ternary power cycle would produce the highest efficiency power plant. The ternary cycle consists of a combination of MHD, gas turbine, and Rankine cycle energy conversion units. Two concepts were investigated — a system with a high temperature regenerator in the helium loop, shown in Fig. 2.1, and a system without a regenerator, shown in Fig. 2.2.

The achieved objectives of the study were as follows:

(1) Model the nuclear MHD power plant cycle.

(2) Analyze the power output from the three energy conversion units and evaluate plant overall efficiency.

(3) Make a parametric study of the effect of changing operating variables on plant overall performance.

All studies used values for input data according to current commercial technology (i.e. efficiencies for steam cycle components, gas turbine, and compressors) or with current use in MHD research.

The modeling of the MHD cycle consisted of defining a pseudo-Brayton cycle and treating the expansion within the MHD generator in a similar manner as in a gas turbine. In order to analyze the two systems it was necessary to write two computer codes:

(1) NMHD-1 — code to analyze the nuclear MHD power plant without regeneration in the helium loop

(2) NMHD-2 — code to analyze the nuclear MHD power plant with regeneration in the helium loop.

Table 2.3 lists input parameters for each system.

A study was made of the effect on overall efficiency of varying the reactor coolant outlet temperature from 3000^{o}K to 4000^{o}K for the two

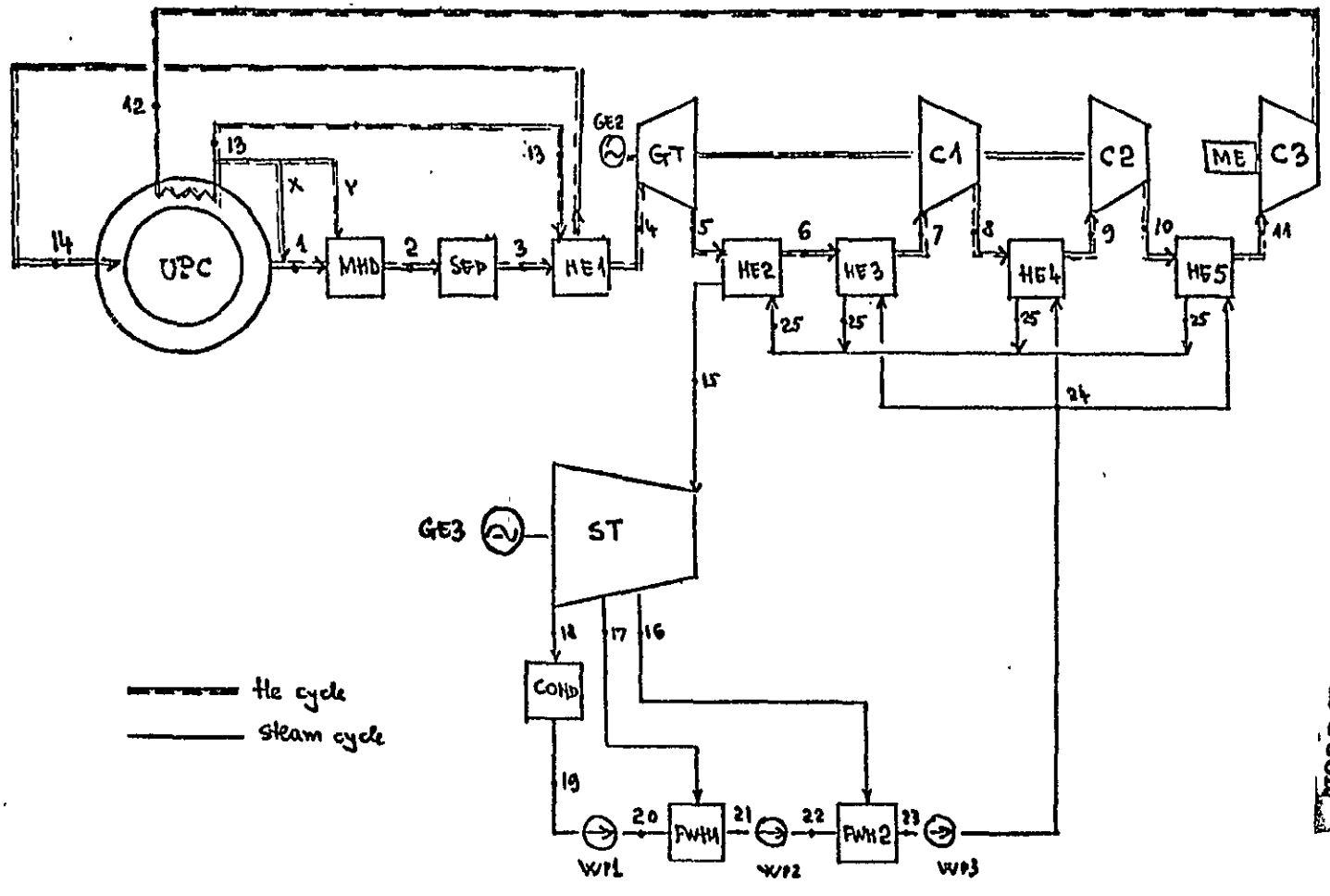

UPC - Uranium Plasma Core; MHD - MHD Generator; SEP - Diffuser and Separator; HE1 - Regenerative Heat Exchanger; HE2,3,4 and 5 - Heat Exchangers; GE - Electric Generator; GT - Gas Turbine; C - Compressor; ME - Electric Motor; ST - Steam Turbine; COND - Condenser; WP - Water Pump; PWH - Feed Water Heater.

Fig. 2.1 Nuclear MHD Power Plant With Regeneration

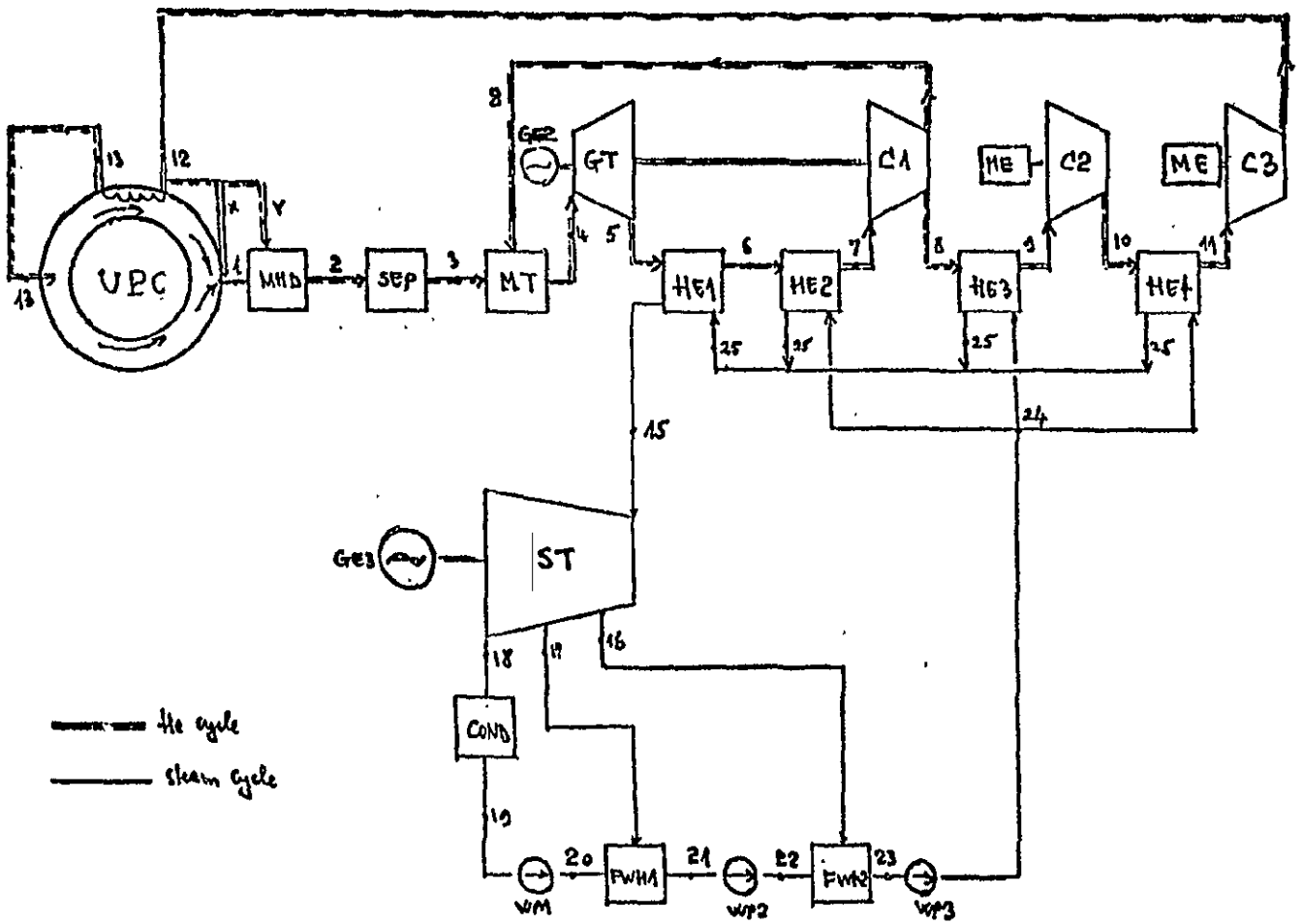

UPC - Uranium Plasma Core; MHD - MHD generator; SEP - Diffuser and Separator; MT - Mixing Tank; GE - Electric Generator; GT - Gas Turbine; C - Compressor; HE - Heat Exchanger; ME - Electric Motor; ST - Steam Turbine; COND - Condenser; WP - Water Pumps; FWH - Feed Water Heater.

Fig. 2.2 Nuclear MHD Power Plant Without Regeneration

Table 2.3 Input Data for NMHD-1 and NMHD-2

Index	NMHD-1		NMHD-2	
1	Boiler Temperature ----	1000°F	Boiler Temperature ----	1000.°F
2	Boiler Pressure -------	1600 psia	Boiler Pressure -------	1600 psia
3	Condenser Pressure ----	1.0 psia	Condenser Pressure ----	1.0 psia
4	Steam Turbine Efficiency	81%	Steam Turbine Efficiency	81%
5	Pump Efficiency -------	80%	Number of Feed Heaters	0,1 or 2
6	Number of Feed Heaters	0,1 or 2	Reactor Temp Difference	200°K
7	Compressor Efficiency -	85%	Compressor Efficiency -	85%
8	MHD Inlet Temp --------	3000°K	MHD Inlet Temp --------	3000°K
9	MHD Inlet Press -------	200 bar	MHD Inlet Press -------	200 bar
10	MHD Pressure Ratio ----	5.0	MHD Pressure Ratio ----	3.0
11	Gas Turbine Pressure Ratio	2.0	Gas Turbine Press. ratio	3.0
12	Feed Heater 1 Pressure	12. psia	Feed Heater 1 press. --	12. psia
13	Feed Heater 2 Pressure -	4. psia	Feed Heater 2 press. --	4.0 psia
14	Bottom Temp Difference -	150°K	Bottom Temp Diff. ----	150°K
15	MHD Inlet Mach No. ----	0.5	MHD Inlet Mach No. ----	0.5
16	Sep Outlet Mach No. ----	0.1	Sep Outlet Mach No. ---	0.1
17	Gas Turbine Inlet Temp -	1500°K	Gas Turbine Inlet Temp	1500°K
18	MHD Efficiency ---------	49%	MHD Efficiency --------	49%
19	Gas Turbine Efficiency -	85%	Gas Turbine Efficiency	85%
20	Number of Compress Stages	3.0	Number of Compress Stages	3.0

systems. Tables 2.4 and 2.5 list typical results, showing an overall plant efficiency as high as 70%.

For Nuclear MHD Power Plant with regeneration (Fig. 2.1), the major contribution of the electric power is produced in the top of the power cycle by the MHD subsystem (33.97% - 45.49% from 100% heat produced by the reactor). The power production has been shifted toward the top of the ternary cycle with a large increase in overall efficiency. This system produces overall efficiencies that are 60 - 80% higher than actual power plants in use and 25 - 45% higher than expected coal-fired MHD power plants.

For Nuclear MHD Power Plants without regeneration (Fig. 2.2), the major contribution of electric power is due to the steam turbine subsystem (36.03% - 36.36% from 100% heat produced by the reactor). Due to a significant fraction of the electric power being produced by the steam cycle at lower efficiencies (40%), it is desirable to shift the power production toward the top of the cycle to improve the overall efficiency. This can be achieved by reducing the mass flow rate of helium within the inner loop and increasing the pressure ratio of the MHD generator. This system produced overall efficiencies that are 40 - 50% higher than actual power plants in use, and 10 - 15% higher than expected coal-fired MHD power plants. Due to the relatively low temperatures within the helium loop, this type of power plant could be considered as a first step in a national program of implementation of MHD power plants with a nuclear source.

Table 2.4 Plant Overall Efficiencies with High Temperature Regenerator

MHD Inlet Temperature	3000°K		3250°K		3500°K		3750°K		4000°K	
Q_R	4973.45	100.0%	5138.94	100.00%	5299.94	100.00%	5458.27	100.0%	5693.55	100.0%
W_{MHD}	1689.52	33.97%	1914.65	37.26%	2139.78	40.37%	2139.78	43.44%	2590.04	45.49%
W_{GT}	319.12	6.42%	319.12	6.21%	319.12	6.02%	319.12	5.85%	319.12	5.60%
W_{ST}	1112.20	22.36%	1112.20	21.64%	1112.20	20.99%	1112.20	20.38%	1112.20	19.53%
η_{PLANT}	62.75%		65.11%		67.38%		69.56%		70.62%	

Q_R = REACTOR HEAT RATE

W_{MHD} = MHD NET ELECTRIC POWER: $W_{MHD} = W_{MHD\ OUTPUT} - W_{COMPRESSOR}$

W_{GT} = GAS TURBINE ELECTRIC POWER: $W_{GT} = W_{GT\ OUTPUT} - 2 \times W_{COMPRESSOR}$

W_{ST} = STEAM TURBINE ELECTRIC POWER: $W_{ST} = W_{ST\ OUTPUT} - W_{PUMP}$

$$\eta_{PLANT} = \left(\frac{W_{MHD}}{Q_R} + \frac{W_{GT}}{Q_R} + \frac{W_{ST}}{Q_R}\right) \times 100 = \left(\frac{W_{MHD}}{Q_R}\,100\right) + \left(\frac{W_{GT}}{Q_R}\,100\right) + \left(\frac{W_{ST}}{Q_R}\,100\right) \quad [\%]$$

Table 2.5 Plant Overall Efficiencies without High Temperature Regenerator

MHD Inlet Temperature	3000°K		3250°K		3500°K		3750°K		4000°K	
Gas Flow Rate Through the GT.	2.33 kg/sec		2.60 kg/sec		2.88 kg/sec		3.15 kg/sec		3.42 kg/sec	
Q_R	12265.71	100.0%	13563.96	100.0%	14862.21	100.0%	16160.46	100.0%	17458.71	100.0%
W_{MHD}	1777.71	14.49%	2077.87	15.32%	2378.55	16.0%	2679.22	16.58%	2929.90	17.07%
W_{GT}	456.46	3.72%	510.00	3.76%	563.54	3.79%	617.68	3.82%	670.62	3.84%
W_{ST}	4419.73	36.03%	4901.75	36.14%	5383.76	36.22%	5865.78	36.30%	6347.80	36.36%
η_{PLANT}	54.24%		55.22%		56.01%		56.70%		57.27%	

Q_R = REACTOR HEAT RATE

W_{MHD} = MHD NET ELECTRIC POWER : $W_{MHD} = W_{MHD\ OUTPUT} - 2W_{COMPRESSOR}$

W_{GT} = GAS TURBINE ELECTRIC POWER : $W_{GT} = W_{GT\ OUTPUT} - W_{COMPRESSOR}$

W_{ST} = STEAM TURBINE ELECTRIC POWER: $W_{ST} = W_{ST\ OUTPUT} - W_{PUMP}$

$$\eta_{PLANT} = \left(\frac{W_{MHD}}{Q_R} + \frac{W_{GT}}{Q_R} + \frac{W_{ST}}{Q_R}\right) \times 100 = \left(\frac{W_{MHD}}{Q_R}\,100\right) + \left(\frac{W_{GT}}{Q_R}\,100\right) + \left(\frac{W_{ST}}{Q_R}\,100\right) \quad [\%]$$

References for Chapter 2

1. Clement, J. D. and Rust, J. H., "Analysis of the Gas Core Actinide Transmutation Reactor," Semi-Annual Report, NASA Grant NSG-1288, Georgia Institute of Technology (September 1977).

2. Bell, M. J., "ORIGEN-The ORNL Isotope Generation and Depletion Code," ORNL-4628 (May 1973).

3. UF_6 BREEDER REACTOR POWER PLANT

A. Neutronics

Neutronics calculations were carried out for a uranium hexafluoride breeder reactor (UF_6BR). The primary objectives of the overall nuclear design were to design a reactor with a low critical mass (less than a few hundred kilograms U-233) and a breeding ratio of 1.0. The latter objective was a precaution to guard against diversion of fissionable material at any stage in the fuel cycle. Since only enough U-233 would be bred in the blanket to replenish the amount depleted in the core, any diversion of U-233 from the fuel cycle would result in an insufficient amount of fissionable material to replenish the core and the reactor would shut down. Both of the objectives were met in the final design.

The MACH-I Code[1] was used as the primary computational tool in the nuclear analysis. MACH-I is a one-dimensional, diffusion theory code. The 26-group ABBN cross section set of Bondarenko, et al[2] was used.

A cylindrical geometry was chosen which is shown in Fig. 3.1. The core consists of a He - UF_6 mixture flowing through a beryllium matrix. Addition of helium improves the heat transfer characteristics of the He - UF_6 mixture and is important in maintaining a small inventory of U-233 in the heat exchanger(s). The beryllium matrix provides the moderation needed by the neutrons. The partial pressures of He and UF_6 are 99 atm. and 0.69 atm., respectively. The core diameter is 200 cm and its height is 600 cm. Surrounding the core radially is a 60 cm thick breeding blanket. The breeding salt composition is 71.7 mole % LiF,

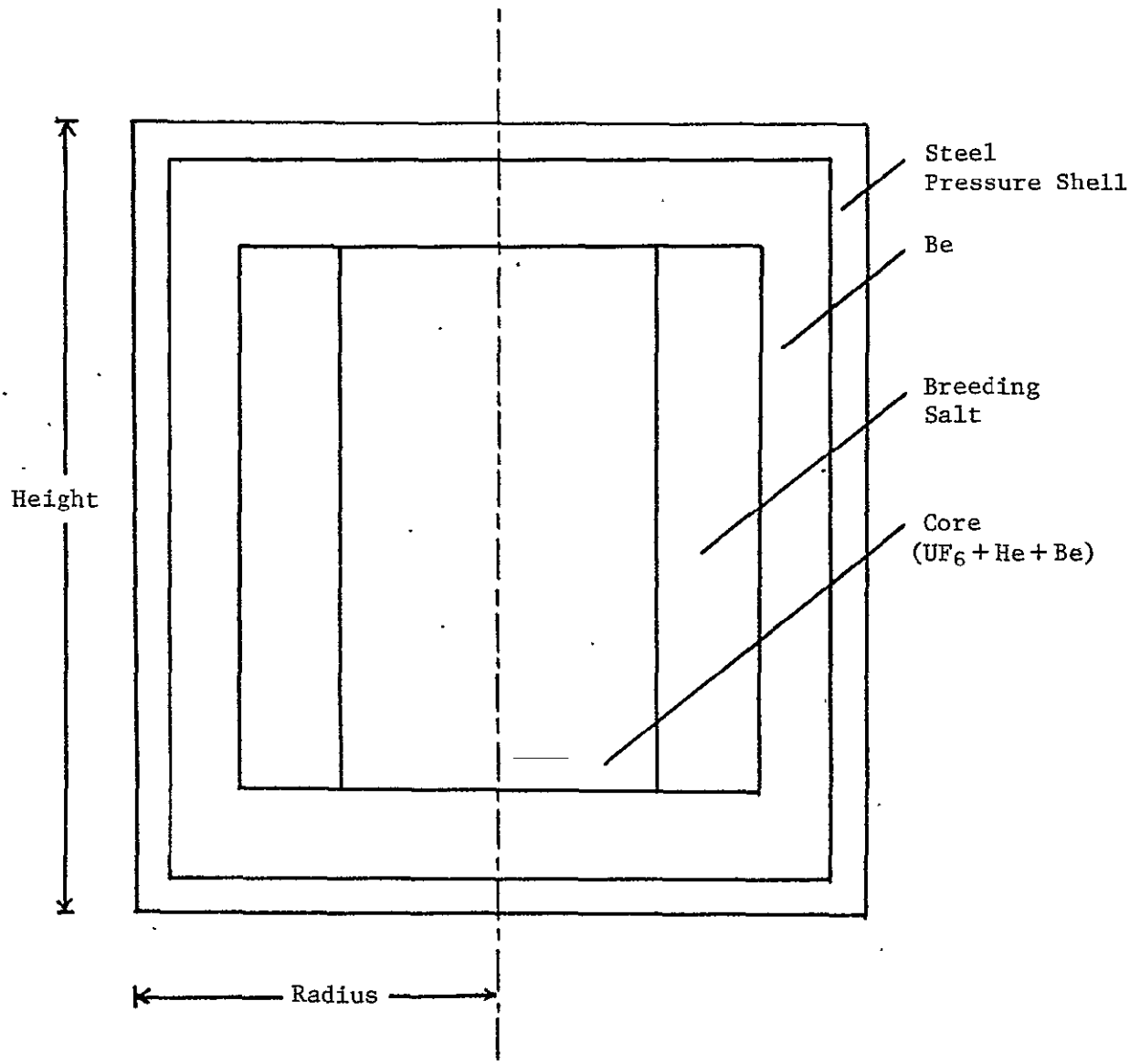

Fig. 3.1 Reactor Configuration of UF_6BR

16 mole % BeF_2, and 12.3 mole % ThF_4. The Li is enriched to essentially 100% Li^7. This composition is based on work done on the molten salt breeder reactor (MSBR) by the Oak Ridge National Laboratory.[3] Beryllium was used as a reflector both axially (20 cm) and radially (50 cm). The entire reactor is encased in a 20 cm thick stainless steel pressure shell.

Since the ABBN cross section set does not have cross sections for helium and fluorine, these were generated from cross section data from BNL-325.[4,5] The group-averaged cross sections were calculated as follows:

$$\langle \sigma_x \rangle_i = \frac{\int_{E_i} \sigma_x(E)\,\phi(E)\,dE}{\int_{E_i} \phi(E)\,dE} \tag{3.1}$$

where $\phi(E) = 0.77E^{\frac{1}{2}}\, e^{-0.776E}$ $\qquad$ $2.5\ \text{MeV} \leq E \leq 10\ \text{MeV}$

$= \frac{1}{E}$ $\qquad$ $E \leq 2.5\ \text{MeV}$

The elastic and inelastic downscattering cross sections were calculated by:

$$\langle \sigma \rangle_{i \to j} = \frac{\int_{E_i}\int_{E_j} \sigma(E)\,\phi(E)\,P(E \to E')\,dE'\,dE}{\int_{E_i} \phi(E)\,dE} \tag{3.2}$$

for elastic scattering, $P(E \to E') = \frac{1}{(1-\alpha)E}$ $\qquad$ $\alpha E < E' < E$

$= 0$ $\qquad$ otherwise (3.3)

where $\alpha = \left(\frac{A-1}{A+1}\right)^2$

for inelastic scattering, $P(E \rightarrow E') = \frac{E'}{T^2} e^{-E'/T}$ (3.4)

with $T = 3.2\sqrt{\frac{E}{A}}$

A = Atomic no. of nuclide

The transport cross section was calculated by

$$\langle \sigma_{tr} \rangle = \langle \sigma_e \rangle (1 - \bar{\mu}_e) + \langle \sigma_{in} \rangle + \langle \sigma_c \rangle + \langle \sigma_f \rangle \quad (3.5)$$

where $\langle \sigma_{tr} \rangle$ = group averaged transport cross section

$\langle \sigma_e \rangle$ = group averaged elastic scattering cross section

$\bar{\mu}_e$ = average cosine of scattering angle

$= \frac{2}{3A}$

$\langle \sigma_{in} \rangle$ = group averaged inelastic scattering cross section

$\langle \sigma_c \rangle$ = group averaged capture cross section

$\langle \sigma_f \rangle$ = group averaged fission cross section

For helium, there are no resonances and all cross sections are smooth functions of energy. Fluorine-19 has a few elastic scattering resonances. It was estimated that for the fluorine in UF_6 and the breeding blanket, the effect of these resonances is small compared to the moderation in the beryllium and lithium. Hence, these resonances were neglected.

In the core and the breeding blanket, self shielding factors were used to take care of dilution effects. For the uranium in the core infinite dilution factors were used because of the low density of the UF_6

gas. For the thorium-232 in the blanket, a self shielding cross section of 61 barns was determined, and appropriate self shielding factors were accounted for.

Since the ABBN cross section set does not treat thermal cross sections accurately, the effective neutron temperature model was used. The thermal flux was assumed to be Maxwellian, $\phi(E) \alpha E\, e^{-E/kT_n}$, where T_n = effective neutron temperature. Following the treatment of Wescott[6] the average thermal cross section is given by

$$\langle \sigma_x \rangle_{th} = \sigma_x(E_o) \quad \frac{\sqrt{\pi}}{2} \quad \sqrt{\frac{T_o}{T}} \quad g_x(T) \tag{3.6}$$

where (E_o, T_o) is, by convention, (0.025 eV, 293.16 °K) and $g_x(T)$ is the non $\frac{1}{v}$ factor for reaction x.

A neutron temperature of 783°K was assumed for the calculations. For this neutron temperature, groups 25 and 26 were combined as the thermal group.

For the cylindrical geometry chosen, a complete calculation would require a two-dimensional calculation. Since MACH-I is a one-dimensional code, the infinite slab and infinite cylinder geometries were used to model the axial and radial neutronics of the reactor. The two geometries were coupled together by group dependent bucklings in the axial and radial directions. Iteration between the axial and radial calculations were carried out until a consistent set of axial and radial bucklings was obtained.

To insure adequate leakage of neutrons to the breeding blanket, a height to diameter ratio of $\frac{600}{200} = 3.0$ was chosen. This was essential to the breeding of the reactor.

In all the MACH-1 calculations, a search was made for the Be concentration in the core. The critical mass of the core could be reduced substantially by increasing the Be to U^{233} ratio, i.e. by making the neutron spectrum more and more thermal. However, for breeding of thorium-232, which has numerous resonances in the epithermal range, too thermal a neutron spectrum would be detrimental. The concentration of Be in the core chosen was a compromise between the requirements of criticality and breeding.

When thorium-232 absorbs a neutron, thorium-233 is formed, and a 7.5 MeV gamma is emitted. Thorium-233 undergoes β^- decay to Pa^{233} emitting a β^- particle of 1.23 MeV. Pa^{233} undergoes further β^- decay to form U^{233} emitting a β^- particle of 0.25 MeV. The reaction is given by:

$$Th^{233}(n,\gamma)\, Th^{233} \xrightarrow[22 \text{ min.}]{\beta^-} Pa^{233} \xrightarrow[27.4 \text{ days}]{\beta^-} U^{233}$$

For a breeding ratio of 1.0, this added up to 8.98 MeV per fission in core. Furthermore, from a MACH-1 calculation, it was found that 0.08%. of the total fissions occurs in the blanket, i.e., 0.157 MeV is available per fission. Assuming a recoverable energy of 196 MeV per fission, the percent of heat generated in the blanket is about 5%.

Characteristics of the reference UF_6BR design are discussed in Section D.

B. Heat Transfer and Thermal Hydraulics

It is necessary to size the heat exchangers in order to determine the total U^{233} inventory in the system. The primary heat exchanger analysis is the same for both the actinide transmutation reactor and the breeder reactor.

The heat exchangers used in this study are simple tube-in-shell counterflow heat exchangers. In the primary heat exchanger (Fig. 3.2) the UF_6-helium mixture passes through a number of modified Hastelloy-N tubes where heat is transferred to a flowing salt mixture composed of 92% $NaBF_4$ and 8% NaF (mole percent). This salt mixture was chosen to eliminate the possibility of criticality occurring in the primary heat exchangers and for its chemical inertness to UF_6. Modified Hastelloy-N was used for the tubing because of its corrosion resistance in a fluoride environment. Properties of UF_6, helium, $NaBF_4$-NaF salt, and modified Hastelloy-N are given in Appendix A.

The primary loop shown in Fig. 3.3 consists of the reactor core, primary heat exchanger, and compressor. The objectives of the analysis was to determine the heat exchanger size so as to determine the amount of fissile uranium in the heat exchanger and to determine the compressor power.

The analysis proceeds as follows. Given the core power, Q_{core}, and the inlet and exit temperatures of the core, T_3 and T_1, respectively, the flow rate in the loop is determined from

$$\dot{m} = \frac{Q_{core}}{C_p(T_1 - T_3)} \tag{3.7}$$

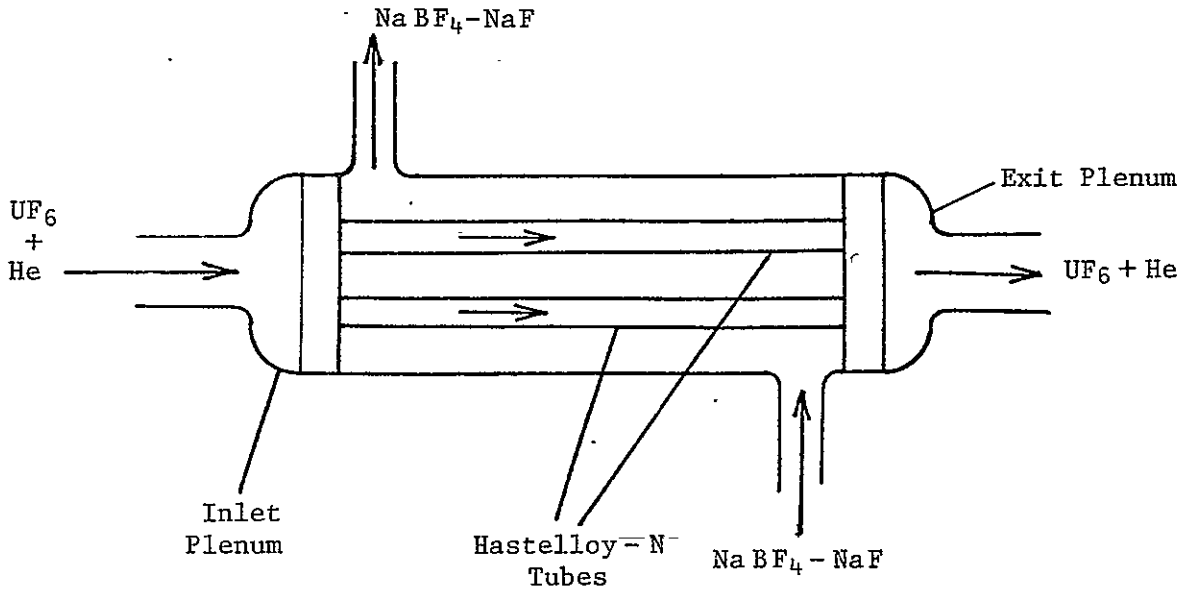

Fig. 3.2 Primary Heat Exchanger

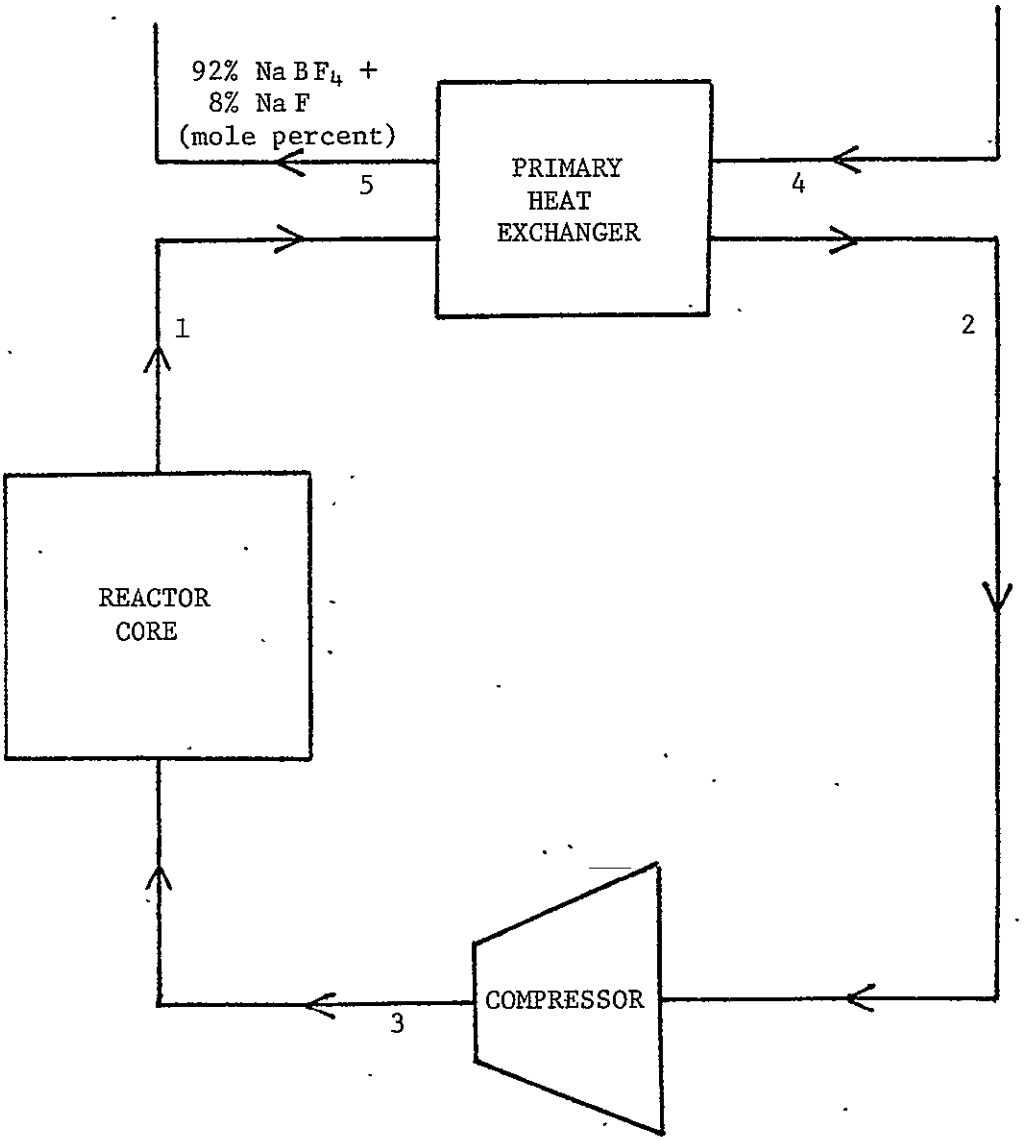

Fig. 3.3 Primary Flow Loop

where C_p is the specific heat of the helium-UF_6 gas mixture.

If the primary heat exchanger exit temperature, T_2, is given, then the power transferred from the UF_6-helium loop to the $NaBF_4$-NaF salt loop is given by

$$Q_{PHX} = \dot{m} C_p (T_1 - T_2) \tag{3.8}$$

The size of the heat exchanger can now be estimated. The equivalent diameter is determined by assuming the tubes are arranged in a triangular lattice structure (Fig. 3.4) and is given by

$$d_{eq} = \frac{4 A_f}{P_w} = \frac{2\sqrt{3}\, c^2 - \pi d_o^2}{\pi d_o} \tag{3.9}$$

where A_f is the channel flow area, P_w is the wetted perimeter, c is the pitch, and d_o is the tube outside diameter. The channel flow area is

$$A_f = \frac{\sqrt{3}}{4} c^2 - \frac{\pi d_o^2}{8} \tag{3.10}$$

The Reynolds and Prandtl numbers for the UF_6-helium mixture in the heat exchanger tubes are

$$Re = \frac{\rho u d_i}{\mu} \tag{3.11}$$

$$Pr = \frac{C_p \mu}{K} \tag{3.12}$$

where ρ, μ, and K are the density, viscosity, and thermal conductivity of the mixture. The average velocity in the tube, u, and tube inside diameter, d_i, must be specified. Similarly, the Reynolds and Prandtl

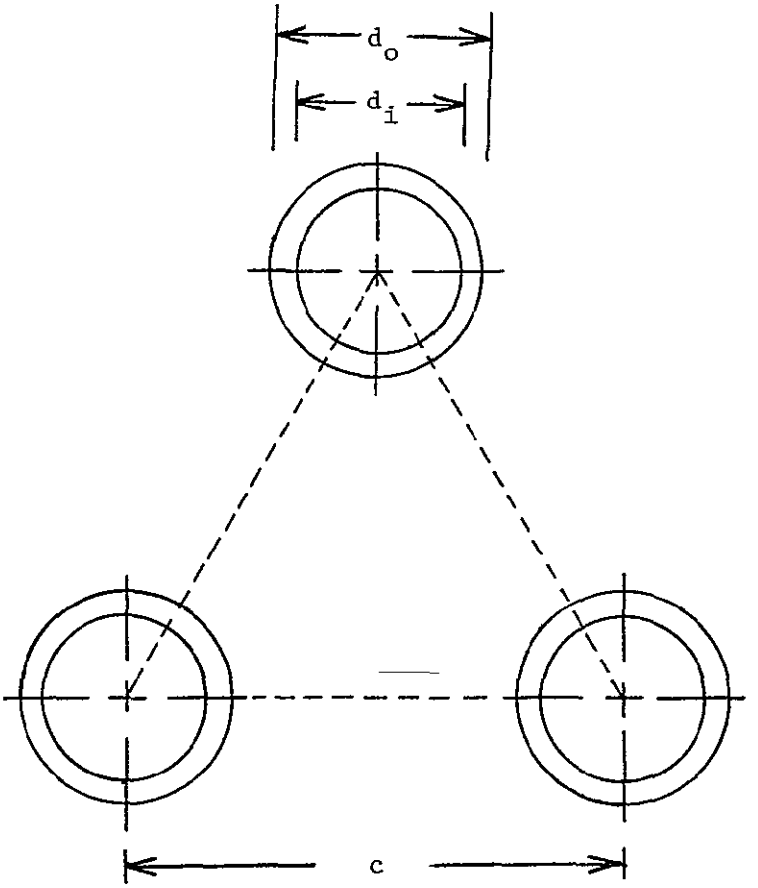

Fig. 3.4 Heat Exchanger Tube
Triangular Lattice Arrangement

numbers for the $NaF - NaBF_4$ salt are

$$Re' = \frac{\rho' u' d_{eq}}{\mu'} \tag{3.13}$$

$$Pr' = \frac{C_p' \mu'}{K'} \tag{3.14}$$

where primes are used to distinguish the salt from the gas mixture.

The convective heat transfer coefficients for the mixture and salt are estimated from the Dittus-Boelter equation[7]

$$h_i = 0.023 \frac{K}{d_i} (Pr)^{0.4} (Re)^{0.8} \tag{3.15}$$

$$h_o = 0.023 \frac{K'}{d_{eq}} (Pr')^{0.4} (Re')^{0.8} \tag{3.16}$$

The overall heat transfer coefficient for flows on each side of a tube is given by[8]

$$U = \frac{1}{\frac{1}{h_o} + \frac{d_o}{2 K_T} \ln \frac{d_o}{d_i} + \frac{d_o}{h_i d_i}} \tag{3.17}$$

where K_T is the thermal conductivity of the tube material.

The total cross sectional area of tubing required is

$$A_t = \frac{\dot{m}}{\rho u} \tag{3.18}$$

or, the number of tubes required is

$$n_t = \frac{4A_t}{\pi d_i^2} \tag{3.19}$$

It is then possible to compute the heat exchanger exit temperature on the salt side from

$$T_5 = T_4 + \frac{Q_{PHX}}{c_p' \rho' u' A_f' n_t} \tag{3.20}$$

The log mean temperature difference for counterflow is given by[8]

$$\Delta T_m = \frac{(T_1 - T_5) - (T_2 - T_4)}{\ln \frac{T_1 - T_5}{T_2 - T_4}} \tag{3.21}$$

from which the heat transfer surface area is determined from

$$S = \frac{Q_{PHX}}{U \Delta T_m} \tag{3.22}$$

and the length of the tubes is then

$$L_t = \frac{S}{n_t \pi d_o} \tag{3.23}$$

The volume of helium-UF_6 mixture in the tubes is

$$V_t = n_t \frac{\pi d_i^2}{4} L_t \tag{3.24}$$

Additional UF_6 and helium reside in the inlet and exit plenums of the heat exchanger. The additional volume is calculated from

$$V_p = n_t L_p \frac{\pi d_i^2}{4 \sigma} \tag{3.25}$$

where L_p is the additional length of the heat exchanger due to the plenums and was taken to be 0.3048 m (1 ft.). Each tube flow area opens up to two corresponding triangular areas so that

$$\sigma = \frac{\pi d_i^2}{2\sqrt{3}\, c^2} \tag{3.26}$$

Therefore, the mass of UF_6 and helium in the heat exchanger is

$$m = \rho(V_t + V_p) \tag{3.27}$$

of which $\frac{233}{347} \frac{\rho^{UF_6}}{\rho}$ is the mass of U^{233}. The salt volume in the heat exchanger is

$$V' = n_t A_f L_t \tag{3.28}$$

and the salt mass is

$$m' = \rho' V' \tag{3.29}$$

The pressure drop has two components. The first is the pressure drop due to the change in flow areas between the plenums and tubes. This drop is given by[9]

$$\Delta P_p = \frac{\rho u^2}{2} (K_c + K_e) \tag{3.30}$$

where K_c and K_e are contraction and expansion coefficients which are functions of σ and the Reynold's number. Reference 9 gives values for K_c and K_e.

The second component is the friction loss in the tubing for the friction factor, f_w. For implementation in a computer code, the Colebrook equation is used[9]:

$$\frac{1}{f_w^{1/2}} = -2 \text{Log}_{10}\left[\frac{\varepsilon/d_i}{3.70} + \frac{2.51}{\text{Re } f_w^{1/2}}\right] \tag{3.31}$$

where ε is a roughness parameter and is 1.524×10^{-6}m (5×10^{-6} ft.) for drawn tubing. f_w is solved iteratively and is used to compute the tube pressure drop

$$\Delta P_t = f_w \frac{\rho u^2}{2} \frac{L}{d_i} \tag{3.32}$$

The compressor power for circulating the UF_6-helium mixture is

$$Q_{comp} = \frac{\dot{m} C_p T_2}{\eta_c} \left[\left(\frac{P_3}{P_2}\right)^{\frac{\gamma-1}{\gamma}} - 1\right] \tag{3.33}$$

where η_c is the compressor efficiency and γ is the mixture specific heat ratio.

Each heat exchanger and superheater were modeled in the same manner. However, pumps are used in the remaining loops. The pump power is calculated from

$$Q_{pump} = \frac{\dot{m} \Delta P}{\eta_p \rho} \tag{3.34}$$

where ΔP is the pressure drop across the pump, and η_p is the pump efficiency.

The boiler is treated differently because water changes into steam over the length of the boiler tubes. Therefore, the boiler is split into two regions for the purposes of analysis. The first region is the subcooled liquid region where the Dittus-Boelter equation is used to calculate the convective heat-transfer coefficient. The second region consists of saturated liquid changing to saturated steam. In this region, the Dittus-Boelter equation cannot be used so a heat-transfer coefficient of $5.68 \times 10^4 \ \frac{W}{m^2 K} \ \left(10^4 \ \frac{Btu}{ft^2 hr F}\right)$ was assumed.

C. Thermodynamic Cycle Analysis

Using the analysis from the previous section, a computer code was written to analyze the breeder power plant cycle. A separate code supplied by Professor R. W. Carlson of the Georgia Institute of Technology was used to obtain the efficiency of the steam cycle.

Several constraints are imposed on temperatures and velocities in the system by the following considerations:

(1) Uranium inventory in the primary heat exchanger cannot be excessive,

(2) Compressor and pump powers must be kept low for good power plant efficiencies,

(3) The breeding salt must be kept above 772°K and the coolant salt must be kept above 658°K to avoid solidification.

Figure 3.5 shows the power plant schematic. The steam cycle consists of high pressure and low pressure turbines, a condenser operating at 1 psia, five feedwater heaters operating at 7, 41, 141, 371, and 820 psia, a boiler operating at 1600 psia and a superheater in which steam is heated to 670°K.

The work used in circulating the various fluids (excluding water) through the heat exchangers is 13.1 MW which is multiplied by 1.5 to account for pressure losses in the piping. An overall plant efficiency of 39.3% is obtained for a steam cycle efficiency of 40.4%.

D. Summary

The design parameters for the breeder reactor are summarized in Table 3.1 while the power plant parameters are summarized in Table 3.2 Temperatures and velocities in the loop are shown in Fig. 3.5.

The critical parameters of interest are the power plant efficiency, reactor thermal power, and the U^{233} inventory. They are 39.3%, 1074 MWt, and 104.8 kg, respectively. In computing the uranium inventory, the uranium in the piping and reprocessing system was not included.

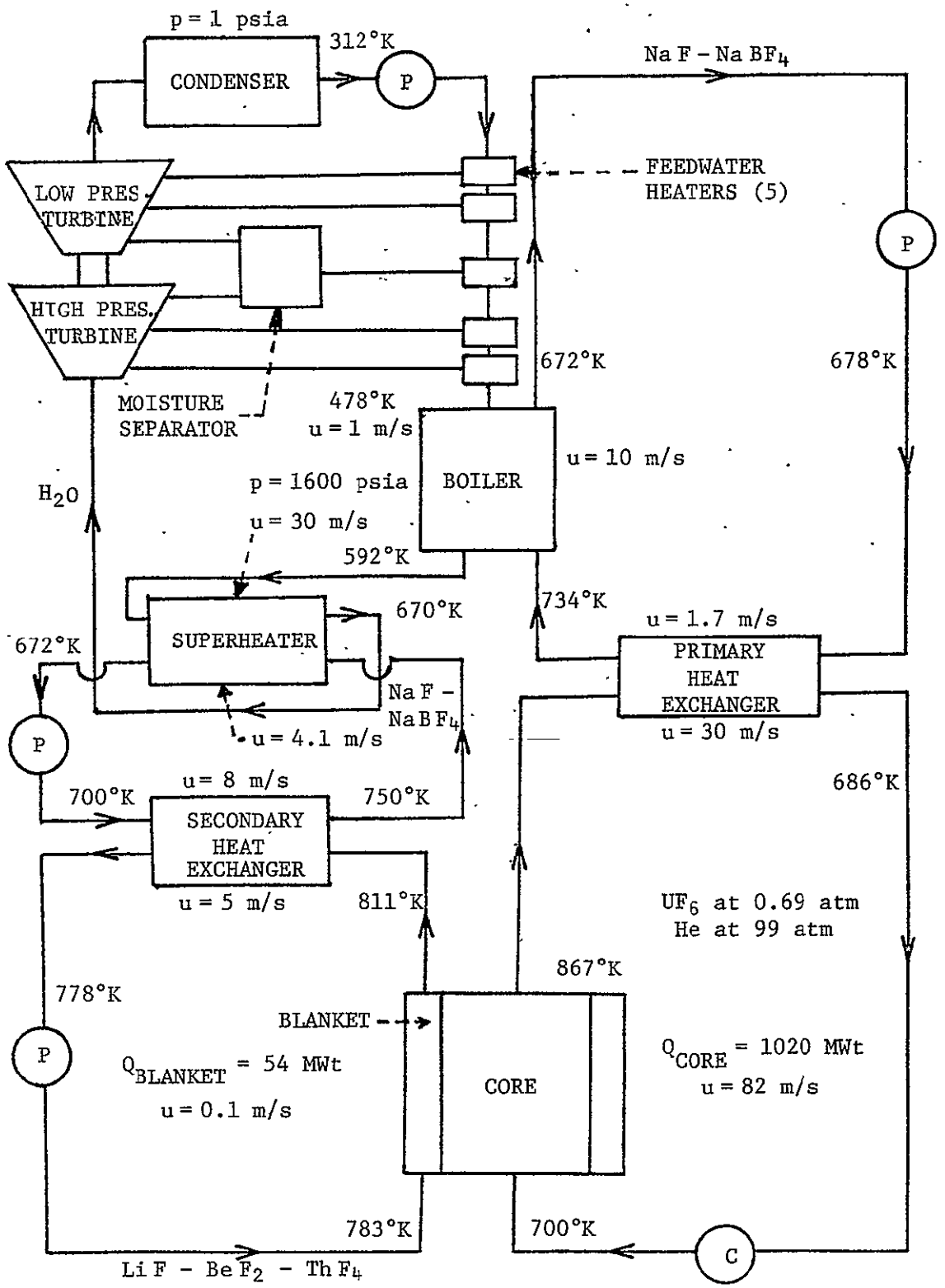

Fig. 3.5 UF_6 Breeder Reactor Power Plant Schematic

Table 3.1. UF_6BR Reactor Design Data Summary

Core Composition

$U^{233}F_6$ partial pressure	=	0.69 atm.
He partial pressure	=	99 atm.
Volume percent of UF_6 + He	=	70%
Volume percent of Be	=	30%

Dimensions

Geometry	=	Cylindrical
Core Diameter	=	2.0 m
Core Height	=	6.0 m
Thickness of Breeding Blanket	=	0.6 m
Thickness of Axial Be Reflector	=	0.5 m
Thickness of Radial Be Reflector	=	0.2 m
Thickness of Steel Pressure Shell	=	0.2 m
Reactor Diameter	=	4.0 m
Reactor Height	=	7.4 m
Core Volume	=	18.85 m^3

Neutronics

Breeding Ratio	=	1.0022
Be to U^{233} Atom Density Ratio	=	8111
Average Core Thermal Flux	=	1.34×10^{15} n/cm^2-sec
Average Core Fission Density	=	1.68×10^{18} fissions/m^3 - sec
Average Core Power Density	=	5.4×10^7 W/m^3
Peak to Average Ratio of Radial Fission Densities	=	1.78
Peak to Average Ratio of Axial Fission Densities	=	1.24
Percent Fission in Blanket	=	0.08%
Average Thermal Flux in Blanket	=	5.3×10^{13} n/cm^2-sec

Table 3.1. UF_6BR Reactor Design Data Summary
(continued)

Masses

U^{233} Mass in Core	=	32.8 kg
UF_6 Mass in Core	=	48.8 kg
Be Mass in Core	=	10,300 kg
Th^{232} Mass in Blanket	=	44,465 kg

Reactor Heat Transfer and Thermal Hydraulics

Total Reactor Power	=	1074 MWt
Core Power	=	1020 MWt
Blanket Power	=	54 MWt
Core Region:		
Inlet Temperature	=	700°K
Exit Temperature	=	867°K
Average UF_6 + He Velocity	=	82 m/sec
Mass Flow Rate of UF_6 + He	=	$1.8 \times 10^3 \frac{kg}{sec}$
Blanket Region:		
Inlet Temperature	=	783°K
Exit Temperature	=	811°K
Average Salt Velocity	=	8.5×10^{-2} m/sec
Mass Flow Rate of Salt	=	$1.42 \times 10^3 \frac{kg}{sec}$

Table 3.2. UF_6BR Power Plant Design Data Summary

Number of Loops = 2

Power Plant Efficiency = 39.3%

Uranium Mass:

Core = 32.8 kg

Primary Heat Exchangers = 72.0 kg

Total = 104.8 kg (Excluding U^{233} in piping and reprocessing system)

Electric Power Output = 426 MWe

UF_6 - He Loop Parameters:

Primary Heat Exchanger:

Number of Tubes = 63595

Inner Tube Diameter = 7.745×10^{-3} m

Outer Tube Diameter = 9.525×10^{-3} m

Pitch to Diameter Ratio = 1.3

Length of Tubes = 3.81 m

Mass Flow Rate = 1.8×10^{3} kg/sec

Compressor Power = 8.6 MW

Na F - Na BF_4 Primary Loop Parameters

Boiler:

Number of Tubes = 3585

Inner Tube Diameter = 1.4148×10^{-2} m

Outer Tube Diameter = 1.5875×10^{-2} m

Pitch to Diameter Ratio = 1.6

Length of Tubes = 7.95 m

Mass Flow Rate = 1.30×10^{4} kg/sec

Pump Power = 3.7 MW

Table 3.2. UF_6BR Power Plant Design Data Summary (continued)

$LiF - BeF_2 - ThF_4$ Loop Parameters

Secondary Heat Exchanger:

Number of Tubes	=	886
Inner Tube Diameter	=	7.745×10^{-3} m
Outer Tube Diameter	=	9.525×10^{-3} m
Pitch to Diameter Ratio	=	1.3
Length of Tubes	=	4.09 m

Mass Flow Rate = $1.42 \times 10^3 \frac{kg}{sec}$

Pump Power = 0.37 MW

$NaF - NaBF_4$ Secondary Loop Parameters

Superheater:

Number of Tubes	=	628
Inner Tube Diameter	=	1.4148×10^{-2} m
Outer Tube Diameter	=	1.5875×10^{-2} m
Pitch to Diameter Ratio	=	1.3
Length of Tubes	=	11.6 m

Mass Flow Rate = 844.5 kg/sec

Pump Power = 0.46 MW

Steam Cycle Parameters

Condenser Pressure = 1 psia

Boiler Pressure = 1600 psia

Feedwater Heater Pressures:

No. 1	=	7 psia
No. 2	=	41 psia
No. 3	=	141 psia
No. 4	=	371 psia
No. 5	=	820 psia

Maximum Steam Temperature = 670°K

Steam Cycle Efficiency = 40.4%

References for Chapter 3

1. Meneley, D. A., et al., "Mach-1, A One-Dimensional Diffusion Theory Package," ANL-7223 (1966).

2. Bondarenko, I. I., Ed., Group Constants for Nuclear Reactor Calculations. Consultants Bureau, New York (1964).

3. Grimes, W. R., "Molten Salt Reactor Chemistry," Vol. 8, Nuclear Applications and Technology 8 (February 1970).

4. Garber, D. I., and Kinsey, R. R., "Neutron Cross Sections," 3rd Edition, Vol. II, BNL-325 (January 1976).

5. Hughes, D. J., and Schwartz, R. B., "Neutron Cross Sections," 2nd Edition, BNL-325 (July 1958).

6. Westcott, C. H., "Effective Cross Section Values for Well-Moderated Thermal Reactor Spectra," 3rd Edition, AECL-1101 (November 1960).

7. El-Wakil, M. M., Nuclear Heat Transport, International Textbook Company (1971).

8. Steam/Its Generation and Use, Babcock and Wilcox Company (1975).

9. Rust, J. H., "Nuclear Power Plant Engineering," Unpublished Notes, Georgia Institute of Technology.

4. UF_6 ACTINIDE TRANSMUTATION REACTOR POWER PLANT

One consequence of the large scale use of fission reactors for production of energy is the accumulation of radioactive wastes. The spent fuel discharged from a LWR consists of structural materials, unfissioned uranium, converted plutonium, other actinides, and fission products. The ratio of these components by weight is as follows:

structural	:	uranium	:	plutonium	:	fission products	:	other actinides
= 256	:	1023	:	9	:	36	:	1

Although the other actinides are the smallest component, they are very important because of their long half lives. After 10^3 years most of the other materials will have decayed to stable isotopes; these actinides will still be radioactive and may present significant health hazards in the future.

Steinberg,[1,2] proposed use of neutron induced transmutation for the disposal of long-lived fission wastes. Under such a scheme, these fission wastes are separated from gross wastes during fuel reprocessing, and converted into forms suitable for insertion into a neutron field, e.g., a fission reactor. In this neutron environment, these nuclides will be converted, or fissioned into short-lived isotopes. The resulting wastes will then be stored for a short period until a harmless activity level is reached. This method allows the possibility of reducing long-lived fission waste inventory at a faster rate than natural decay, and hence of reducing the long-term risk of exposure to radioactivity.

The first step in the actinide transmutation scheme is the chemical extraction of actinides from the bulk wastes. The Oak Ridge National Laboratory is currently performing a fairly extensive study in this area.[3]

Since no chemical extraction process is 100% efficient, there will always be a small quantity of actinides left unextracted in the bulk wastes. What, then, should the extraction efficiency be so that the risk associated with the unextracted actinides be considered acceptable? Radioactive material has been present in the earth's crust and surface at all times in the form of uranium and thorium minerals and ores. Claiborne[4] compared the long-term hazard of actinides for different extraction efficiencies with the calculated hazard of pitchblende (~ 70% U), the most radioactive mineral, and with the calculated hazard of high grade uranium ore (~ 0.2% U). He showed that it is possible to reduce the hazard (after 1000 years) associated with high-level wastes to values comparable to those from high grade uranium ore provided that 99.99% of Pu, 99.9% of U, Am, Cm, and ^{129}I and 95% of the Np are recovered from LWR fuels.

After the actinides are extracted from the bulk wastes, they are placed into a reactor for irradiation.

Claiborne[5] performed detailed calculations on actinide transmutation in LWR's. Assuming separation efficiencies of 99.5% and 99.9% for U, Pu, and the other actinides, the actinides (no U and Pu) are recycled back into a PWR for many cycles. A thermal flux of 3×10^{13} n/cm^2-sec was used. With this strategy the actinides are removed by two paths. One, they are converted to plutonium and uranium, and are then extracted during chemical reprocessing. Most of the plutonium extracted is Pu^{238}, formed by the reaction Np^{237} (n,γ) $Np^{238} \xrightarrow{\beta-} Pu^{238}$. A small quantity of Pu^{239} is also formed. This mix of Pu^{238} - Pu^{239} can be used as reactor fuel just like Th^{232} - U^{233}. The other path is for the actinides to be fissioned directly inside the PWR. The total

actinide inventory approaches an equilibrium value that is several times that produced in the first cycle (1.6 times for Np, 1.2 times for Am, 9.0 times for Cm). Np reaches equilibrium after ~ 4 to 5 recycles, Am after ~ 2 to 3 recycles, and Cm after 50 to 60 recycles. Claiborne also concluded that the introduction of actinide wastes perturbs the reactor very slightly. Similar results have been obtained at Battelle Northwest Laboratories.[6]

Beaman et al.[7] performed actinide transmutations calculations for an LMFBR. His scheme consisted of an LMFBR recycling the actinide wastes produced by itself and 3 BWR's. The actinides are removed in 2 ways: (1) by conversion to Pu, and (2) by fission. Equilibrium concentrations of recycled actinides in a LMFBR are qualitatively similar to the LWR case. In Np^{237} equilibrium is reached after about 14 recycles; for Cm about 30 recycles. An equilibrium concentration of the actinide mixture is achieved after approximately 26 recycles. The equilibrium inventory is 3.1 times the quantity charged in the first cycle. Introduction of the actinide wastes into an LMFBR have a very slight effect on other reactor characteristics. Similar studies were done by Oliva, et al.[8]

These schemes for recycling actinide wastes in LWRs and LMFBRs are not satisfactory in two respects. First, since only a small number of reactors are serviced by a LWR or a LMFBR, many transmuters (LWRs and/or LMFBRs) will be required. Second, even then it will require very long irradiation times (> 20 recycles) to reach equilibrium. This gives rise to the idea of designing of a special burner reactor capable of servicing a large number of LWRs and operating at high fluxes to shorten the irradiation time.

One candidate for this special burner reactor is the gas core reactor. Because of the low fissile fuel inventory a high flux can be maintained. Continuous reprocessing of the fuel means better fuel economy and the possibility of continuous irradiation.

Clement and Rust[9] performed actinide burnup calculations in a plasma core actinide transmutation reactor. The calculations assumed 100% extraction efficiency for U, Pu and other actinides and the reactor was designed to dispose of actinide wastes from 27 LWRs. Due to constraints imposed by the high temperature uranium plasma, the neutron flux in the actinide region was only 7×10^{12} n/cm^2-sec. Approximate equilibrium actinide inventory is reached after 13 recycles, and the equilibrium actinide inventory is about 2.6 times the initial actinide loading.

This study continues the previous investigation; however, a uranium hexafluoride fueled reactor was investigated for its potential as a gas core actinide transmuter (UF_6ATR).

A. Neutronics

A flow chart of the computation strategy is shown in Fig. 4.1. The ABBN[10] cross section set is used for imput into the MACH-I[11] code. Cross sections for Np^{237}, Am^{241}, Am^{243}, Cm^{244} are generated from ENDF/III by the code MC^2.[12] Cross sections for the He and fluorine are generated from the cross section data from BNL-325.[13,14] The detailed formalism is described in Chapter 3. The depletion and decay of the actinide isotopes are calculated by the code ORIGEN.[15]

The cylindrical reactor configuration is shown in Fig. 4.2. Since MACH-I is a one-dimensional code, the infinite slab and cylinder geometries were used to model the axial and radial neutronics of the reactor. The two calculations were coupled together by group dependent bucklings in

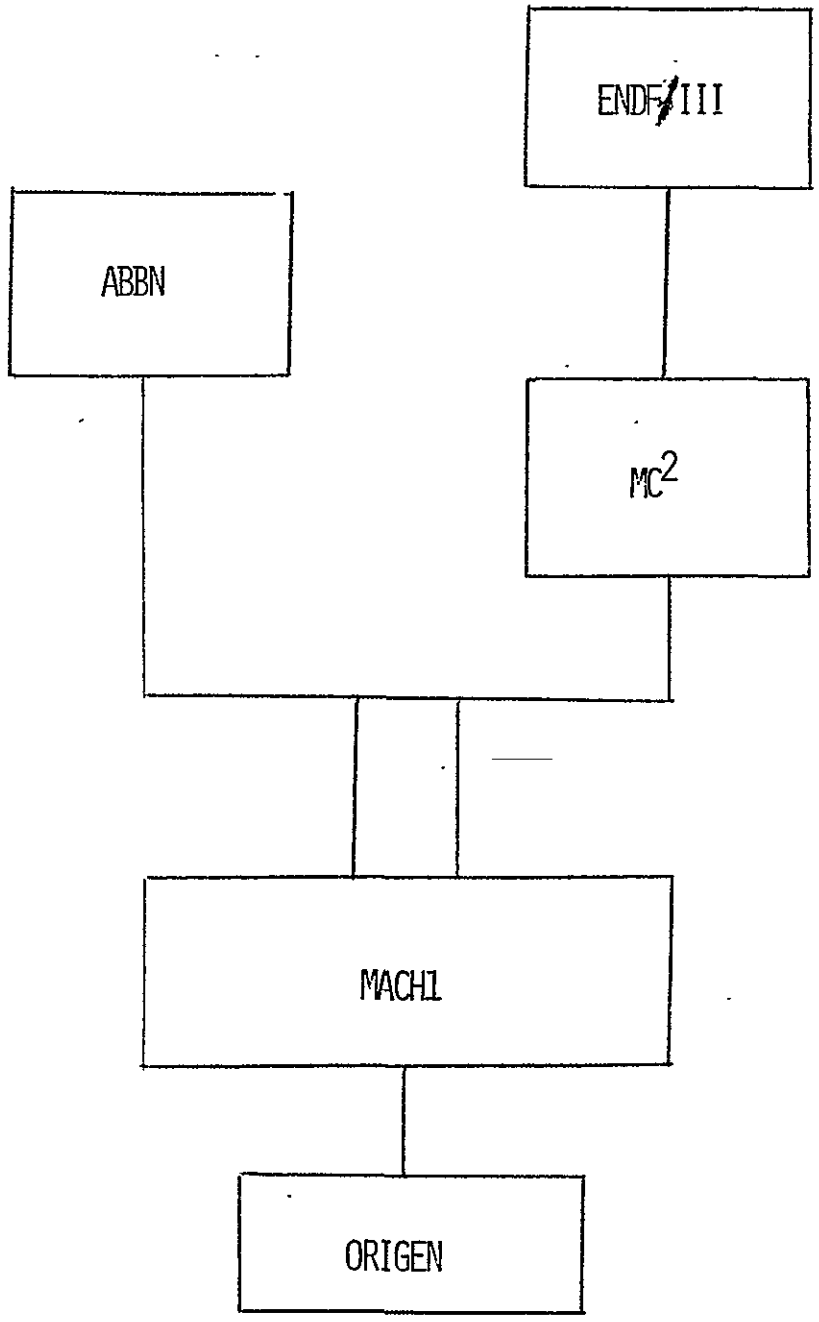

Fig. 4.1 Flowsheet of Nuclear Analysis Computation

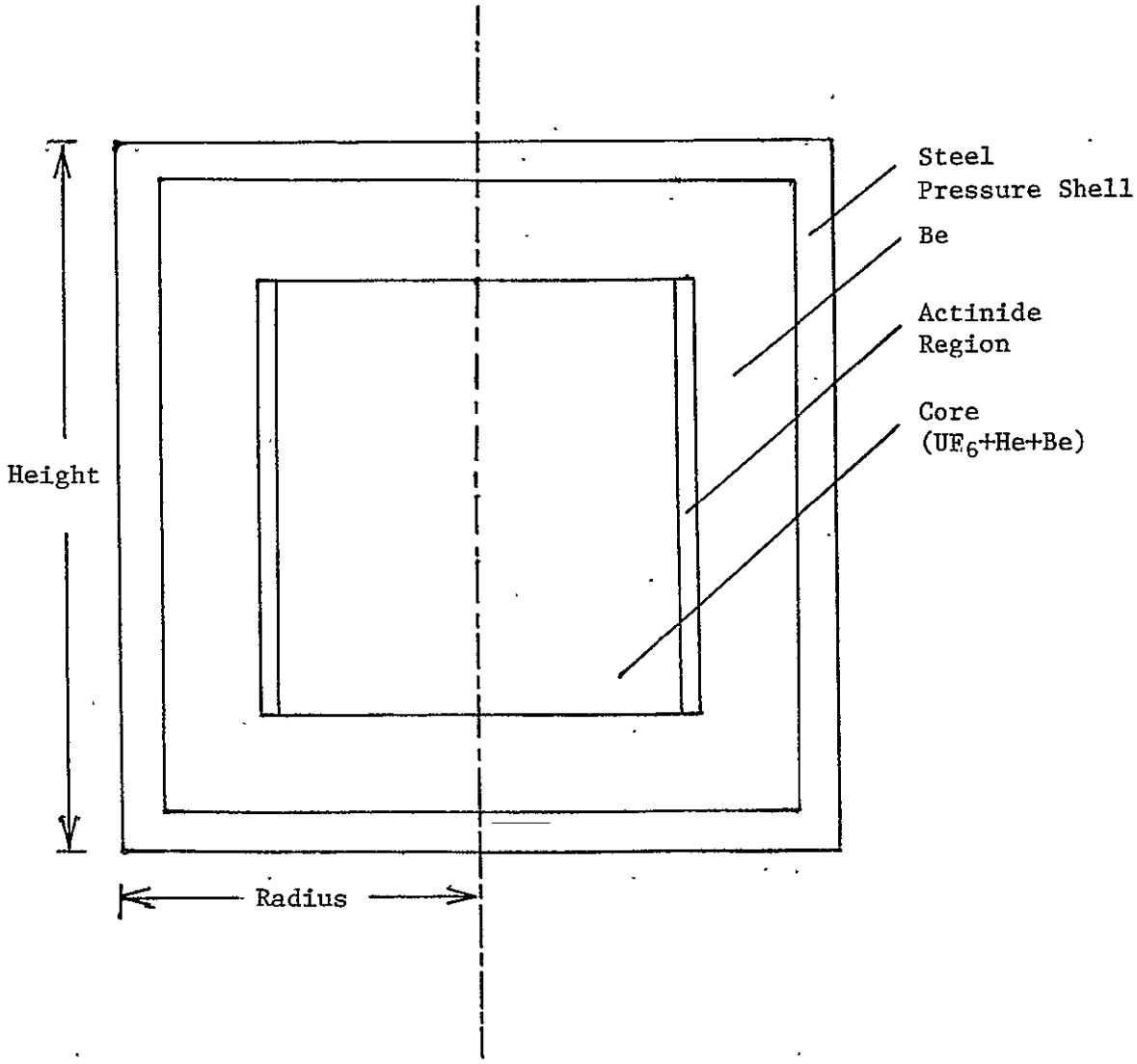

Fig. 4.2 Reactor Configuration of UF_6ATR

the axial and radial directions. Several iterations were required before a consistent set of axial and radial bucklings was obtained.

The core consists of a He-UF_6 mixture flowing through a beryllium matrix. Addition of helium greatly improves the heat transfer characteristics of the gas, since UF_6 is a very poor heat transfer agent. The neutron spectrum is thermalized by a beryllium matrix in the core. Surrounding the core is an actinide blanket region consisting of He cooled, zirconium clad actinide fuel rods. The actinides are assumed to be present as oxides. Only the principal actinides, Np^{237}, Am^{241}, Am^{243}, and Cm^{244} are included. The actinide blanket is surrounded by a beryllium reflector and a steel pressure shell. Characteristics of the reactor are summarized in Section 4D.

B. Heat Transfer and Thermal Hydraulics

The analysis for the heat exchangers is the same as that described in Section 3.B. The heat transfer for the actinide transmuter reactor is unique in that the core power decreases from 504 MWt at beginning of life to 180 MWt at the end of life of the first core. This is due to buildup of fissile plutonium in the actinide blanket. Therefore, the flux in the actinide region and the core has to be decreased to maintain the same volumetric heat generation rate in the actinide rods. The consequence is that a time dependent study is needed. However, in this study, heat transfer calculations were only made for beginning-of-life conditions.

C. Thermodynamic Cycle Analysis

Figure 4.3 shows the schematic for the actinide power plant at beginning-of-life conditions. The overall plant efficiency is 39.2%.

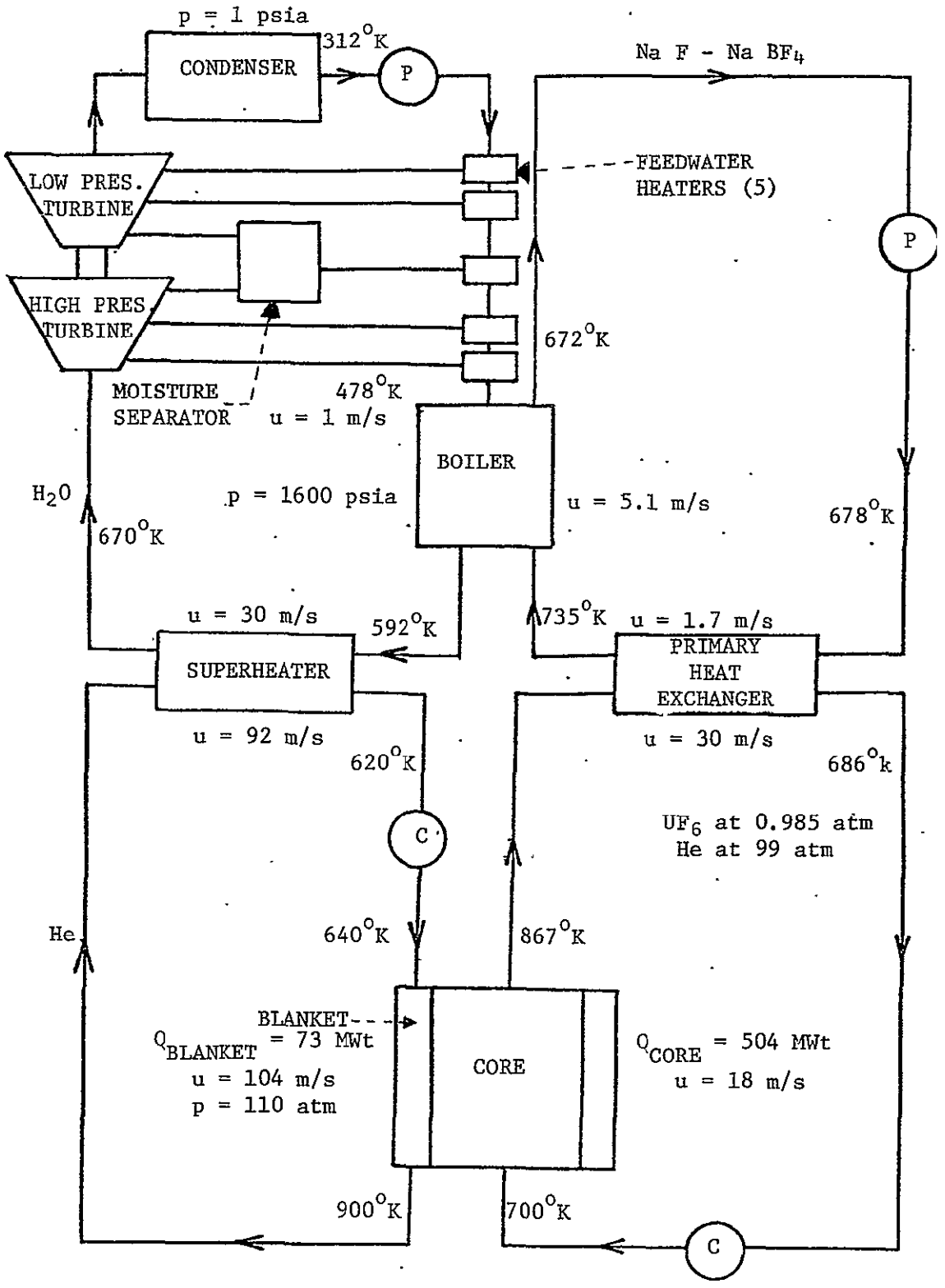

Fig. 4.3 UF_6 Actinide Transmutation Reactor Power Plant
(Beginning-of-Life Conditions)

D. Summary

Characteristics of the beginning-of-life UF_6ATR are shown in Table 4.1 By virtue of the low density of the U^{233} fuel, an average flux of 4×10^{14} n/cm^2 sec can be reached in the core, and an average flux of 1.3×10^{14} n/cm^2 sec can be reached in the actinide region. This high actinide region flux will bring about a very rapid transmutation of the actinides. However, as the quantity Pu^{239} and other fissile isotopes increases, the flux in the actinide region must be lowered to stay within the safety limits of the actinide rods. Thus the flux in the actinide region must be gradually lowered, as the inventory of fissile isotopes gradually builds up so as to maintain an acceptable volumetric heat generation rate (q''') in the actinide region.

The transmutation strategy used for the present study is shown in Fig. 4.4. Each LWR is loaded with 88 metric tonnes of uranium (3.3% U^{235}) and operated at a constant and average specific power of 30 MW/MTU. At the end of 1100 days, a burnup of 33,000 MWD/MTU is reached. The fuel is discharged from the reactor and cooled for 160 days. Next, the spent fuel is reprocessed during which 100% of Np, Am, Am, and higher actinides are separated from the bulk wastes. The concentrations of these actinides are calculated by ORIGEN. These actinides are then manufactured into fuel rods and charged into the UF_6ATR. These actinides are irradiated for 1100 days in the UF_6ATR until an average burnup of 100,000 MWD/MTA is attained. The actinide rods are discharged from the UF_6ATR and undergo reprocessing during which fission products and converted U and Pu are extracted. These actinides are mixed with a batch of freshly produced actinides from the LWRs and manufactured into oxide rods and charged back into the UF_6ATR. In the present calculation the UF_6ATR services 14 PWRs,

Table 4.1 UF_6ATR Reactor Design Data Summary
(Beginning-of-Life)

Core Composition

U^{233} F_6 partial pressure	=	0.985 atm.
He partial pressure	=	99 atm.
Volume percent of UF_6 + He	=	83.3%
Volume percent of Be	=	16.7%

Actinide Composition

Actinide Dioxide	=	28 volume %
Zirconium Clad	=	7 volume %
Helium Coolant	=	65 volume %
Actinides		
Np^{237}	=	74 atomic %
Am^{241}	=	7 atomic %
Am^{243}	=	14 atomic %
Cm^{244}	=	5 atomic %

Dimensions

Geometry = Cylindrical
Core Diameter = 2.74 m
Core Height = 3.0 m
Thickness of Actinide Blanket = 1.32×10^{-2} m
Thickness of Axial Be Reflector = 0.5 m
Thickness of Radial Be Reflector = 0,43 m
Thickness of Pressure Shell = 0.2 m
Reactor Diameter = 4.0 m
Reactor Height = 4.4. m
Core Volume = 17.7 m^3
Volume of Actinide Region = 0.343 m^3
Fuel Pins in Actinide Region

Fuel Pin Radius	=	2.175×10^{-3} m
Gap Thickness	=	1.5×10^{-4} m
Clad Thickness	=	3.5×10^{-4} m
Wire Wrap Diameter	=	1.42×10^{-3} m

Table 4.1 UF_6ATR Reactor Design Data Summary
(continued)

Neutronics

Type of Reactor = Thermal

Be to U^{233} Atom Density Ratio = 2660

Average Core Thermal Flux = 4.07×10^{14} n/cm^2-sec

Average Core Fission Density = 8.90×10^{17} fissions/m^3 sec

Peak to Average Ratio of Radial Fission Densities = 1.82

Peak to Average Ratio of Axial Fission Densities = 1.42

Percent Fissions in Actinide Blanket = 12.6%

Average Thermal Flux in Actinide Region = 1.26×10^{14} n/cm^2-sec

Masses

U^{233} Mass in Core = 52.5 kg

UF_6 Mass in Core = 78.2 kg

Actinide Mass = 800 kg (~ output from 14 LWRs)

Reactor Heat Transfer and Thermal Hydraulics

Total Reactor Power = 577 MWt

Core Power = 504 MWt

Actinide Region Power = 73 MWt

Core Region

- Inlet Temperature = 700°K
- Exit Temperature = 867°K
- Average UF_6 + He Velocity = 18 m/sec
- Mass Flow Rate = 1008 kg/sec
- Average Core Power Density = 28.5 MW/m^3

Actinide Region

- He Coolant Pressure = 110 atm.
- Inlet Temperature = 640°K
- Exit Temperature = 900°K
- Average He Velocity = 104 m/sec
- Mass Flow Rate = 54 kg/sec
- Average Power Density of Region = 210 MW/m^3

Table 4.1 UF_6ATR Reactor Design Data Summary
(continued)

Average q''' of Actinide Rod	=	760 MW/m^3
Average q''_w of Actinide Rod	=	0.83 MW/m^2
Average q' of Actinide Rod	=	11.3 kW/m

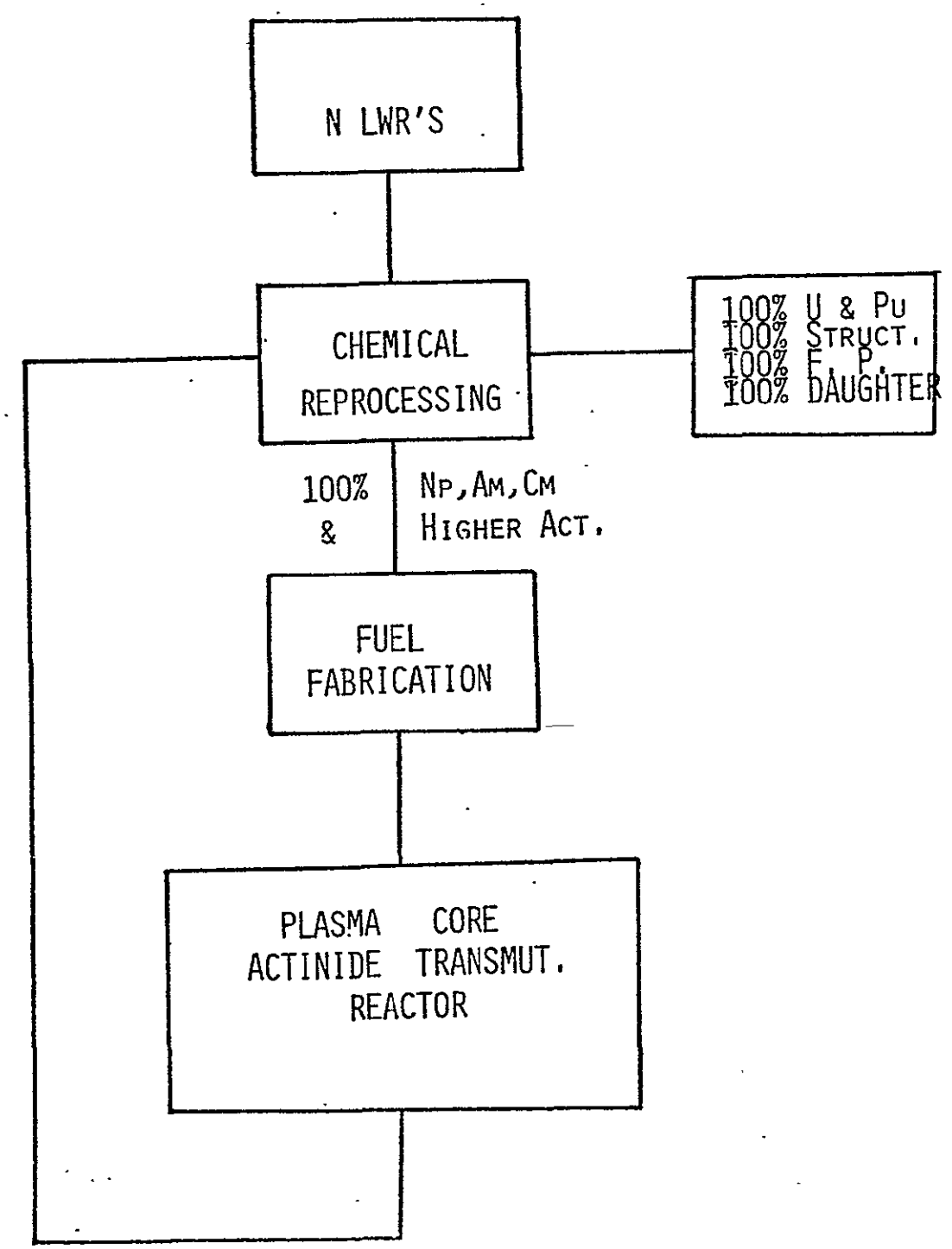

Fig. 4.4 Strategy for Actinide Transmutation

i.e., 800 kg of actinides per cycle. To maintain an acceptable volumetric heat generation rate (q''') in the actinide region, the flux must be varied as a function of time. To approximate this occurrence, a flux of 5.6×10^{13} n/cm^2-sec was used for the first 100 days and a flux of 1.6×10^{13} n/cm^2-sec for the rest of the 1100 day period. Approximate equilibrium is reached after 15 recycles. The equilibrium actinide inventory is about 2.3 times its initial loading. In the equilibrium cycle, about 10.8% of the actinides are fissioned and about 32.1% is removed by reprocessing. These results are shown in Table 4.2.

The UF_6ATR is capable of maintaining a flux of 10^{14} n/cm^2-sec in the actinide region; however, heat transfer limitations in the actinide region force the UF_6ATR to operate at a much lower flux. Assuming that the heat transfer problem in the actinide region can be solved, an ORIGEN calculation was performed for a UF_6ATR with a constant flux of 1.25×10^{14} n/cm^2-sec in the actinide region. The actinides were irradiated for 165 days. The results were compared with those of a typical low flux UF_6ATR case with 1100 days of irradiation in Table 4.3. As shown, the 2 cases are comparable, indicating that with a high flux of 1.25×10^{14} n/cm^2-sec it may be possible to cut the irradiation time by a factor of 6-7.

Table 4.4 summarizes the power plant parameters for beginning-of-life conditions. The power plant operates at 577 MWt with an efficiency of 39.2% and with 102.2 kg of U^{233} in the core and heat exchanger.

Table 4.2 Actinide Burnup in Uranium Hexafluoride Actinide Transmutation Reactor 1100 Days of Irradiation, 365 Days of Cooling, 730 Days of Reprocessing (100% Removal of U and Pu, F. P. and Daughters, and Fuel Fabrication, 14 PWRs Serviced (0.800 Metric Tonne of Actinides Charged per Cycle) THERM = 0.54227, RES = 0.375, FAST = 1.50, Φ(0-100 days) = 1.6×10^{13}.

Batch No.	Cycle No.														
	1	2	3	4	5	6	7	8	9	10	11	12	13	14	15
1	0.800	0.426	0.233	0.128	0.073	0.045	0.030	0.022	0.017	0.015	0.013	0.012	0.011	0.011	0.010
2		0.800	0.426	0.233	0.128	0.073	0.045	0.030	0.022	0.017	0.015	0.013	0.012	0.011	0.011
3			0.800	0.426	0.233	0.128	0.073	0.045	0.030	0.022	0.017	0.015	0.013	0.012	0.011
4				0.800	0.426	0.233	0.128	0.073	0.045	0.030	0.022	0.017	0.015	0.013	0.012
5					0.800	0.426	0.233	0.128	0.073	0.045	0.030	0.022	0.017	0.015	0.013
6						0.800	0.426	0.233	0.128	0.073	0.045	0.030	0.022	0.017	0.015
7							0.800	0.426	0.233	0.128	0.073	0.045	0.030	0.022	0.017
8								0.800	0.426	0.233	0.128	0.073	0.045	0.030	0.022
9									0.800	0.426	0.233	0.128	0.073	0.045	0.030
10										0.800	0.428	0.233	0.128	0.073	0.045
11											0.800	0.426	0.233	0.128	0.073
12												0.800	0.426	0.233	0.128
13													0.800	0.426	0.233
14														0.800	0.426
15															0.800
TOTAL	0.8	1.23	1.46	1.59	1.66	1.69	1.71	1.73	1.74	1.76	1.77	1.78	1.79	1.80	1.81

Table 4.3 Comparison of Low Flux UF_6ATR and High Flux UF_6ATR for the First Cycle.

Avg. flux	$5.60 \times 10^{13} - 1.60 \times 10^{13}$	1.25×10^{14}
Irradiation time	1100 days	165 days
Burnup	59,900 MWD/MTA	47,800 MWD/MTA
% Actinides fissioned	6.0%	5.2%
% Actinides removed by reprocessing	32.3%	27.9%

Table 4.4 UF_6ATR Power Plant Design Data Summary
(Beginning-of-Life)

Number of Loops = 1

Power Plant Efficiency = 39.2%

Uranium Mass:

- Core = 52.5 kg
- Primary Heat Exchanger = 49.7 kg
- Total = 102.2 kg (Excluding U^{233} in piping and reprocessing system)

Electric Power Output = 226 MWe

UF_6 - He Loop Parameters:

Primary Heat Exchanger:

- Number of Tubes = 61496
- Inner Tube Diameter = 7.74×10^{-3} m
- Outer Tube Diameter = 9.525×10^{-3} m
- Pitch to Diameter Ratio = 1.3
- Length of Tubes = 3.81 m

Mass Flow Rate = 1015 kg/sec

Compressor Power = 4.73 MW

NaF - $NaBF_4$ Loop Parameters:

Boiler:

- Number of Tubes = 3535
- Inner Tube Diameter = 1.4148×10^{-2} m
- Outer Tube Diameter = 1.5875×10^{-2} m
- Pitch to Diameter Ratio = 1.6
- Length of Tubes = 9.19 m

Mass Flow Rate = 6308 kg/sec

Pump Power = 0.66 MW

He Coolant Loop Parameters

Superheater:

- Number of Tubes = 994
- Inner Tube Diameter = 1.4148×10^{-2} m
- Outer Tube Diameter = 1.5875×10^{-2} m
- Pitch to Diameter Ratio = 1.3
- Length of Tubes = 9.95 m
- Mass Flow Rate = 54 kg/sec
- Compressor Power = 2.42 MW

Table 4.4 UF_6ATR Power Plant Design Data Summary
(continued)

Steam Cycle Parameters

Condenser Pressure = 1 psia

Boiler Pressure = 1600 psia

Feedwater Heater Pressures:

No. 1 = 7 psia

No. 2 = 41 psia

No. 3 = 141 psia

No. 4 = 371 psia

No. 5 = 820 psia

Maximum Steam Temperature = $670^{o}K$

Steam Cycle Efficiency = 40.4%

References for Chapter 4

1. Steinberg, M., Wotzak, G. and Manowitz, B., "Neutron Burning of Long-Lived Fission Products for Waste Disposal," BNL-8558 (September 1964).

2. Gregory, M. V., and Steinberg, M., "A Nuclear Transformation System for Disposal of Long-Lived Fission Product Waste in an Expanding Nuclear Power Economy," BNL-11915 (November 1967).

3. Blomeke, J. O., "A Program to Establish the Technical Feasibility and Incentives for Partitioning," NR-CONF-001, Proceedings of Nuclear Regulatory Commission Workshop (June 1976).

4. Claiborne, H. C., "Effect of Actinide Removal on the Long-Term Hazard of High-Level Waste," ORNL-TM-4724 (January 1975).

5. Claiborne, H. C., "Neutron-Induced Transmutation of High-Level Radioactive Waste," ORNL-TM-3964 (December 1972).

6. Schneider, K. J., and Platt, A. M., "High-Level Radioactive Waste Management Alternative," BNWL-1900, Battelle Pacific Northwest Laboratories (1974).

7. Beaman, S. L., and Aitken, E. A., "Feasibility Studies of Actinide Recycling in LMFBRs as a Waste Management Alternative," General Electric Company.

8. Oliva, G., Palmiotti, G., Salvatores, M., and Tondinelli, L., "Elimination of Transuranium Elements by Burnup in a Power Fast Breeder Reactor," Nuclear Science and Engineering 37 (March 1978).

9. Clement, J. D., and Rust, J. H., "Analysis of the Gas Core Actinide Transmutation Reactor (GCATR)," NASA-GRANT-NSG-1288 (September 1977).

10. Bondarenko, I. I., Ed., Group Constants for Nuclear Reactor Calculations, Consultants Bureau, New York (1964).

11. Meneley, D. A., et al., "MACH-I, A One-Dimensional Diffusion Theory Package," ANL-7223 (1966).

12. Toppel, B. J., Rago, A. L., and O'Shea, D. M., "MC^2 - A Code to Calculate Multigroup Cross Sections," ANL-7318 (1967).

13. Garber, D. I., and Kinsey, R. R., "Neutron Cross Sections," 3rd Edition, Vol. II, BNL-325 (January 1976).

14. Hughes, D. J., and Schwartz, R. B., "Neutron Cross Sections," 2nd Edition, BNL-325 (July 1958).

15. Bell, M. J., "ORIGEN - The ORNL Isotope Generation and Depletion Code," ORNL-4628 (May 1973),

5. CONCLUSIONS AND RECOMMENDATIONS

This report shows that gas core reactors can be very versatile in terms of power, temperature, and application. Four types of systems were studied: plasma core breeder, plasma core actinide transmuter, UF_6 breeder, and UF_6 actinide transmuter.

In addition to breeding and transmuting actinides, the plasma core reactor can serve as a high temperature source for MHD power conversion. For a reactor exit temperature of 4000°K, a power plant employing a ternary cycle consisting of a MHD generator, gas turbine, and steam cycle with a high temperature regenerator may have an efficiency as high as 70%. However, great advances in materials technology are necessary for the development of this system. If the reactor exit temperature is decreased to 3000°K, the power plant efficiency is decreased to 63%, but materials requirements would be considerably lessened. For exit temperatures considerably below 3000°K, advanced solid core reactors such as high temperature gas cooled reactors and liquid metal fast breeder reactors utilizing plasma or liquid metal MHD may become competitive with the gas core reactor - MHD system.

The on-going UF_6 reactor experiments at Los Alamos and the DOE coal-fired MHD program will provide valuable information on the feasibility of a plasma core reactor - MHD system. However, research and development of this system is a long term proposition so that studies are needed now to define the problems and to formulate a modest research program.

On the other hand, the UF_6 reactor would require only a modest extension of present day technology for its development. In particular, the UF_6 breeder reactor is an attractive near term application. The

on-line reprocessing systems for the core and blanket are major features of this system since they improve the fuel economy. Although no calculations were made on the reprocessing systems, they are qualitatively discussed in Appendix B. It is important to note that much of the molten salt technology is available from the molten salt breeder program, helium purification techniques are available from the high temperature gas-cooled reactor program, and UF_6 handling techniques are available from the gaseous diffusion program. It appears that no radically new technology is required for the development of this reactor.

Both this report and that of Ref. 1 show attractive features of the UF_6 breeder reactor. A comparison of the two systems is given in Table 5.1. The Los Alamos core design is unique in that seven cylindrical cells are arranged in a scalloped fashion while the Georgia Tech design uses a beryllium matrix. The former design allows a wider design range based on breeding ratio.

The Los Alamos reactor is designed for 200 MWt while the Georgia Tech reactor is designed for 1074 MWt. These powers are low but acceptable for use in developing countries where the power grid system is not well developed. Higher powers may be obtained by increasing the reactor pressure, but this introduces materials problems.

It is seen that the uranium inventories are small (less than 100 Kg for the Los Alamos system). Only the uranium inventory in the core and heat exchangers were estimated in the Georgia Tech design; but, if the uranium in the piping, circulators, and reprocessing system were added, the inventory would still be small compared to present day reactor power plants.

Table 5.1 Comparison of Los Alamos[1] and Georgia Tech UF_6 Breeder Power Plants

	Los Alamos[1]	Georgia Tech
Core Configuration	Seven Cylindrical Cells Scallop Design	Beryllium Matrix
Reactor Power, MWt	200	1074
UF_6 Partial Pressure, atm.	0.6	0.69
He Partial Pressure, atm.	99	99
Reactor Exit Temperature, °K	1225	867
Type of Cycle	Brayton - Steam	Superheated Steam
Power Plant Efficiency, %	36.6	39.3
U^{233} in Core, kg	45.0	32.8
U^{233} in Heat Exchangers, kg	4.0	72.0
Total U^{233} in Core and Heat Exchangers, kg	49.0	104.8
Total U^{233} in Entire System, kg	91.0	---

The efficiency was slightly higher for the Georgia Tech UF_6 breeder power plant due to the superheated steam cycle which has an efficiency of 40.4% compared to the 34% steam cycle employed in the Los Alamos design.

The main advantage of the Georgia Tech reactor versus the Los Alamos reactor is that the reactor exit temperature is much less for the Georgia Tech reactor. This is important because more UF_6 dissociates at higher temperatures creating fluorine which may cause corrosion problems. Operating at lower temperatures will also alleviate materials problems and increase the lifetime of the power plant. In addition, the Los Alamos design used a Brayton cycle which needs additional development work, whereas the superheated steam cycle is already used in most power plants.

Therefore, UF_6 breeder reactor power plants can be developed using present day or near term technology with-power plant efficiencies comparable or slightly greater than present day nuclear power plants and with a lower uranium inventory.

For the purpose of transmutation of actinides, gas core reactors can be designed to act as special burner reactors; servicing large numbers of LWRs and capable of maintaining a high flux. The plasma core actinide transmuter was designed to service 27 LWRs. Due to the many constraints imposed on the high temperature uranium plasma core, a low flux of 7×10^{12} n/cm^2-sec was used for the actinide region. As a result of the low flux, long irradiation times (~ 13 recycles) are required to attain equilibrium. These irradiation times were comparable to those obtained by Claiborne[2] and Beaman.[3] The uranium hexafluoride gas core

reactor can sustain higher fluxes (10^{14} n/cm^2-sec) in the actinide region. However, since the actinide region consisted of conventional solid actinide fuel rods, the buildup of fissile isotopes in this high flux actinide region posed severe heat transfer problems. As a result, the actinide region neutron flux must be decreased with increasing time to maintain a constant volumetric heat generation rate.

The heat transfer problems in the actinide region arise principally from the buildup of fissile plutonium isotopes. If the actinides can be used in a molten salt blanket, the converted plutonium isotopes can be continually removed and the heat transfer problems greatly alleviated.

One consequence of loading a large quantity of actinide nuclides into a transmuter is that the core and the actinide region become closely coupled. Hence, the criticality of the reactor is greatly affected by the composition change in the actinides. A detailed neutronic study of such a reactor will require a detailed set of cross sections for the actinides.

Again, the U^{233} inventory in the core and heat exchanger is seen to be low (102 kg for the case under study). The power plant efficiency at the beginning of life was 39.2%, assuming that the heat transfer problems mentioned previously can be solved in such a way that the model in Section 4.C is feasible.

The UF_6 reactor need not be designed for breeding and actinide transmutation applications. The relaxation of some of the constraints enables the reactor to operate at high powers under different conditions. Examples of UF_6 power reactors is given in Table 5.2 which summarizes work done by the University of Florida.[4] The main criticism of these

Table 5.2 University of Florida's UF_6 Reactor Designs[4]

Characteristics	HGCR1	HGCR2
Total Power	3000 MW(th)	1000 MW(th)
Moderator/coolant Material	H_2O	D_2O
Core Barrel Material	Be or BeO	Be or BeO
Moderator/coolant Channel Tube Material	Nb-alloy	Be or BeO
Reflector Material	H_2O	D_2O
Core Diameter	340 cm	340 cm
Core Height	360 cm	360 cm
Core Volume	32.69 m^3	32.69 m^3
Tube Thickness	0.1 cm	0.5 cm
Core Barrel Thickness	20 cm	20 cm
Reflector Thickness	40 cm	80 cm
Unit Cell Radius	3.2 cm	7.5 cm
Number of Coolant Channels	2800	514
Fuel Volume Fraction in the Core	0.88	0.64
Average UF_6 Pressure	20 atm	20 atm
U_{235} Enrichment (Average)	12 wt%	3 wt%
He Pressure	21 atm	21 atm
Coolant Pressure	1100 psi	1100 psi
Power Density	92 kW/litre	31 kW/litre
Uranium Mass in the Core	1665 kg	1665 kg
U_{235} Mass in the Core	200 kg	50 kg
Average Gas Temperature	~1000 K	~1000 K
Average Coolant Temperature	~540 K	~540 K
Estimated HGCR Overall Efficiency	~40%	~40%

designs is that the UF_6 to He partial pressure ratio is too high so that excessive amounts of uranium will be present in the heat exchangers.

In conclusion, it can be seen that the gas core reactor can operate under a wide range of conditions. No optimization was performed in this study, but it was shown that the UF_6 reactor can be used as a breeder with low uranium inventory and high power plant efficiency. The superior actinide transmutation features of the UF_6 reactor was also demonstrated, but further work is needed to solve the heat transfer problems. Plasma core reactors will require more extensive research, but the high power plant efficiencies that may be obtained when the reactor is coupled to a MHD generator is a strong motivating factor for further investigation of this system.

References for Chapter 5

1. Lowry, L. L., "Gas Core Reactor Power Plants Designed for Low Proliferation Potential," LA-6900-MS (September, 1977).

2. Claiborne, H. C., "Neutron Induced Transmutation of High-Level Radioactive Waste," ORNL-TM-3964 (December, 1972).

3. Beaman, S. L. and Aitken, E. A., "Feasibility Studies of Actinide Recycling in LMFBRs as a Waste Management Alternative," General Electric Company.

4. Han, K. I., Dugan, E. T., and Diaz, N. J., "Heterogeneous Gas Core Reactor Power Plants," Transactions of the American Nuclear Society, 27, 721-724 (November 27 - December 2, 1977).

Appendix A. Material Properties

UF_6 - helium gas mixture properties were calculated in the manner suggested by Ref. 1. The UF_6 thermophysical properties listed in Table A.1 were obtained from Ref. 2 which used data from Ref. 3. Helium properties shown in Table A.2 were obtained from Refs. 4 and 5. The properties of pure UF_6 and helium were used to obtain mixture properties following the procedures given in Ref. 6.

The mixture density is calculated from

$$\rho_{mix} = \rho_{UF_6} + \rho_{He} \tag{A.1}$$

while the specific heat at constant pressure of the mixture is obtained from

$$C_p^{mix} = \frac{C_p^{UF_6} \rho_{UF_6} + C_p^{He} \rho_{He}}{\rho_{mix}} \tag{A.2}$$

The specific heat at constant volume for UF_6 and for helium are

$$C_v^{UF_6} = \frac{C_p^{UF_6}}{\gamma_{UF_6}} \tag{A.3}$$

$$C_v^{He} = \frac{C_p^{He}}{\gamma_{He}} \tag{A.4}$$

which are used to determine the ratio of specific heats for the mixture,

$$\gamma_{mix} = \frac{C_p^{UF_6} \rho_{UF_6} + C_p^{He} \rho_{He}}{C_v^{UF_6} \rho_{UF_6} + C_v^{He} \rho_{He}} \tag{A.5}$$

Table A.1

UF_6 Thermophysical Properties[2]

Density, $\rho = 4.2675 \times 10^{-2} \frac{p}{T}, \frac{kg}{m^3}$
Specific Heat, $C_p = 391.22 + 0.09574\,T - \frac{3.8685 \times 10^6}{T^2}, \frac{J}{kg\ ^\circ K}$
Thermal Conductivity, $k = [0.0257\,T - 0.9093] \times 10^{-3}, \frac{W}{m\ ^\circ K}$
Viscosity, $\mu = [0.469 + 0.0044\,T] \times 10^{-5}$, pascal - sec
Ratio of Specific Heats, $\gamma = 1.06$

Pressure is in pascals
Temperatures are in degrees Kelvin

Table A.2

Helium Thermophysical Properties[4,5]

Density, $\rho = 4.8146 \times 10^{-4} \frac{p}{T}, \frac{kg}{m^3}$
Specific Heat, $C_p = 5192.6, \frac{J}{kg\ °K}$
Thermal Conductivity, $k = [6457 + 28.285\,T] \times 10^{-5}, \frac{W}{m\ °K}$ $200\ °K \leq T \leq 1000\ °K$
Viscosity, $\mu = 8.358 \times 10^{-6} + 3.659 \times 10^{-8}\,T$, pascals-sec $200\ °K \leq T \leq 1000\ °K$
Ratio of Specific Heat, $\gamma = 1.6667$

Pressure is in pascals
Temperatures are in degrees Kelvin

Given the mixture mass flow rate, $\dot{m}_{mix}$, and the ratio of UF_6 partial pressure to total pressure, r, the mass flow rates of UF_6 and helium are found from

$$\dot{m}_{UF_6} = \frac{\dot{m}_{mix}}{1 + \frac{M_{He}}{M_{UF_6}} \frac{1-r}{r}} \tag{A.6}$$

$$\dot{m}_{He} = \dot{m}_{mix} - \dot{m}_{UF_6} \tag{A.7}$$

where M_{He} and M_{UF_6} are the molecular weights of helium and UF_6, respectively.

The mole flow rates are defined by

$$\dot{x}_{UF_6} = \frac{\dot{m}_{UF_6}}{M_{UF_6}} \tag{A.8}$$

$$\dot{x}_{He} = \frac{\dot{m}_{He}}{M_{He}} \tag{A.9}$$

The mixture viscosity and conductivity are then given by

$$\mu_{mix} = \sum_i \frac{\dot{x}_i \mu_i}{\sum_j \dot{x}_j \tilde{\Phi}_{ij}} \tag{A.10}$$

$$k_{mix} = \sum_i \frac{\dot{x}_i k_i}{\sum_j \dot{x}_j \tilde{\Phi}_{ij}} \tag{A.11}$$

where the summation is taken over the helium and UF_6 species and $\tilde{\Phi}_{ij}$ is given by

$$\Phi_{ij} = \frac{1}{\sqrt{8}} \frac{\left[1 + \left(\frac{\mu_i}{\mu_j}\right)^{\frac{1}{2}} \left(\frac{M_j}{M_i}\right)^{\frac{1}{4}}\right]^2}{\left[1 + \left(\frac{M_i}{M_j}\right)\right]^{\frac{1}{2}}} \qquad \text{(A.12)}$$

Values of C_p^{mix}, μ_{mix}, and k_{mix} as functions of helium mole fraction are given in Tables A.3 to A.5 for various temperatures. These properties are also shown graphically in Figs. A.1 to A.3.

The molten salt used in the breeding blanket is composed of LiF (71.7 mole %), BeF_2 (16 mole %), and ThF_4 (12.3%). Its properties listed in Table A.6 were obtained from Ref. 7.

The properties of NaF (8 mole %)-$NaBF_4$ (92 mole %) salt is given in Table A.7 and were obtained from Ref. 8.

Hastelloy-N is a nickel alloy which is compatible with fluorides. Modified Hastelloy-N is very similar in composition and other related physical properties to standard Hastelloy-N, but the addition of 2% titanium increases the ability of Hastelloy-N to resist helium embrittlement due to neutron irradiation. A thorough discussion of this material is given in Ref. 9 as only the physical properties are summarized in Table A.8 which was obtained from Ref. 10.

Further discussion of the corrosion problem is made in Ref. 11. As pointed out in that report, nickel or one of its alloys, is the best candidate for containing UF_6. However, nickel has a high capture cross section which prevents it from being used in large amounts in the reactor core. But it may be possible to use small amounts of nickel in the core by utilizing it as a clad. For example, nickel may be electroplated onto a beryllium substrate. Further work is needed to determine the optimum material and geometry of structural material in the core.

Table A.3. Specific Heats at Constant Pressure for UF_6-Helium Mixtures For Various Mole Fractions of He

$\frac{x^{He}}{x^{TOT}}$	$C_p \left(\frac{J}{kg\ °K}\right)$		
	T = 600°K	T = 700°K	T = 800°K
0	437.92	450.35	461.76
0.1	443.87	456.29	467.68
0.2	451.29	463.69	475.06
0.3	460.80	473.17	484.52
0.4	473.41	485.75	497.07
0.5	490.96	503.25	514.54
0.6	517.04	529.27	540.49
0.7	559.87	571.99	583.10
0.8	643.22	655.12	666.03
0.9	876.20	887.49	897.84
0.91	924.77	935.93	946.16
0.92	983.96	994.97	1005.1
0.93	1057.7	1068.5	1078.4
0.94	1152.1	1162.7	1172.3
0.95	1277.2	1287.5	1296.8
0.96	1451.0	1460.8	1469.8
0.97	1708.8	1717.9	1726.2
0.98	2130.6	2138.7	2146.0
0.99	2946.6	2952.5	2957.8
0.995	3727.4	3731.3	3734.8
0.998	4475.4	4477.3	4479.0
1.0	5192.6	5192.6	5192.6

Table A.4. Viscosities for UF_6-Helium Mixtures at Various Mole Fractions of He

$\frac{x^{He}}{x^{TOT}}$	μ (pascal-sec)		
	T = 600°K	T = 700°K	T = 800°K
0	3.1090×10^{-5}	3.5490×10^{-5}	3.9890×10^{-5}
0.1	3.1444×10^{-5}	3.5889×10^{-5}	4.0335×10^{-5}
0.2	3.1860×10^{-5}	3.6359×10^{-5}	4.0857×10^{-5}
0.3	3.2356×10^{-5}	3.6917×10^{-5}	4.1478×10^{-5}
0.4	3.2955×10^{-5}	3.7590×10^{-5}	4.2224×10^{-5}
0.5	3.3689×10^{-5}	3.8412×10^{-5}	4.3135×10^{-5}
0.6	3.4601×10^{-5}	3.9430×10^{-5}	4.4258×10^{-5}
0.7	3.5735×10^{-5}	4.0687×10^{-5}	4.5636×10^{-5}
0.8	3.7071×10^{-5}	4.2143×10^{-5}	4.7213×10^{-5}
0.9	3.8007×10^{-5}	4.3071×10^{-5}	4.8132×10^{-5}
0.91	3.7971×10^{-5}	4.3008×10^{-5}	4.8043×10^{-5}
0.92	3.7877×10^{-5}	4.2878×10^{-5}	4.7876×10^{-5}
0.93	3.7708×10^{-5}	4.2660×10^{-5}	4.7608×10^{-5}
0.94	3.7439×10^{-5}	4.2325×10^{-5}	4.7207×10^{-5}
0.95	3.7036×10^{-5}	4.1834×10^{-5}	4.6630×10^{-5}
0.96	3.6452×10^{-5}	4.1134×10^{-5}	4.5814×10^{-5}
0.97	3.5619×10^{-5}	4.0147×10^{-5}	4.4673×10^{-5}
0.98	3.4435×10^{-5}	3.8757×10^{-5}	4.3078×10^{-5}
0.99	3.2748×10^{-5}	3.6791×10^{-5}	4.0833×10^{-5}
1.00	3.0312×10^{-5}	3.3971×10^{-5}	3.7630×10^{-5}

Table A.5. Thermal Conductivities For UF_6-Helium Mixtures at Various Mole Fractions of He

$$k\left(\frac{W}{m\ °K}\right)$$

$\frac{x^{He}}{x^{TOT}}$	T = 600°K	T = 700°K	T = 800°K
0	1.4511×10^{-2}	1.7081×10^{-2}	1.9651×10^{-2}
0.1	1.8913×10^{-2}	2.2076×10^{-2}	2.5239×10^{-2}
0.2	2.4178×10^{-2}	2.8049×10^{-2}	3.1918×10^{-2}
0.3	3.0591×10^{-2}	3.5316×10^{-2}	4.0038×10^{-2}
0.4	3.8569×10^{-2}	4.4349×10^{-2}	5.0125×10^{-2}
0.5	4.8765×10^{-2}	5.5880×10^{-2}	6.2989×10^{-2}
0.6	6.2251×10^{-2}	7.1107×10^{-2}	7.9954×10^{-2}
0.7	8.0919×10^{-2}	9.2139×10^{-2}	1.0335×10^{-1}
0.8	1.0843×10^{-1}	1.2304×10^{-1}	1.3763×10^{-1}
0.9	1.5286×10^{-1}	1.7267×10^{-1}	1.9245×10^{-1}
0.91	1.5883×10^{-1}	1.7931×10^{-1}	1.9977×10^{-1}
0.92	1.6518×10^{-1}	1.8637×10^{-1}	2.0753×10^{-1}
0.93	1.7195×10^{-1}	1.9388×10^{-1}	2.1579×10^{-1}
0.94	1.7917×10^{-1}	2.0188×10^{-1}	2.2958×10^{-1}
0.95	1.8688×10^{-1}	2.1042×10^{-1}	2.3394×10^{-1}
0.96	1.9512×10^{-1}	2.1954×10^{-1}	2.4393×10^{-1}
0.97	2.0395×10^{-1}	2.2928×10^{-1}	2.5458×10^{-1}
0.98	2.1340×10^{-1}	2.3968×10^{-1}	2.6594×10^{-1}
0.99	2.2351×10^{-1}	2.5078×10^{-1}	2.7804×10^{-1}
1.00	2.3428×10^{-1}	2.6257×10^{-1}	2.9085×10^{-1}

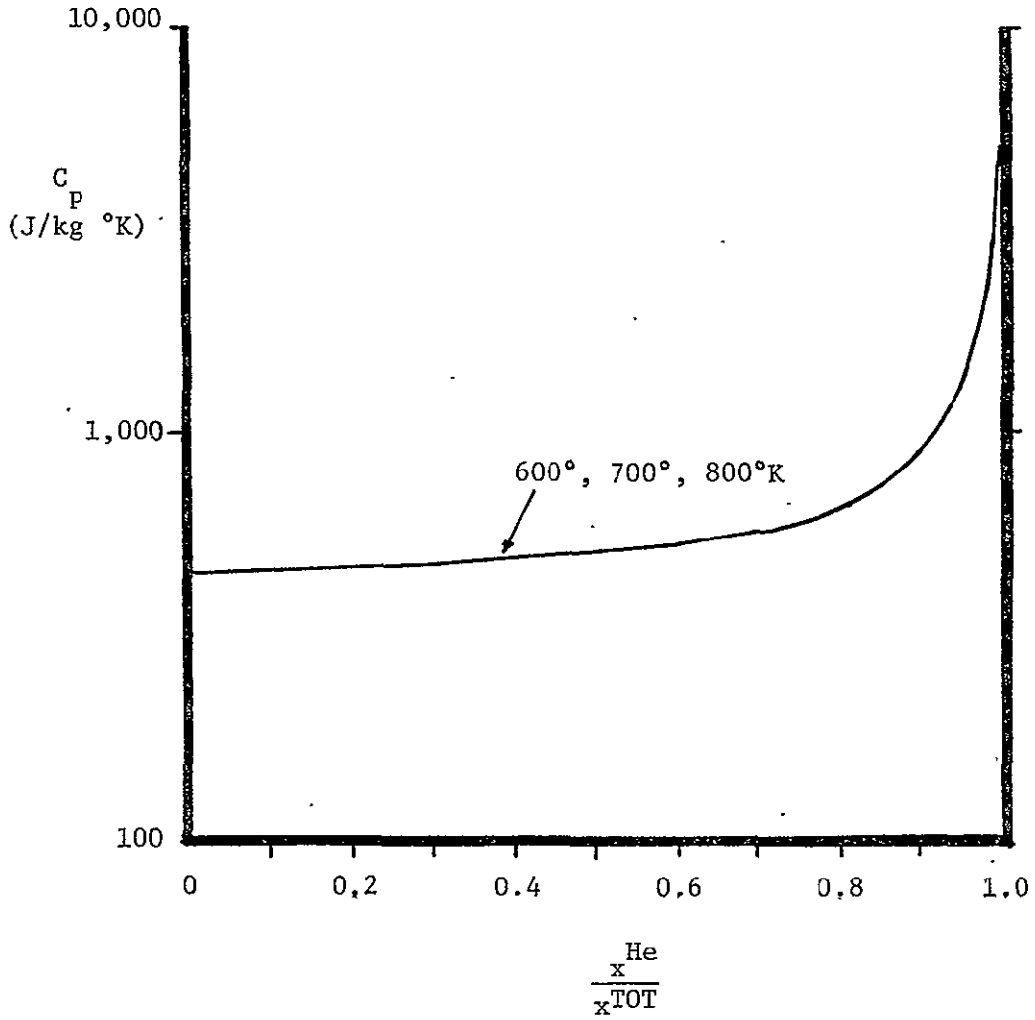

Fig. A.1. Specific Heats at Constant Pressure for UF_6-Helium Mixtures at Various Mole Fractions of He

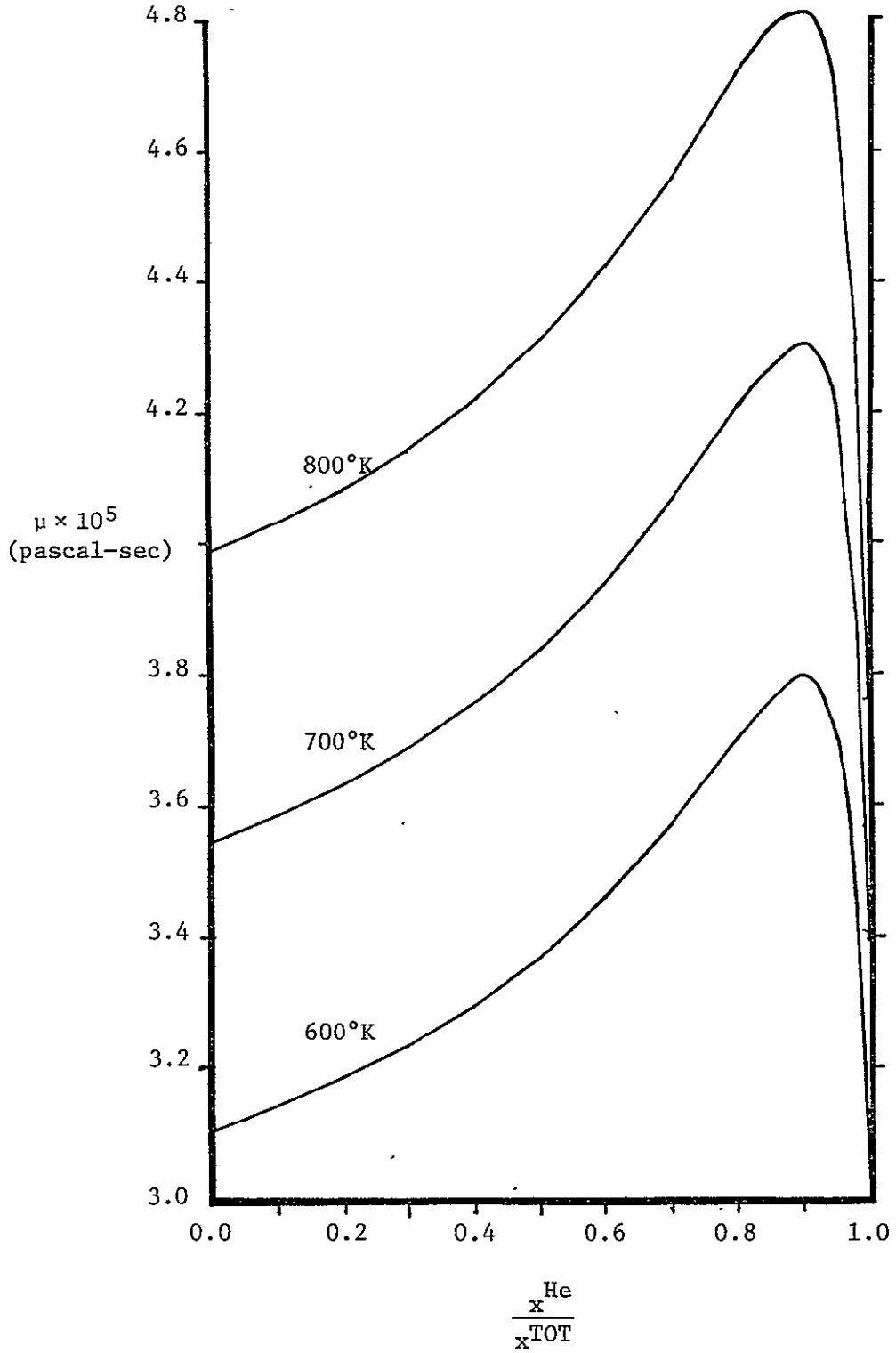

Fig. A.2. Viscoscities of UF_6-Helium Mixtures at Various Mole Fractions of He

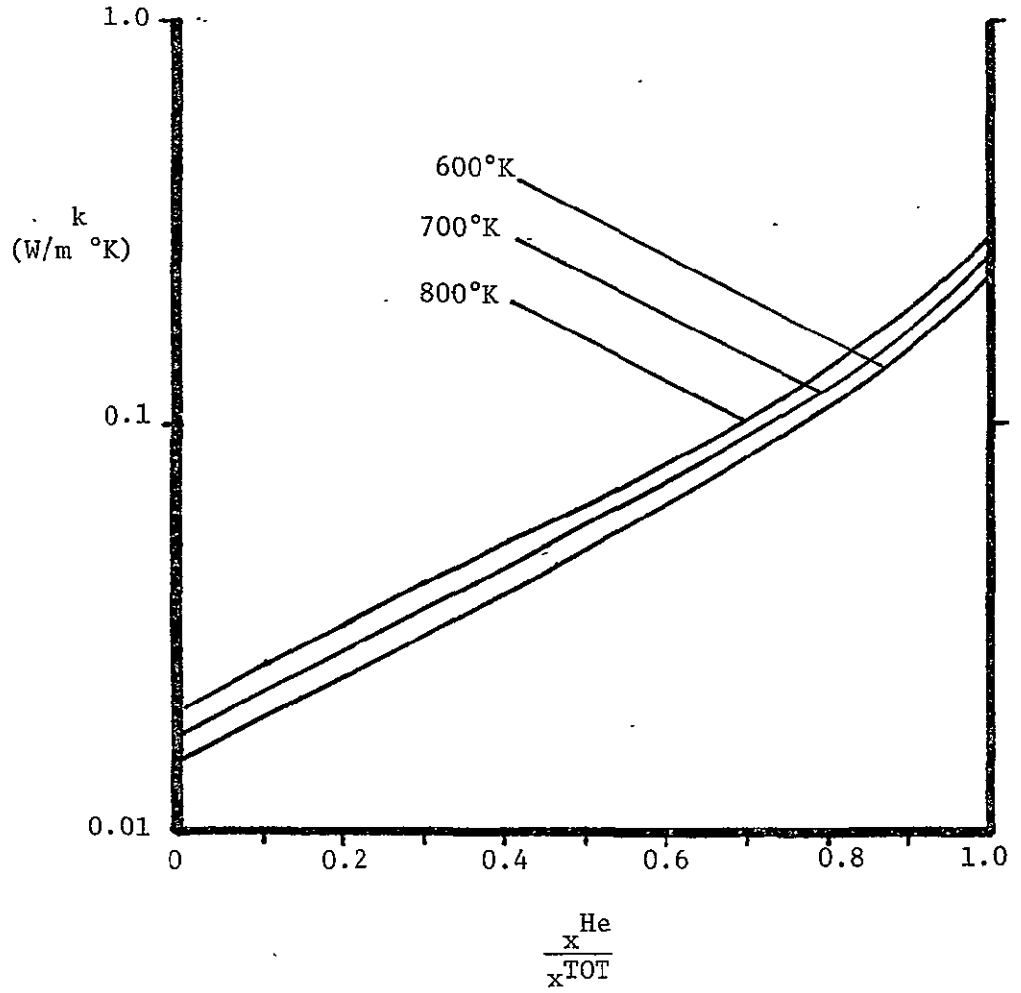

Fig. A.3. Thermal Conductivities for UF_6-Helium Mixtures at Various Mole Fractions of He

Table A.6. Thermophysical Properties of LiF (71.7 mole %), BeF_2 (16 mole %), and ThF_4 (12.3 mole %) Molten Salt (7)

Molecular Weight = 64

Melting Point = 772 °K

Specific Heat at Constant Pressure = 1356.6 $\frac{J}{kg\ °K}$

Density = 3935.4 - 0.6682 T $\frac{kg}{m^3}$, T is in °K

Viscosity = 1.0901×10^{-4} exp (4090/T) pascals-sec , T is in °K

Thermal Conductivity = 1.19 $\frac{W}{m\ °K}$ at 978 °K

1.23 $\frac{W}{m\ °K}$ at 908 °K

1.19 $\frac{W}{m\ °K}$ at 839 °K

Vapor Pressure at 894 °K is less than 13.33 pascals (1 mm Hg)

Table A.7. Thermophysical Properties of NaF (8 mole %), $NaBF_4$ (92 mole %) Salt[8]

Melting Point = 658 °K

Physical Properties at 727 °K

Density = 1938.4 $\frac{kg}{m^3}$

Specific Heat at Constant Pressure = 1507.3 $\frac{J}{kg\ K}$

Viscosity = 0.0025 pascals-sec

Thermal Conductivity = 0.5 $\frac{W}{m\ °K}$

Vapor Pressure at 880 °K* = 2.667×10^3 pascals (200 mm Hg)

*Highest permissible operating temperature.

Table A.8. Properties of Hastelloy N[9]

Yield Strength	3.103×10^8 pascals
Tensile Strength	7.929×10^8 pascals
Elongation	51%
Brinell Hardness	96
Density	$8489.3 \frac{kg}{m^3}$
Specific Gravity	8.79
Melting Point	1672 °K
Specific Heat	$418.7 \frac{J}{kg\ °K}$
Coefficient of Thermal Expansion	3.44 m/m/°K
Thermal Conductivity	$10.25 \frac{W}{m\ °K}$
Electrical Resistivity	1.388×10^{-6} ohm-m
Young's Modulus of Elasticity	2.186×10^{11} pascals

Nominal Composition

Chromium	7%	Molybdenum	16.5%
Iron	8%	Nickel	65.5%
Titanium	3%		

References for Appendix A

1. Private communication with John S. Kendall of the United Technologies Research Center, East Hartford, Connecticut (January 25, 1978).

2. Rodgers, R. J., Latham, T. S., and Krascella, M. L., "Analysis of Low-Power and Plasma Core Cavity Reactor Experiments," United Aircraft Research Laboratories Report, R75-911908-1 (May 1975).

3. Katz, J. J. and Rabinowitch, E., Chemistry of Uranium, USAEC, Technical Information Service, Oak Ridge, Tennessee (1958).

4. Lick, W. J. and Emmons, H. W., Thermodynamic Properties of Helium to 50,000°K, Harvard University Press (1962).

5. Lick, W. J. and Emmons, H. W., Transport Properties of Helium to 50,000°K, Harvard University Press (1965).

6. Holmes, J. T. and Baerns, M. G., "Predicting Physical Properties of Gases and Gas Mixtures," Chemical Engineering (May 24, 1965).

7. Robertson, R. C., "Conceptual Design Study of a Single-Fluid Molten Salt Breeder Reactor," ORNL-4541 (June 1971).

8. Grimes, W. R., "Molten Salt Reactor Chemistry," Nuclear Applications and Technology, 8 (February 1970).

9. Clement, J. D. and Rust, J. H., "Analysis of UF_6 Breeder Reactor Power Plants," Final Report, NASA Grant NSG-1168, Georgia Institute of Technology (February 1976).

10. Properties of Some Metals and Alloys, International Nickel Company, Inc., New York (1968).

11. Wagner, P., "Materials Considerations for UF_6 Gas-Core Reactor. Interim Report for Preliminary Design Study," LA-6776-MS (April 1977).

Appendix B Reprocessing Systems

No quantitative analysis was made of the reprocessing systems for the UF_6 breeder and actinide transmutation reactors. However, since the reprocessing systems are important to the operation of the power plants, a qualitative discussion is included in this study which is based on proposed systems given in Refs. 1-3. Although these studies were preliminary in nature, they did not encounter major obstacles.

There are three major reprocessing systems to be considered. The first is the cleanup of fission products in the UF_6-helium mixture. For the breeder power plant, the bred material must be separated from the breeding salt. Finally, actinides must be separated from other waste products to be used in the actinide transmutation reactor. These systems will be described in the following sections.

B.1 Fission Product Cleanup

Fission products must be removed from the UF_6-helium mixture continuously to avoid buildup of reactor poisons and condensation of volatiles. Fortunately, the technology for UF_6 separation and purification is available from the Molten Salt Breeder Reactor Program at Oak Ridge National Laboratory and helium purification technology is available from the High Temperature Gas Cooled Reactor developed by General Atomics.

It is expected that some UF_6 will dissociate in the core and that the fluorine formed will combine with metallic fission products to form fluorides. According to Ref. 1, the fluorides and gases in Table B.1 will be formed. The fluorides are divided into volatile, mobile, intermediate and refractory fluorides according to their boiling points. The mole

Table B.1

Gaseous and Fluoride Fission Products[1]

Gases	Volatile Fluorides	Mobile Fluorides	Intermediate Fluorides	Refractory Fluorides
Kr	SeF_6 (236°K)*	SbF_5 (423°K)	Cs F (1524°K)	RaF_2 (2410°K)
Xe	MoF_6 (308°K)	NbF_5 (509°K)	Rb F (1663°K)	YF_3 (2500°K)
I	TeF_6 (309°K)	RuF_5 (523°K)		CeF_3 (2573°K)
Br		ZrF_5 (873°K)		NdF_3 (2573°K)
		SuF_4 (978°K)		PrF_4 (2600°K)
				LaF_3 (2600°K)
				SrF_2 (2762°K)

*numbers in parantheses are the boiling points of the various fluorides

fractions of the fission product gases, volatile fluorides, and mobile fluorides are on the order of 10^{-5} less than the mole fraction of helium while the mole fractions of the intermediate and refractory fluorides are 10^{-3} less than the other fluorides.

Due to their low boiling points, the volatile and some of the mobile fluorides will remain in the UF_6-helium circulating gas loop until they are removed for reprocessing. The other fluorides will be deposited in the heat exchangers and piping. The problem is further complicated by radioactive decay of various species, resulting in a change of their chemical nature and the relocation of their deposition sites.

Reference 1 suggests that replaceable getter pads made of nickel wire be placed in the reactor outlet piping to capture the intermediate and refractory fluorides.

Lowry[1] of the Los Alamos Scientific Laboratory proposed the fission product cleanup system shown in Fig. B.1. A small amount of UF_6-helium gas mixture is bled from the circulating loop and is reduced in pressure to 1.5 atmospheres. The mixture then passes into a high temperature bed of Na F pellets at 500°K where most of the volatile fluorides are absorbed and is cooled to 300°K before entering a low temperature bed of Na F pellets. The low temperature bed absorbs the UF_6 and remaining metal fluorides while the helium containing xenon, krypton, bromine, iodine and other gases pass through the filter to the helium purification system.

Two low temperature beds are utilized. When one bed becomes loaded with UF_6, the flow into this bed is valved out and the fresh bed is placed in service. The bed loaded with UF_6 is then heated to 700°K which drives

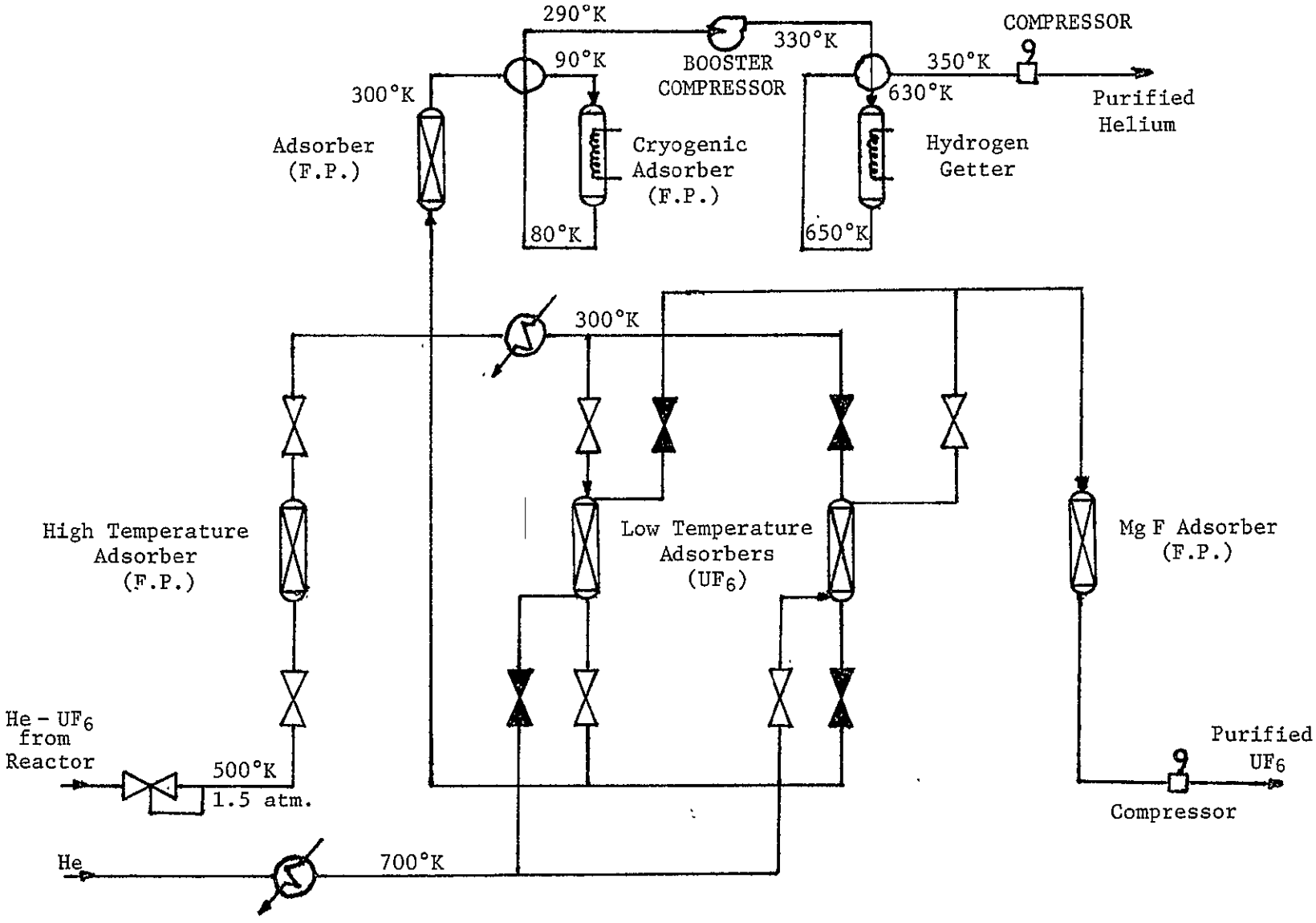

Fig. B.1 Fission Product Removal System[1]

off UF_6 as a gas along with small amounts of TeF_6. A helium purge gas is used to help remove the UF_6. Finally, the UF_6 passes through a bed of MgF_2 to remove the TeF_6 before being filtered, pressurized, and cooled to produce a purified liquid which is recycled to the reactor. The NaF and MgF_2 beds containing fission products are either stored or sent to a waste treatment plant.

Helium at 300°K flows into one of two parallel systems consisting of high and low temperature charcoal absorbers. The high temperature absorber contains activated charcoal impregnated with potassium. The charcoal removes the condensable metallic fission products while the potassium removes iodine by chemisorption.

The helium is then cooled to 90°K in a helium regenerator and passes through the low temperature absorber which removes krypton, xenon, nitrogen, and some hydrogen and tritium. Helium is cooled in the absorber to 80°K by liquid nitrogen. The purified helium then enters the cold side of the regenerator where it is heated to 290°K and is filtered to remove dust before being compressed and sent to the hydrogen removal section.

Helium leaving the compressor enters another regenerator before passing through one of two parallel hydrogen getters consisting of titanium sponges to remove hydrogen and tritium. Helium enters the getters at 630°K and is heated by the electrically heated sponges to 650°K. The helium then reenters the regenerator and is cooled to 350°K, filtered and recompressed.

The uranium inventory in the reprocessing system is not a function of reactor power but of regeneration frequency and volume of the NaF bed.

Distillation[1] is an alternative method for fission product removal especially if a large part of the primary stream must be cleaned up. The bled stream enters a distillation column where most of the fluorides are removed as a concentrate at the bottom of the column. An aqueous wash removes the fluorides from the concentrate and residual UF_6 is returned to the column for further purification. The UF_6 and volatile fluorides are condensed and fed to a second column which produces pure UF_6 at the bottom of the column.

Another method for UF_6 purification is a combination of a cold trap process and fluoride volatility process proposed by Rust and Clement.[2]

Clearly, there are several possible methods for UF_6 purification. The method that will be selected should be based on consideration of economics, minimum uranium inventory, effectiveness in keeping the system as clean as possible, and compatibility with power plant operation.

B.2 Breeding Salt Reprocessing System

The description of the molten salt breeding blanket reprocessing system is summarized from Ref. 3. Additional information was taken from Ref. 1.

Since it is desirable to have the Gas Core Breeder Reactor (GCBR) be a self-contained unit, generating its own new fuel, an on-line reprocessing system for the molten salt blanket is a necessity. This section describes protactinium removal and salt purification processes, and calculational procedures for expected flow rates and equilibrium concentrations of various isotopes present in the system.

The salt used in the blanket is an eutectic mixture composed of LiF, BeF_2, and ThF_4 in the ratios of 72:16:12 mole percent. This particular combination was developed at the Oak Ridge National Laboratory in conjunction with the Molten Salt Breeder Reactor program.

When thorium atoms contained in the salt are irradiated with neutrons, some of the atoms absorb a neutron and transmute to protactinium as shown in Fig. B.2. The protactinium eventually decays to uranium which can then be fed to the core as new fuel. However, as seen in Figure B.2, Pa^{233} has a substantial cross section (22 barns) and since its half life is 27 days, Pa acts as a poison, siphoning off neutrons which could otherwise irradiate Th atoms. In addition, the daughter of Pa^{233} $\left(U^{233}\right)$ would be lost. For these reasons, it is desirable to remove Pa from the molten salt loop and allow it to decay outside the core.

However, since it is impossible to have a zero protactinium concentration in the molten salt blanket, there will be some uranium present in the core. Some of these atoms will fission and, consequently, there will be some uranium fission products in the molten salt loop. Some of these fission products have large cross sections as shown in Table B.2. Note that Xe and other gaseous fission product poisons are not listed because it is assumed that the blanket can be vented and these gaseous products easily removed. As will be shown later, the necessity of keeping the concentration of fission products at a low level determines the amount of time which the salt can stay in the irradiated blanket region.

In order to achieve the above neutronics goals, a fluorination-reductive extraction system was developed at Oak Ridge National Lab. A description of this process is as follows:[5]

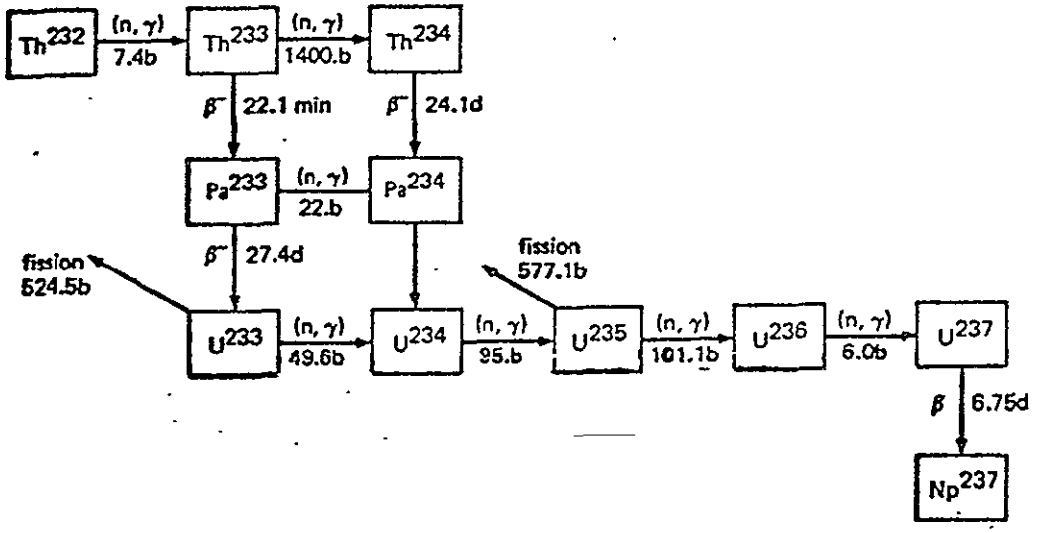

Fig. B.2 The chain of isotopes created by neutron irradiation of Th232.

Table B.2

Rare Earth Fission Product Absorption Cross Section

Nd-143	330 barns
La-139	8.9 barns
Eu-153	320 barns

The fluorination-reductive extraction system for isolating protactinium is shown in its simplest form in Figure B.3. The salt stream from the reactor first passes through a fluorinator, where most of the uranium is removed by fluorination. Approximately 90% of the salt leaving the fluorinator is fed to an extraction column, where it is countercurrently contacted with a bismuth stream containing lithium and thorium. The uranium is preferentially removed from the salt in the lower extractor, and the protactinium is removed by the upper contactor. A tank through which the bismuth flows is provided for retaining most of the protactinium in the system.

The bismuth stream leaving the lower contactor contains some protactinium as well as the uranium that was not removed in the fluorinator and the uranium that was produced by the decay of protactinium. This stream is contacted with a H_2-HF mixture in the presence of approximately 10% of the salt leaving the flourinator in order to transfer the uranium and the protactinium to the salt. The salt stream, containing UF_4 and PaF_4, is then returned to a point upstream of the fluorinator, where most of the uranium is removed. The protactinium passes through the fluorinator and is subsequently extracted into the bismuth. Reductant (Li and Th) is added to the Bi stream leaving the oxidizer, and the resulting stream is returned to the upper contractor. The salt stream leaving the upper contactor is essentially free

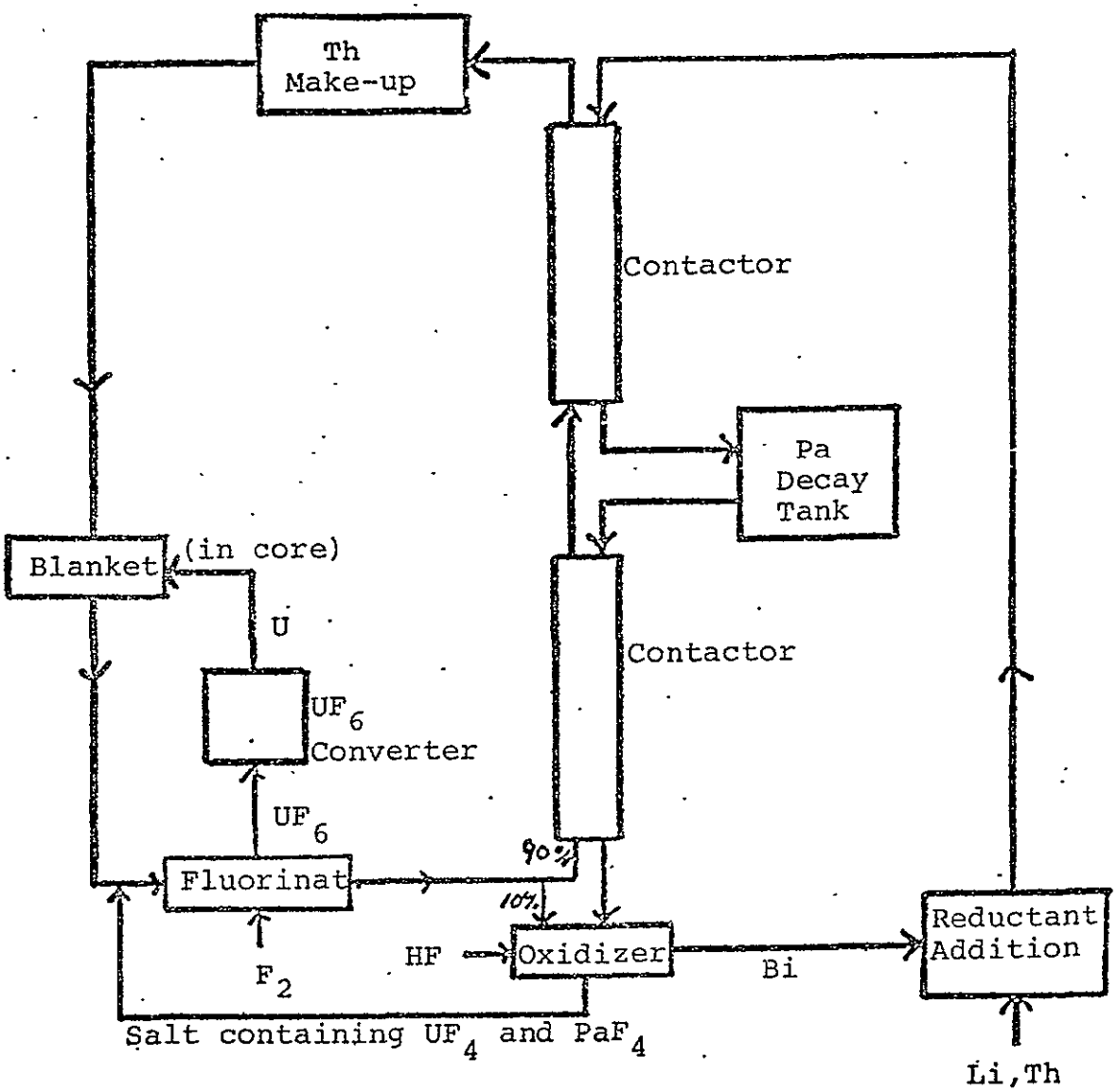

Fig. B.3 UF_6 Breeder Reactor Salt Reprocessing System

of uranium and protactinium and would be processed for removal of any fission product gases and additional thorium added to compensate for that which had been consumed.

Figure B.4 describes the UF_6 to U metal conversion process. Unfortunately this is a batch process instead of a continuous flow system as is present in the remainder of the reprocessing set-up. However, there should be no problem providing temporary storage tanks for UF_6.

The UF_6 initially enters a reaction chamber where it is mixed with hydrogen. A reaction is triggered and UF_4 powder and HF gas is produced. The UF_4 is then loaded into a steel "bomb" which has been coated with fused dolomitic lime--lime is one of the few oxides that does not react with molten uranium. The "bomb" is then heated to 565°C where an exothermic reaction takes place and uranium metal solidifies on the bottom of the "bomb". The MgF_2 is removed and U metal of high purity can then be taken from the bottom of the "bomb" and sent to the plasma core reactor.(7)

Given certain constraints on the reprocessing system it is possible to calculate the flow rates which would exist in both the molten salt and bismuth loops. It is also possible to calculate protactinium concentrations throughout the reprocessing system and therefore determine uranium concentrations throughout the system. The constraints which are placed on the reprocessing system are as follows:

1) The protactinium concentration in the molten salt blanket is allowed to reach 95% of the equilibrium value obtained if the salt remained in the active region of the reactor for an infinite amount of time, provided that the concentration of protactinium does not cause

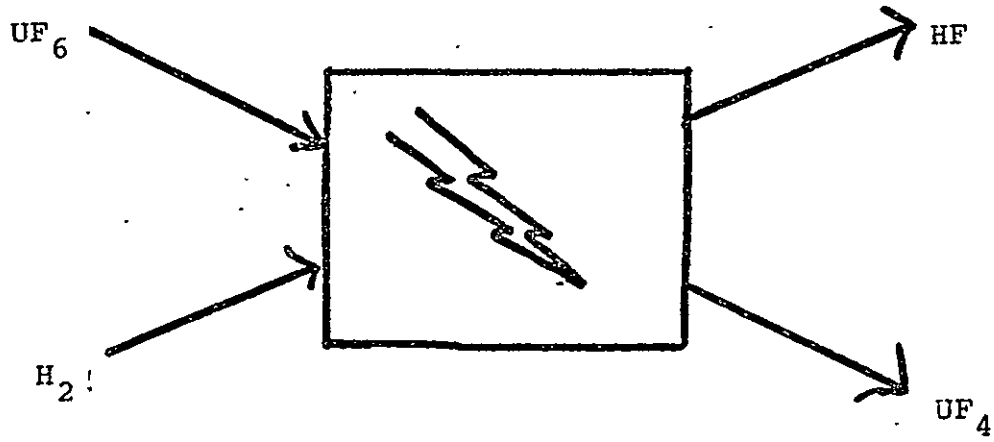

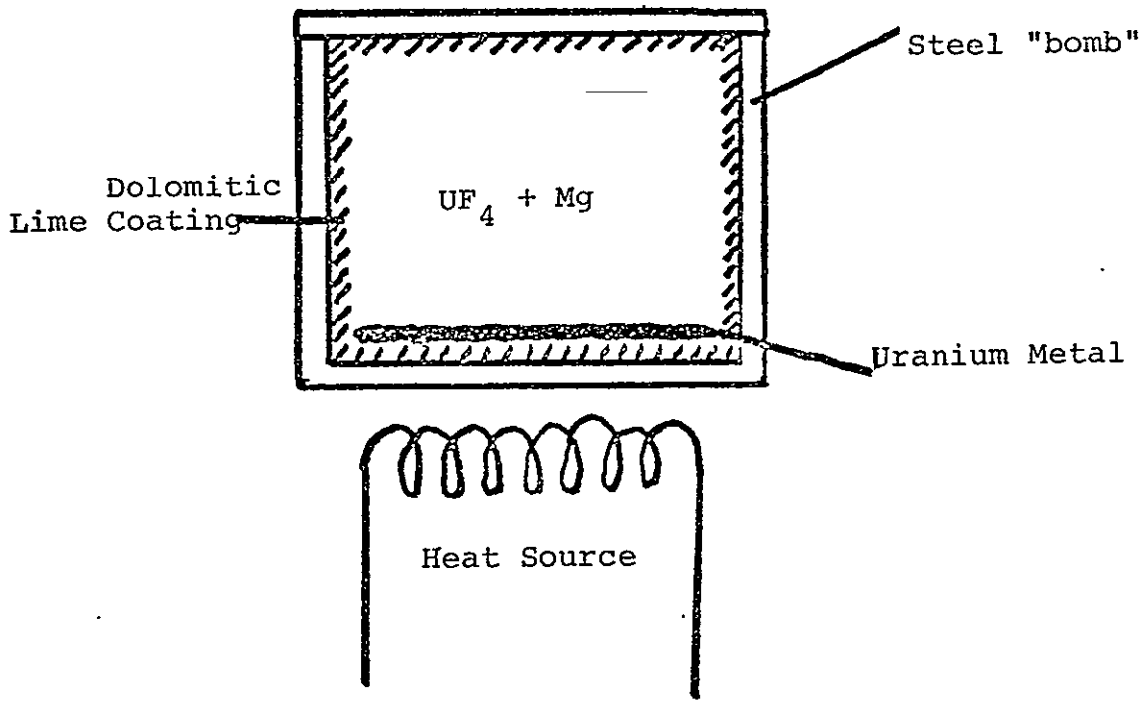

Fig. B.4 UF_6 to U Metal Batch Process

parasitic absorption of neutrons by fission products greater than 1% of the absorptions which are due to thorium captures.

2) The volume of the blanket and the flux in the blanket is determined by breeding ratio constraints as explained elsewhere in this report.

3) The uranium removal efficiency of the fluorinator and oxidizer is 98%.[7]

4) The operating temperature of the system is 640°C (necessary because the salt is a eutectic mixture).[7]

5) The Li concentration in the Bi loop is 1%. The Th concentration in the Bi loop is held at less than 50% of the solubility of Th in Bi.[8]

6) The Pa distribution coefficient for the contactors, defined as (mole fraction of Pa in Bi at equilibrium)/(mole fraction of Pa in salt at equilibrium), can be taken to be 100.[8]

The following physics data is required:

Neutron Flux

Volume of Blanket

Molar Volume of Salt

Molar Volume of Bi

Pa Absorption Cross Section

Th Absorption Cross Section

U Absorption Cross Section

U Fission Cross Section

Pa Decay Constant

Concentration of Th in Salt

To satisfy assumption 1, it is necessary to examine if the Pa concentration in the salt from the output of the blanket will be governed by the rate of fission product captures. To determine the number of fission product captures the Pa and U concentrations are first calculated as follows:

$$\frac{d\ Pa}{dt} + \lambda Pa = \sigma_a^{Th}\ \phi\ Th \tag{B.1}$$

where ϕ is the flux, Th is the thorium concentration, and λ the Pa decay constant.

Solving Eq. B.1 gives

$$Pa = \frac{\sigma_a^{Th}\phi\ Th}{\lambda} - e^{-\lambda t}\left[\frac{\sigma_a^{Th}\phi\ Th}{\lambda} - Pa_o\right] \tag{B.2}$$

The equation for the uranium concentration as a function of time is

$$\frac{dU}{dt} = -\ \phi\ \sigma_a^{u}\ U + \lambda\ Pa \tag{B.3}$$

where U is the U-233 concentration.

Solving this equation we have

$$U = U_o e^{-\sigma_a^{u}\phi t} + \frac{\sigma_a^{Th}\ Th}{\sigma_a^{u}}\left(1 - e^{-\sigma_a^{u}\phi t}\right) - \lambda\left[\frac{\sigma_a^{Th}\phi\ Th}{\lambda} - Pa_o\right]\left[\frac{e^{-\lambda t} - e^{-\sigma_a^{u}\phi t}}{\sigma_a^{u}\phi - \lambda}\right] \tag{B.4}$$

If a material is assumed to spend time T in the blanket, then the number of fissions which occurs during this time is

$$\text{No. of fissions} = \int_o^T \sigma_f{}^u \phi \; U(t)\,dt \tag{B.5}$$

Evaluating this integral we have

$$\text{No. of fissions} = \sigma_f{}^u \phi \left[\frac{\sigma_a{}^{Th}\, Th}{\sigma_a{}^u} \left(T - \frac{e^{-\sigma_a{}^u \phi T} - 1}{\sigma_a{}^u \phi} \right) - \right.$$

$$\left. \frac{\lambda}{(\sigma_a{}^u \phi - \lambda)} \left[\frac{\sigma_a{}^{Th} \phi Th}{\lambda} - P_{ao} \right] \left[\frac{1 - e^{-\lambda T}}{\lambda} + \frac{e^{-\sigma_a{}^u \phi T} - 1}{\sigma_a{}^u \phi} \right] \right] \tag{B.6}$$

and the fission product concentration at the end of a cycle of length T is given by

$$[\text{F.P.}] = \left[\int_o^T \sigma\phi \; U(t) \; e^{\sigma_f{}^u \phi t} \, dt \right] e^{-\sigma_f{}^u \phi T} \ll \gamma \text{ (No. of fissions)} \tag{B.7}$$

where γ is the probability per fission of getting a particular fission product. Since the fluorinater removes 98% of the uranium in the molten salt on each pass through the system, the entering concentration to the blanket region can be taken as effectively zero.

Solving Eq. B.7 for a variety of times T, the results can be given as $\frac{\Sigma_{Eu}}{\Sigma_{Th}}$ where Σ_{Eu} is the absorption cross section of one of the most troublesome rare earth fission products, Eu^{153}. It should be stated that the estimate of the Eu^{153} concentration is high due to the approximation in Eq. B.7. If the concentration is sufficiently small, no fission product removal system is necessary; otherwise, a removal system similar to those discussed in Section B.1 is needed.

To determine the flow rates and concentrations in the system, use must be made of the following mass balance equations.[9] Referring to the hypothetical exchange column shown in Fig. B.5

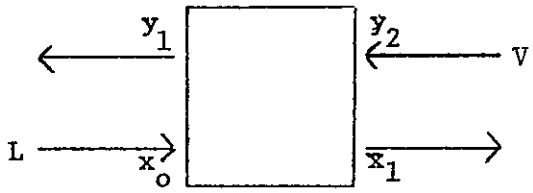

Figure B.5: Exchange Column Flows

then a material balance yields the following equation:

$$Lx_o + Vy_2 = Lx_1 + Vy_1 \tag{B.8}$$

or

$$L\,(x_o - x_1) = V\,(y_1 - y_2) \tag{B.9}$$

where L and V are flow rates in moles/$\overline{\text{sec}}$ and x and y are concentrations of the transferring material expressed in mole fractions. Now at equilibrium

$$y_1 = K \cdot x_1 \tag{B.10}$$

where K is a constant known as the distribution coefficient. Substituting for x_1 in Equation B.9 and solving for y_1 we have

$$y_1 = \frac{y_2 + \frac{L}{V} x_o}{\frac{L}{KV} + 1} \tag{B.11}$$

So if the two inlet concentrations and the flow rates are known, then the outlet concentrations can be calculated.

The value of the flow rates in the Bi and blanket loops must be solved for iteratively. A flow chart of the solution process is shown in Fig. B.6. A value for the Bi flow rate is assumed and for given Pa core concentration, neutron flux, and core volume, the flow rate in the blanket, residence time in the core, and input concentration of Pa to the core can be solved for iteratively.

Reference 8 gives the distribution coefficient of Pa as a function of time of contact and relative volumes of salt and Bi. Picking a specific distribution coefficient determines the time of contact and the relative volume of the two components. A new value for the Bi flow rate can then be calculated by using the value of the blanket flow rate calculated above. The entire iterative procedure is then repeated with the new Bi flow rate.

Once the flow rates have been calculated, the output Pa concentration in the Bi loop from the contactor can then be found from Eq. B.11 and the input concentration from Eq. B.9.

It should be noted at this point that if a contactor is composed of several stages with K being the distribution coefficient in each stage, then the procedure described above can be applied to the whole system with the number of stages, N, given by the expression[9]

$$N = \frac{\log \left[\frac{A-1}{A} \left(\frac{y_{n+1} - Kx_o}{y_1 - Kx_o} \right) + \frac{1}{A} \right]}{\log A} \qquad \text{(B.12)}$$

where A is the absorption factor and is defined by $A = L/(KV)$.

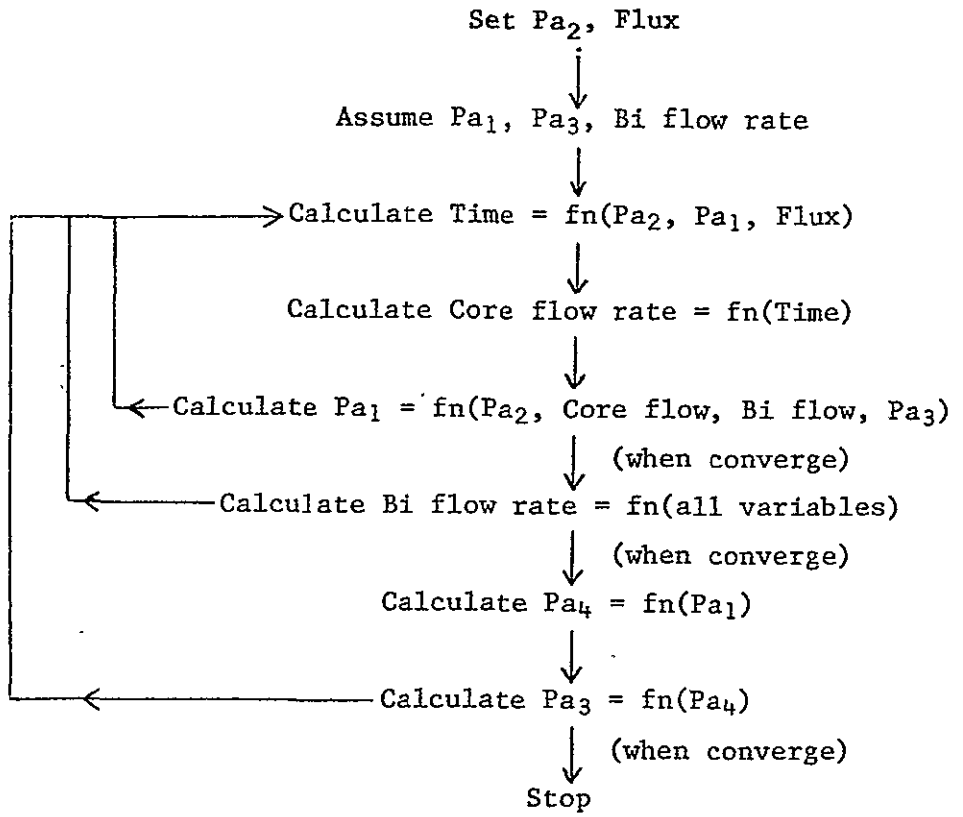

Pa_1 = Core input Pa concentration

Pa_2 = Core output Pa concentration

Pa_3 = Bi loop contactor input Pa concentration

Pa_4 = Bi loop contactor output Pa concentration

Fig. B.6 Flowchart for Calculation of Reprocessing System Flow Rates and Pa Concentration

Calculations performed for the Plasma Core Breeder Reactor salt reprocessing system[3] indicate the proposed system is feasible. The technology is presently available and the chemical processes involved in uranium separation have been proven by experiments in connection with the Molten Salt Breeder program.

Reference 1 points out that extraction of U^{233} from the salt requires a concentration of 100 parts per million or more.[10] At start-up, no U^{233} exists in the blanket so that the reactor must run from an auxiliary bottle until enough has formed. This would add to the uranium inventory.

B.3 Actinide Reprocessing System

Because of the hazardous radionuclides present in high-level wastes from present day reactors, schemes are needed which provide waste management programs of one million years or longer.

One alternative to this would be to remove the long-lived actinides which require long term surveillance. If this could be achieved, the remaining fission products and wastes would require a waste management program on the order of 1000 years. The actinides would then be transmuted in a fission or other type reactor to reduce the long half-lives to short ones, and thus reduce the radioactive hazard. The main problem to be overcome is separation of actinides from the rest of the waste products.

With the assumption that this separation can be done, an investigation was made to determine the necessary separation factors. The study indicated that separations beyond certain limits may not yield enough to substantiate such separation factors. The separations of 99.99% for plutonium, 99.9% for uranium, americium and curium, and 99% for neptunium will reduce the hazard potential to about five percent of that for natural uranium.[11] After 99.9% removal of iodine, it will then be the long-lived remaining fission products which control the waste hazard. Higher removal factors for the actinides do not appear to be warranted unless long-lived fission products are also removed, especially Tc-99.

As means of recovering actinides from the spent waste, several schemes are available. Several schemes can be ruled out mainly due to expense and complexity. For example, a centrifuge is too "dirty" because of associated alpha emitters from the actinides.[12] This would require tight contamination control, and hence much shielding. Other processes require a gaseous form, but there are no gaseous forms of americium or curium.

Present feasibility studies indicate that separations based on solvent extraction, ion exchange, and scavenging precipitation have greatest possibilities. Solvent extraction by itself has not been shown to achieve desired results; however, multi-step solvent extraction processes have a greater probability of success.[13] If particular waste stream recycles are solved, processes based on cation exchange may be a viable method for partitioning the actinides. Another method with potential in waste partitioning may be precipitation.

Figure B.7 illustrates the reprocessing scheme for fission products and actinides generated from Light Water Reactors. Spent fuel from LWRs containing fission products and actinides listed in Table B.3 is sent to storage for about 150 days. The wastes from storage, which is listed in Table B.4, is then sent to a reprocessing plant. This plant discharges Kr-85 and tritium to the air. Ninety-nine percent of the uranium is removed from the waste and sent for enrichment and 98 percent of the plutonium is separated for further fuel fabrication.

The rest of the high-level waste goes to a high-level liquid waste storage for about 215 days. These high-level wastes are listed in Table B.5. After further storage these wastes (listed in Table B.6) go to a fission product/actinide fractionation plant.

Fractionation Schemes

Studies to date indicate that the best methods for removing actinides from wastes will be obtained by improving present state-of-the-art methods.[14] One of the present schemes is shown in the Fig. B.8. In this scheme, neptunium, uranium, and plutonium, are recovered in the primary PUREX plant. Various exhaustive extractions or further PUREX processes are used to accomplish complete removal of the neptunium, plutonium, and uranium. Through the PUREX plant process, a recovery rate of 95-99% for neptunium and improvements in uranium and plutonium recovery to 99.5% or better are expected.[15]

The interim waste storage is for the purpose of reducing the radiation hazard from the remaining high level wastes during subsequent processing. The radiation hazard will be high unless the fission product yttrium and rare earths, which are associated with americium and curium, are allowed to

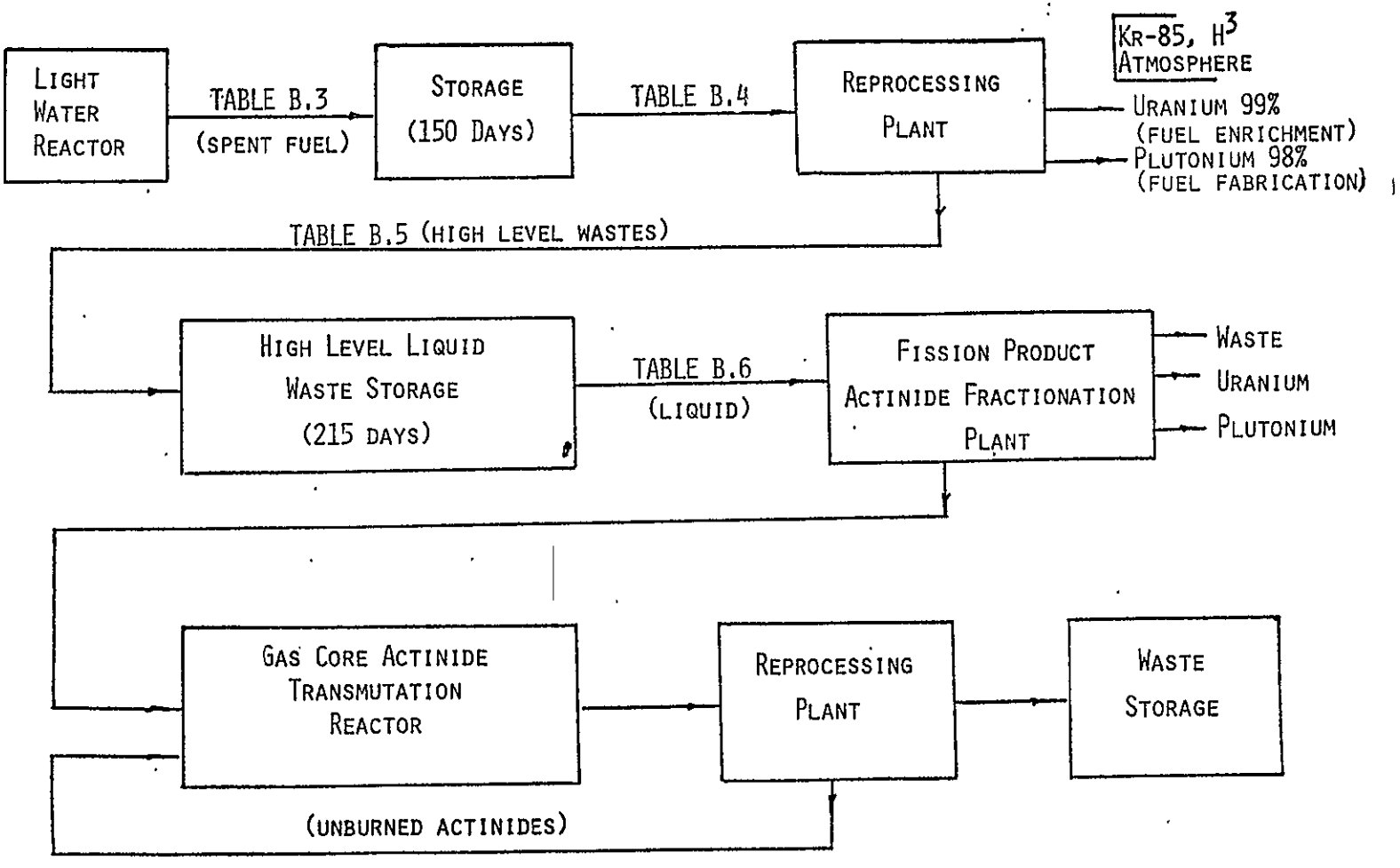

Fig. B.7. Actinide Reprocessing Scheme

Table B.3

FISSION PRODUCT AND ACTINIDE CONCENTRATIONS LEAVING A LWR

PWR FUEL CYCLE - DECAY TIMES OF FUEL DURING COOLING PERIOD
POWER= 30.00MW, BURNUP= 33000.MWD, FLUX= 2.92E+13N/CM**2-SEC
NUCLIDE INGESTION HAZARD, M**3 OF WATER AT RCG
BASIS = PER METRIC TONNE OF U LOADED IN REAC

Actinides

	DISCHARGE
PB212	7.50E+01
BI212	3.75E+00
RA223	1.27E+00
RA224	7.50E+02
TH228	2.13E+02
TH230	8.88E+00
TH231	5.99E+03
TH234	1.57E+04
PA231	2.71E+01
PA233	3.24E+03
PA234M	1.60E+01
PA234	6.52E+01
U232	2.02E+02
U233	1.52E+00
U234	2.55E+04
U235	5.70E+02
U236	9.61E+03
U237	8.55E+09
U238	7.85E+03
NP237	1.11E+05
NP239	1.85E+11
PU236	1.17E+04
PU238	5.45E+08
PU239	6.30E+07
PU240	9.55E+07
PU241	5.25E+08
PU242	2.76E+05
AM241	2.15E+07
AM242M	2.29E+06
AM242	6.34E+08
AM243	4.54E+06
CM242	1.67E+09
CM243	7.42E+05
CM244	3.49E+08
CM245	8.54E+04
CM246	1.71E+04
CM248	1.98E+00
BK249	8.96E+00
CF250	3.76E+00
CF252	2.52E+00
SUBTOT	1.98E+11
TOTALS	2.16E+11

Fission Products

	DISCHARGE
H 3	2.36E+05
KR 85	1.13E+04
RB 86	2.47E+07
SR 89	2.39E+11
SR 90	2.59E+11
Y 90	4.03E+09
Y 91	3.13E+10
ZR 93	2.36E+03
NB 93M	3.61E+02
ZR 95	2.29E+10
NB 95M	2.80E+04
NB 95	1.38E+10
MO 99	3.81E+10
TC 99	7.14E+04
RU103	1.52E+10
RH103M	1.22E+08
RU106	5.45E+10
RH106	7.40E+05
PD107	1.10E+02
AG110M	1.23E+08
AG110	1.59E+05
AG111	9.90E+08
CD113M	1.05E+01
IN114M	7.75E+04
CD115M	1.84E+07
SN119M	1.64E+01
SN123	8.88E+03
SB124	2.03E+07
SN125	6.76E+08
SB125	8.70E+07
TE125M	3.11E+07
TE127M	3.07E+08
TE127	3.60E+08
TE129M	2.86E+09
TE129	4.21E+08
I129	6.18E+05
I131	2.87E+12
XE131M	6.39E+03
TE132	5.92E+10
I132	1.53E+11
XE133	1.61E+06
CS134	2.74E+10
CS135	2.86E+03
CS136	1.01E+09
CS137	5.39E+09
BA137M	1.01E+05
BA140	7.27E+10
LA140	7.50E+10
CE141	1.54E+10
PR143	2.41E+10
CE144	1.11E+11
PR144	1.12E+06
ND147	9.81E+09
PM147	5.12E+08
PM148M	5.89E+04
PM148	1.99E+05
SM151	3.12E+06
EU152	1.57E+05
GD153	1.78E+05
EU154	3.49E+08
EU155	5.74E+07
EU156	2.26E+05
TB160	3.21E+07
SUBTOT	4.11E+12
TOTALS	6.40E+12

Table B.4

FISSION PRODUCT AND ACTINIDE CONCENTRATIONS AFTER 150 DAYS STORAGE

PWR FUEL CYCLE - DECAY TIMES OF FUEL DURING COOLING PERIOD
POWER= 30.00MW, BURNUP= 33000.MWD, FLUX= 2.92E+13N/CM**2-SEC
NUCLIDE INGESTION HAZARD, M**3 OF WATER AT RCG
BASIS = PER METRIC TONNE OF U LOADED IN REAC

Actinides

	150. D
PB212	1.10E+02
BI212	5.49E+00
RA223	1.70E+00
RA224	1.10E+03
TH228	3.18E+02
TH230	1.02E+01
TH231	8.55E+01
TH234	1.57E+04
PA231	2.74E+01
PA233	3.40E+03
PA234M	1.57E+01
PA234	3.14E+00
U232	2.46E+02
U233	1.54E+00
U234	2.52E+04
U235	5.70E+02
U236	9.61E+03
U237	2.69E+04
U238	7.85E+03
NP237	1.13E+05
NP239	1.82E+05
PU236	1.86E+04
PU238	5.84E+08
PU239	6.46E+07
PU240	9.55E+07
PU241	3.15E+08
PU242	2.76E+05
AM241	3.85E+07
AM242M	2.29E+06
AM242	9.13E+04
AM243	4.54E+06
CM242	8.38E+08
CM243	7.66E+05
CM244	3.44E+08
CM245	8.54E+04
CM246	1.74E+04
CM248	1.98E+00
BK249	6.24E+00
CF250	3.93E+00
CF252	2.26E+03
SUBTOT	2.52E+09
TOTALS	2.52E+09

Fission Products

	150. D
H 3	2.31E+05
KR 85	1.10E+04
RB 86	9.49E+04
SR 89	3.24E+10
SR 90	2.56E+11
Y 90	3.84E+09
Y 91	5.37E+09
ZR 93	2.36E+03
NB 93M	4.52E+02
ZR 95	4.62E+09
NB 95M	3.88E+03
NB 95	5.29E+09
MO 99	2.55E-06
TC 99	7.17E+04
RU103	1.16E+09
RH103M	8.83E+06
RU106	4.10E+10
RH106	4.10E+05
PD107	1.10E+02
AG110M	3.14E+07
AG110	3.17E+02
AG111	9.47E+02
CD113M	1.03E+01
IN114M	9.69E+03
CD115M	1.64E+06
SN119M	1.08E+01
SN123	3.86E+03
SB124	3.59E+06
SN125	1.06E+04
SB125	7.95E+07
TE125M	3.20E+07
TE127M	1.23E+08
TE127	3.04E+07
TE129M	1.35E+08
TE129	2.17E+06
I129	5.23E+05
I131	7.28E+06
XE131M	3.19E+00
TE132	7.57E-04
I132	1.95E-03
XE133	5.35E-03
CS134	2.38E+10
CS135	2.36E+05
CS136	3.41E+05
CS137	5.04E+09
BA137M	9.99E+04
BA140	2.16E+07
LA140	2.48E+07
CE141	6.27E+08
PR143	1.06E+07
CE144	7.71E+10
PR144	7.71E+05
ND147	8.39E+05
PM147	4.30E+08
PM148M	3.27E+03
PM148	3.83E+02
SM151	3.12E+06
EU152	1.53E+05
GD153	1.16E+05
EU154	2.48E+08
EU155	3.20E+07
EU156	2.21E+02
TB160	7.58E+06
SUBTOT	4.58E+11
TOTALS	4.58E+11

Table B.5

FISSION PRODUCT AND ACTINIDE CONCENTRATIONS EXITING FROM THE REPROCESSING PLANT

PWR FUEL CYCLE DECAY TIMES OF FUEL AFTER 1ST PROCESSING
POWER= 30.00MW, BURNUP= 33000.MWD, FLUX= 2.92E+13N/CM**-SEC
NUCLIDE INGESTION HAZARD, M**3 OF WATER AT RCG
BASIS = PER METRIC TONNE OF U LOADED IN REAC

Actinides

	DISCHARGE
PB212	1.10E+02
BI212	5.49E+00
RA223	1.70E+00
RA224	1.10E+03
TH228	3.18E+02
TH230	1.02E+01
TH234	1.57E+04
PA234	2.74E+01
PA233	3.40E+03
U232	2.46E+00
U234	2.52E+02
U235	5.70E+00
U236	9.61E+01
U237	2.65E+02
U238	7.85E+01
NP237	1.13E+05
NP239	1.82E+05
PU236	2.12E+02
PU238	1.13E+07
PU239	1.29E+06
PU240	1.91E+06
PU241	1.03E+07
PU242	5.52E+03
AM241	3.85E+07
AM242M	2.29E+06
AM242	9.15E+04
AM243	4.54E+06
CM242	3.88E+08
CM243	7.36E+05
CM244	3.44E+08
CM245	8.54E+04
CM246	1.71E+04
CM248	1.90E+00
BK249	6.44E+00
CF249	8.96E-01
CF250	3.69E+00
CF252	2.26E+00
SUBTOT	1.30E+09
TOTALS	1.30E+09

Fission Products

	DISCHARGE
H 3	2.31E+05
KR 85	1.10E+04
RB 86	9.49E+04
SR 89	3.24E+10
SR 90	2.56E+11
Y 90	3.84E+09
Y 91	5.37E+09
ZR 93	2.36E+03
NB 93M	1.52E+02
ZR 95	1.02E+09
NB 95M	5.88E+03
NB 95	5.20E+09
TC 99	7.17E+04
RU103	1.19E+09
RH103M	8.32E+06
RU106	4.10E+10
RH106	4.10E+09
PD107	1.10E+02
AG110M	8.14E+07
AG110	3.17E+02
CD113M	1.03E+01
IN114M	9.59E+03
CD115M	1.64E+06
SN119M	1.08E+01
SN123	5.30E+03
SB124	3.59E+06
SB125	7.95E+07
TE125M	3.20E+07
TE127M	1.23E+08
TE127	5.04E+07
TE129M	1.35E+08
TE129	2.17E+06
I129	6.23E+05
I131	7.28E+06
CS134	2.58E+10
CS135	2.69E+03
CS136	3.41E+05
CS137	5.54E+09
BA137M	9.99E+04
BA140	2.16E+07
LA140	2.48E+07
CE141	6.27E+08
PR143	1.36E+07
CE144	7.71E+10
PR144	7.71E+05
ND147	8.39E+05
PM147	4.90E+08
PM148M	3.27E+03
PM148	2.63E+02
SM151	3.12E+06
EU152	1.33E+05
GD153	1.16E+05
EU154	3.43E+08
EU155	3.20E+07
TB160	7.93E+06
SUBTOT	4.58E+11
TOTALS	4.58E+11

Table B.6

FISSION PRODUCT AND ACTINIDE CONCENTRATIONS AFTER 215 DAYS
STORAGE IN HIGH LEVEL LIQUID WASTE STORAGE FACILITY

PWR FUEL CYCLE DECAY TIMES OF FUEL AFTER 1ST PROCESSING
POWER= 30.00MW, BURNUP= 33000.MWD, FLUX= 2.92E+13N/CM**2-SEC
NUCLIDE INGESTION HAZARD, M**3 OF WATER AT RCG
BASIS = PER METRIC TONNE OF U LOADED IN REAC

Actinides

	CHARGE	215. D
PB212	0.	9.11E+01
BI212	0.	4.55E+00
RA223	0.	2.33E+00
RA224	0.	9.11E+02
TH228	0.	2.59E+02
TH230	0.	1.02E+01
TH234	0.	1.89E+02
PA231	0.	2.74E+01
PA233	0.	3.40E+03
U232	0.	3.56E+00
U234	5.45E+04	2.56E+02
U235	2.36E+03	5.70E+00
U236	0.	9.61E+01
U237	0.	4.81E+02
U238	8.05E+03	7.85E+01
NP237	0.	1.13E+05
NP239	0.	1.82E+05
PU236	0.	1.84E+02
PU238	0.	2.19E+07
PU239	0.	1.29E+06
PU240	0.	1.94E+06
PU241	0.	1.00E+07
PU242	0.	5.52E+03
AM241	0.	3.90E+07
AM242M	0.	2.28E+06
AM242	0.	9.12E+04
AM243	0.	4.54E+06
CM242	0.	3.56E+08
CM243	0.	7.26E+05
CM244	0.	3.36E+08
CM245	0.	8.54E+04
CM246	0.	1.71E+04
CM248	0.	1.98E+00
BK249	0.	4.61E+00
CF249	0.	1.49E+00
CF250	0.	3.58E+00
CF252	0.	1.94E+00
SUBTOT	6.50E+04	7.74E+08
TOTALS	6.50E+04	7.74E+08

Fission Products

	215. D
H 3	2.23E+05
KR 85	1.06E+04
RB 86	3.28E+01
SR 89	1.84E+09
SR 90	2.52E+11
Y 90	3.79E+09
Y 91	4.26E+08
ZR 93	2.36E+05
NB 93M	5.78E+02
ZR 95	4.67E+08
NB 95M	5.94E+02
NB 95	5.96E+08
TC 99	7.17E+04
RU103	2.56E+07
RH103M	2.05E+05
RU106	2.73E+10
RH106	2.73E+05
PD107	1.10E+02
AG110M	4.51E+07
AG110	1.76E+02
CD113M	9.99E+00
IN114M	4.92E+02
CD115M	5.11E+04
SN119M	5.96E+00
SN123	1.17E+03
SB124	2.99E+05
SB125	6.83E+07
TE125M	2.83E+07
TE127M	3.13E+07
TE127	7.74E+06
TE129M	1.69E+06
TE129	2.71E+04
I129	6.24E+05
I131	6.64E-02
CS134	1.95E+10
CS135	2.06E+03
CS136	3.58E+00
CS137	5.27E+09
BA137M	3.85E+04
BA140	1.89E+02
LA140	2.18E+02
CE141	6.31E+06
PR143	2.56E+02
CE144	4.56E+10
PR144	4.56E+05
ND147	1.24E+00
PM147	4.19E+08
PM148M	9.46E+01
PM148	7.55E+00
SM151	3.11E+06
EU152	1.48E+05
GD153	6.25E+04
EU154	3.35E+08
EU155	2.55E+07
TB160	9.60E+05
SUBTOT	3.56E+11
TOTALS	3.56E+11

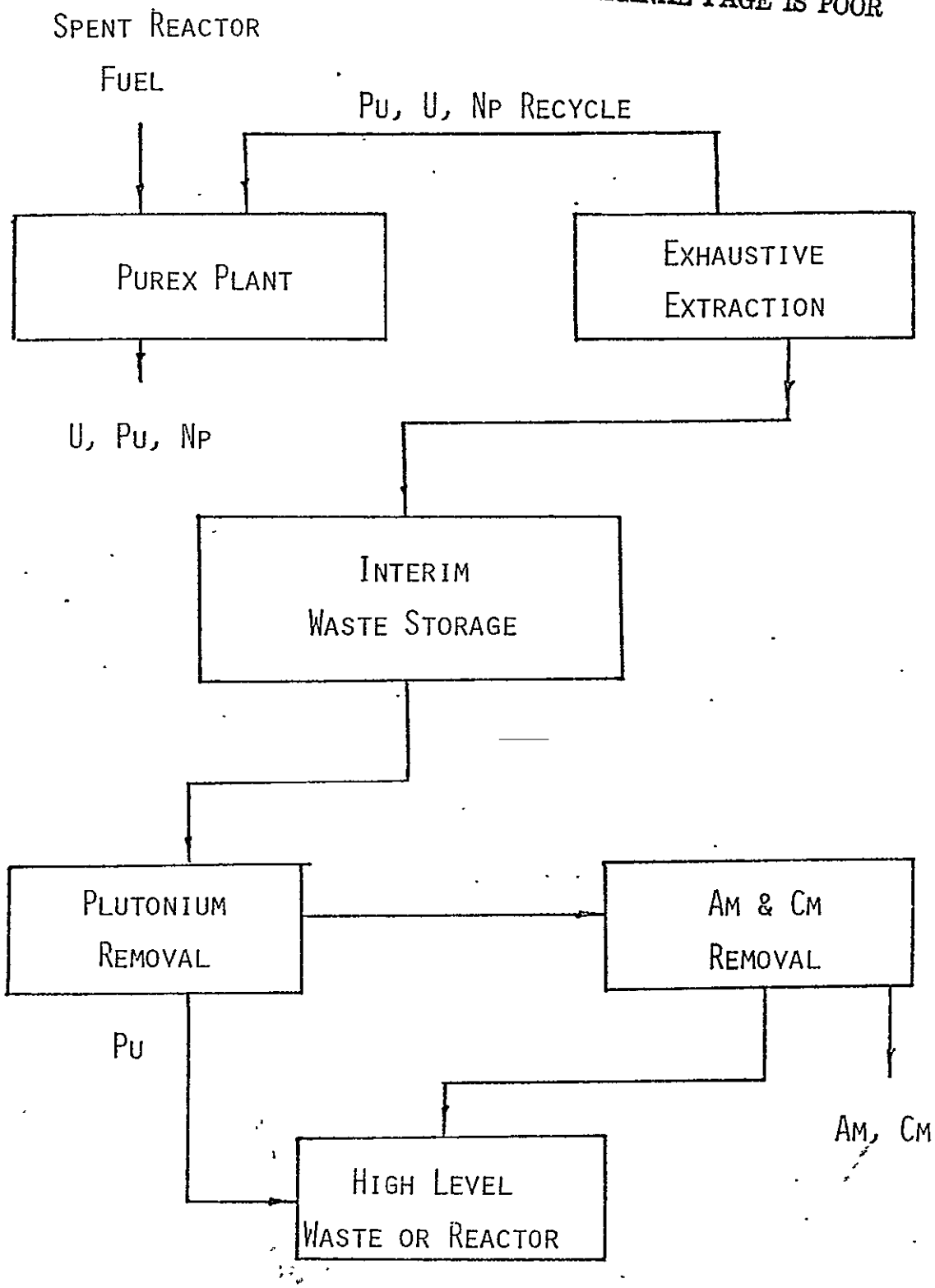

Fig. B.8 Present Processing Sequence for the Removal of Actinides

decay to less hazardous levels.[15] By considering the most important decay times, storage times of ten years would significantly reduce the hazards. Current NRC regulations require that wastes be solidified within five years. However, because of difficulties in working with a solid waste, it will be assumed that the americium and curium are removed from the liquid wastes after a five year period.

One disadvantage of interim waste storage is that the amount of plutonium in the waste grows by curium decay. Therefore, plutonium removal from the stored waste is necessary after several years of interim storage. The process showing most potential for recovering the plutonium is an all ion-exchange process.[16]

After removal of plutonium, the americium and curium are isolated from the rest of the waste. The problems associated with americium and curium removal are centered around finding a suitable chemical separation process for commercial high level wastes. Recovery of americium and curium has been done at the Oak Ridge National Laboratory and Savannah River Laboratory on a multigram basis using a Tramex process.[15] This process has problems with corrosive solutions that require processing equipment constructed of special and expensive materials. Because of these reasons, the process is not recommended. However, there is some possibility that the Tramex processing equipment can be constructed so as to allow safe working of both corrosive solutions in the process and toxic radionuclides at little additional cost.

Other processes that have been developed and claim to give high americium and curium separation are Cation Exchange Chromatography (CEC) and Trivalent Actinide-Lanthanide Separation by Phosphorous Reagent Extraction from Aqueous

Complexes (TALSPEAK).[15] Cation Exchange Chromatography was developed at the Savannah River Laboratory and successfully used to separate about twenty-five percent of the necessary amounts of americium, curium, and rare earths in one metric ton of Light Water Reactor fuel.[15] A schematic flowsheet of CEC is shown in Fig. B.9. The TALSPEAK process, shown in Fig. B.10, has been developed only to the point of tracer-level laboratory studies at Karlsruhe for americium and curium removal.[15]

As means of separating Am and Cm from other wastes, the Tramex, CEC, and TALSPEAK processes require considerable developmental work and data gathering to determine their applicability to the commercial (high volume) extraction of actinides from high-level wastes.

Proposed Schemes

Present proposals for actinide partitioning are based on a sequence of separation processes using solvent extraction, ion exchange, and precipitation. These techniques have not yet been developed.[14] A multistep solvent extraction process combined with other processes, such as cation exchange, may work well in the removal of uranium, neptunium, and plutonium, as well as separations of americium and curium from other wastes.

Tributylphosphate (TBP) may be used as the solvent in the solvent extraction method.[14,17] As demonstrated in the PUREX process, TBP achieved highly efficient recovery of uranium, plutonium, and neptunium.[11]

As a means of separating americium and curium from the rest of fission products and wastes, two steps of cation exchange is quite promising. The potential here appears to be 99.9 percent or better.[14] In the first step the lanthanides and actinides are absorbed on a cation exchange resin

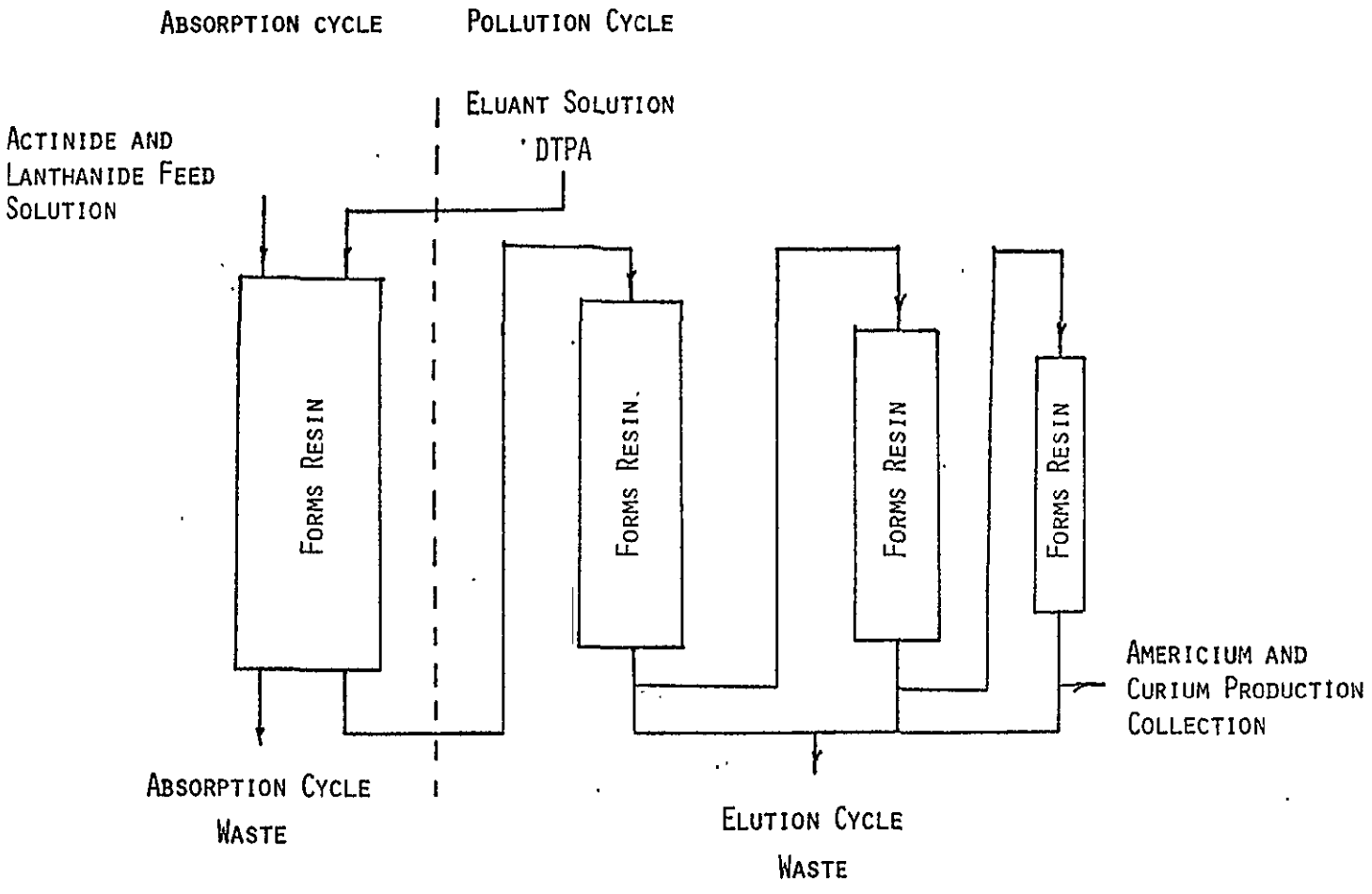

Fig. B.9. Schematic Flowsheet of Cation Exchange Chromatographic Process for Recovery of Americium and Curium[15]

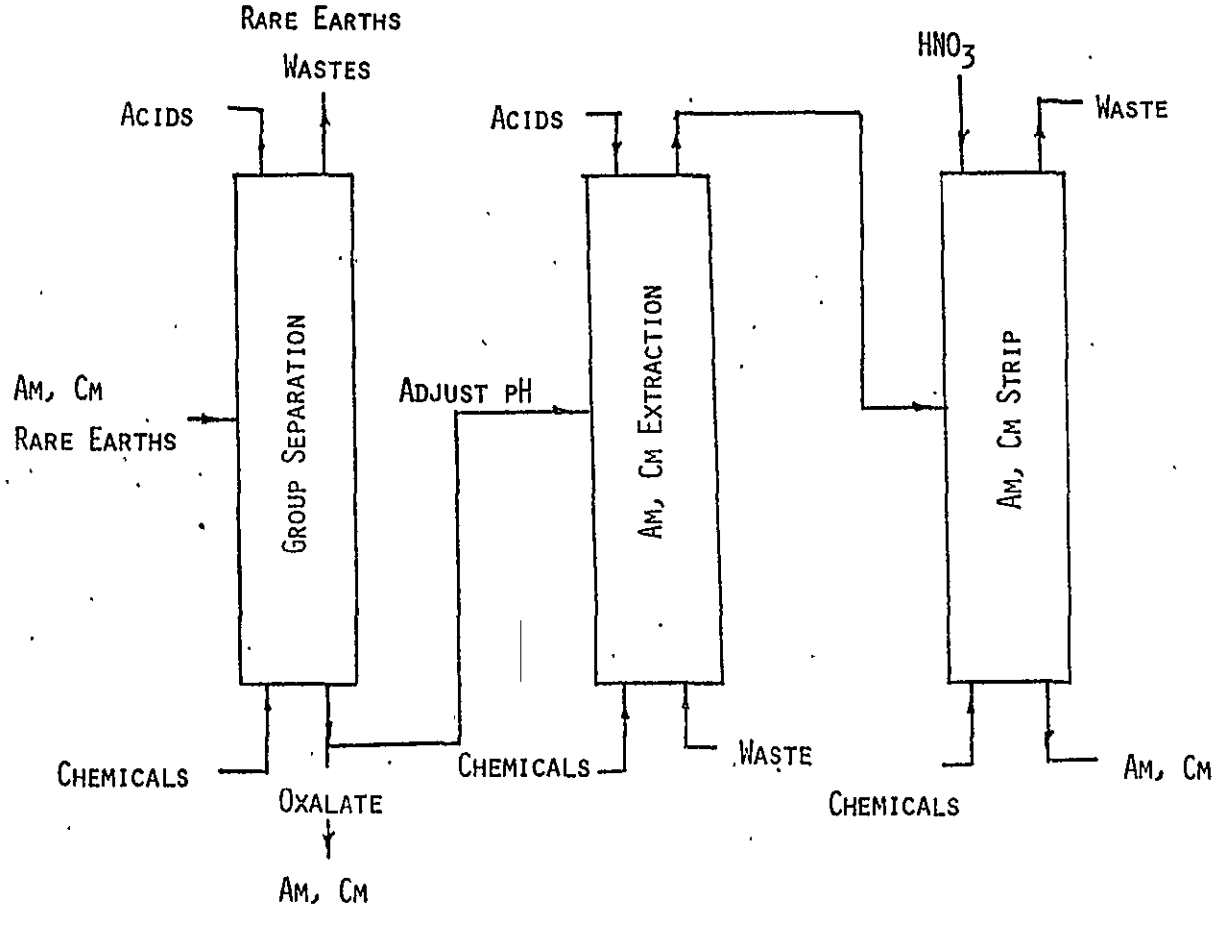

Fig. B.10. Conceptual Flow Sheet for Recovery of Americium and Curium by a TALSPEAK

column and eluted with nitric acid. In the following step the lanthanides and actinides are separated by cation exchange chromatography. Problems to be solved with this process are in converting the spent ion exchange resin to acceptable levels for waste generated in the chromatographic separation.

Precipitation methods combined with ion exchange and/or solvent extraction may be another possible method for partitioning actinides. Even though solid waste handling is unavoidable, ways are now under study for obtaining crude concentrations of plutonium, americium, curium, and fission products. These actinides would then be separated from the lanthanides in further ion exchange or solvent extraction steps. Oak Ridge National Laboratory is studying the use of oxalate[16] precipitation together with ion exchange to isolate the lanthanides and actinides.[14,19] A removal factor of 0.95 is achieved by precipitation while the remaining is removed in the cation exchange column.[15] Tracer-level studies indicate removal of 0.999 for americium and curium.[15] Almost complete removal has been demonstrated for americium and curium by use of multiple oxalate precipitation stages.[14] Further work in this area is still needed to determine the effect of the handling problems.

Technical feasibility, resultant benefits, and costs of partitioning actinides from high-level wastes are yet to be established. It must be decided if the net benefits will justify the use of partitioning. It must also be kept in mind that the separation schemes do not solve the long-term actinide problem. In order to justify this, the actinides must somehow be transmuted to shorter-lived radionuclides or disposed of from our environment. These and many more problems still need research and investigation before a feasible actinide-separation-transmutation process can be substantiated.

From research done to date, it is concluded that much research and development is still needed in the area of actinide partitioning. Work being performed at the Oak Ridge National Laboratory may show encouraging results by the end of 1978. Present state-of-the-art methods will not yield the results needed to establish a practical, economically feasible operating partitioning plant. It is believed that research in the area of combined methods of solvent extraction and ion exchange will yield the necessary separations factors.

References for Appendix B

1. Lowry, L. L., "Gas Core Reactor Power Plants Designed for Low Proliferation Potentials," LA-6900-MS (September 1977).

2. Clement, J. D. and Rust, J. H., "Analysis of the Gas Core Actinide Transmutation Reactor (GCATR)," Annual Report, Georgia Institute of Technology, NASA Grant NSG-1288 (February 1977).

3. Clement, J. D. and Rust, J. H., "Analysis of the Gas Core Actinide Transmutation Reactor (GCATR)," Semi-Annual Report, Georgia Institute of Technology, NASA Grant NSG-1288, Supplement No. 1 (September 1, 1977).

4. Henry, A. F., Nuclear Reactor Analysis, M.I.T. Press, 763 (1975).

5. McNeese, L. E., "Engineering Development Studies for Molten-Salt Breeder Reactor Processing No. 5," ORNL-TM-3140, 15-16 (October 1971).

6. Benedict, M. and Pigford, T. H., Nuclear Chemical Engineering, McGraw-Hill, 156-158 (1957).

7. McNeese, L. E., Op. Cit., 18.

8. "Molten Salt Reactor Program Semiannual Progress Report for Period Ending August 31, 1968," ORNL-4344, 292-298 (1969).

9. Foust, A. S., Principal of Unit Operations, Wiley, 45, 77 (1964).

10. Rosenthal, M. W., Houbenreich, P. N., and Briggs, R. B., "The Development Status of the Molten Salt Breeder Reactors," ORNL-4812 (August 1972).

11. Claiborne, H. C., "Effect of Actinide Removal on the Long Term Hazard of High-Level Waste," ORNL-TM-4724 (January 1975).

12. Schneider, A., Georgia Institute of Technology, Personal consultation (April 1976).

13. Bocola, W., Frittelli, L., Gera, F., Grossi, G., Moccia, A., and Tondinelli, L., "Considerations on Nuclear Transmutation for the Elimination of Actinides," IAEA-SM-207/86.

14. Blomeke, J. O., "Technical Alternatives Documents," ORNL, Prepublication Paper (1976).

15. Bond, W. D., and Leuze, R. E., "Feasibility Studies of the Partition of Commercial High-Level Wastes Generated in Spent Nuclear Fuel Processing: Annual Progress Report for FY-1974," ORNL-5012 (January 1975).

16. Bond, W. D., Claiborne, H. C., and Leuze, R. E., "Methods for Removal of Actinides from High-Level Wastes," Nuclear Technology, 24, 367 (1974).

17. LaRiviere, J. R., et al., "The Hanford Isotopes Production Plant Engineering Study," HW-77770, Hanford Atomic Products Operation (July 1963).

18. Rupp, A. F., "A Radioisotope-Oriented View of Nuclear Waste Management," ORNL-4776 (May 1972).

19. Ferguson, D. W., et al., "Chemical Technology Division Annual Progress Report for Period Ending March 31, 1975," ORNL-5050, 6-11, 30-31 (October 1975).